UNIVERSITÀ
DEGLI STUDI
DI PADOVA

Università degli Studi di Padova

Dipartimento di Ingegneria Civile, Edile e Ambientale

Corso di Laurea Magistrale in Environmental Engineering DM 270/04

Tesi di Laurea

Treating urban wastewaters with microalgae: batch and continuous flow experiments and preliminary process design

Relatore: Prof. Ing. Alberto Bertucco,
Dipartimento di Ingegneria Industriale
Correlatore: Dr.ssa Barbara Gris,
Dipartimento di Ingegneria Industriale

Laureando: Francesco Bettin
n° matr.:1020058

Anno Accademico 2012 / 2013

RIASSUNTO

É stata valutata la possibilità di integrare gli attuali processi a fanghi attivi con la coltivazione di microalghe.

La crescita di *Chlorella protothecoides* in un refluo urbano non sterilizzato è stata testata attraverso esperimenti in batch, effettuati a diverse temperature, per simulare la variazione annuale di temperatura del refluo in ingresso all'impianto di trattamento di Camposampiero (PD). Durante questi esperimenti è stata osservata una forte dipendenze della costante di crescita di *C. protothecoides* rispetto alla temperatura.

Inoltre, è stato rilevato e coltivato in modalità batch un consorzio di microalghe native dal refluo di Camposampiero, con l'obiettivo di caratterizzare la composizione di specie microalgali in previsione di future ricerche e sviluppi.

È stata effettuata una ricerca sulla capacità di crescita di *C. protothecoides* in urina umana sintetica, ma gli esperimenti sono falliti, probabilmente a causa di una errata scelta della composizione dell'urina sintetica.

Sono stati eseguiti esperimenti in continuo con un fotobioreattore piatto verticale, sia a illuminazione costante che con cicli simulati giorno/notte: durante questi esperimenti sono stati monitorati sia la produttività di biomassa che la capacità di rimozione dei nutrienti e i risultati sono stati integrati con i dati ottenuti in precedenti lavori di tesi.

Infine, sono stati proposti e analizzati, con un approccio di dimensionamento preliminare, tre possibili processi di trattamento dei reflui integrati con la produzione di biomassa microalgale.

ABSTRACT

The possibility of integrating existing activated sludge processes with microalgae cultivation was addressed.

The growth of *Chlorella Protothecoides* in urban non-sterilized wastewater was tested with batch experiments, carried out at different temperatures in order to simulate the annual temperature variation of the influent wastewater of Camposampiero (PD) treatment plant. During this temperature screening, a strong dependence of *C. protothecoides* growth rate constant on temperature was observed.

Furthermore, native microalgae consortium from Camposampiero wastewater was detected and grown in batch mode in order to characterize its strain composition for future researches and developments.

An investigation on *C. protothecoides* growth capacity in diluted synthetic human urine was performed, but experiments failed, probably due to an incorrect synthetic human urine composition.

Continuous flow experiments with a vertical flat panel photobioreactor were performed both at constant illumination and under simulated day/night cycles: during these experiments both biomass productivity and nutrients depletion capacity were monitored and results were integrated with data obtained in previous thesis works.

Finally, three possible wastewater treatment processes integrated with microalgae production were proposed and analyzed by a preliminary process design approach.

CONTENTS

1 INTRODUCTION

In recent decades, the exploitation of fossil fuels proved all its limitation: the energy demand is increasing worldwide due to the raise of life quality in developing countries and the inability of industrialized countries in finding alternatives, and the conventional oil production have difficulty in reaching this increasing demand. Alternative energy source, such as photovoltaic, thermal, wind and hydrogen fuel cells are technologies still characterized by high costs and low efficiencies. Besides, these technologies cannot be easily implemented in the transportation sector without costly upgrading.

In addition to these economic problems, fossil fuels have raised a lot of environmental concerns, such as greenhouse gases (GHG) effect on global warming.

In this scenario, biofuels are now being recognized as a valid and green alternative to fossil fuels from researchers and governors. The greatest benefits of biofuels are that they are non-toxic, biodegradable and do not contribute to carbon dioxide or sulphur net emissions (Lam & Lee 2012).

First generation biofuels are produced starting from edible vegetable oils such as soybean, rapeseed, sunflower and palm oil. However, the use of these feedstock is severely limited by the competition with food cultures. Second generation biofuels, instead, derive from non-edible oils such as jatropha oil, waste cooking oil and animal fats, thus not affecting food production. However, the sustainability of second generation biofuels is not favorable (Rawat et al. 2013).

In this situation, biofuels production from microalgae is more and more considered the best available alternative. These microorganisms have a shorter life cycle that terrestrial plants, allowing a continuous harvesting of biomass over the year and they need less freshwater for cultivation, which can be accomplished in non-arable lands (Rawat et al. 2011). Besides, oil content of microalgae is on the average higher with respect to terrestrial plants used for the production of first and second generation biofuel (Table 1.1).

Table 1.1 Comparison of microalgae with other biodiesel feedstock (Mata et al. 2010).

Plant source	Seed oil content (% oil by wt in biomass)	Oil yield (L oil/ha year)	Land use (m^2 year/kg biodiesel)	Biodiesel productivity (kg biodiesel/ha year)
Corn/Maize (*Zea mays* L.)	44	172	66	152
Hemp (*Cannabis sativa* L.)	33	363	31	321
Soybean (*Glycine max* L.)	18	636	18	562
Jatropha (*Jatropha curcas* L.)	28	741	15	656
Camelina (*Camelina sativa* L.)	42	915	12	809
Canola/Rapeseed (*Brassica napus* L.)	41	974	12	862
Sunflower (*Helianthus annuus* L.)	40	1070	11	946
Castor (*Ricinus communis*)	48	1307	9	1156
Palm oil (*Elaeis guineensis*)	36	5366	2	4747
Microalgae (low oil content)	30	58,700	0.2	51,927
Microalgae (medium oil content)	50	97,800	0.1	86,515
Microalgae (high oil content)	70	136,900	0.1	121,104

However, according to results of many researches (Raehtz 2009; Lardon et al. 2009), the environmental and economic benefits, when passing from laboratory scale to plan scale, are not always clear and effective.

LCA (Life Cycle Assessment) on microalgae biomass production recommended the coupling with wastewater treatment, thus to minimize the heavy dependence on inorganic nutrients, necessary for its growth (Lam & Lee 2012). Other studies (Lardon et al. 2009) suggest that the coupling with wastewater treatment is necessary for achieve a net reduction on CO_2 emissions.

Besides, wastewater treatment processes can improve their sustainability by the utilization of microalgae: nitrification-denitrification processes usually implemented for nutrient reduction are high energy-intensive and require high capital costs (Metcalf & Eddy 2004) and only a small part of this energy can be recovered by the anaerobic digestion of the bacterial biomass produced.

A careful engineered approach could improve the overall process yield, reducing the total energy demand and, at the same time, producing a biomass feedstock with high energy content.

1.1 WASTEWATER TREATMENT PLANT

Sewage wastewater represents one of the primary sources of soil and water bodies' pollution: it generally contains high nutrient and organic substances loadings, with variable characteristics depending on the basin extent, presence of industrial or commercial discharges and other factors. The main issue, related to discharge of this loadings in superficial water bodies, is the depletion of dissolved oxygen due to the aerobic digestion of organic matter by bacteria naturally presents and eutrophication phenomena. The first case regards primarily river bodies, where oxygen depletion can cause the death of fish species and, in some cases, it can lead to anoxic conditions, causing problems of odorous compounds. The second case is related to water bodies with low water exchange (lakes and lagoons): excessive nutrient loadings cause an abnormal algal bloom; when this biomass die it is degraded by bacteria, that consume oxygen and cause fish death.

Besides, sewage wastewater contains high concentration of pathogens and, in some cases, excessive loadings of inorganic pollutants, like heavy metals.

In the following paragraphs, typical wastewater treatment processes are described and law limits imposed by Italian legislation are recalled.

1.1.1 ITALIAN LEGISLATION ON WASTEWATER TREATMENT AND DISCHARGE

The reference standard for the EU Member States on the treatment of urban wastewater is the Directive 91/271/EEC, which concerns the entire management system of urban wastewater,

starting from the collection, the treatment and final discharge of wastewater from certain industrial sectors. Its aim is to protect the environment from any adverse effects caused by the discharge of such waters.

The competent authorities lay down the regulations which urban wastewater treatment plants are subjected to. The Directive, further, establishes a timetable, which Member States must adhere to, for the provision of collection and treatment systems for urban waste water in agglomerations corresponding to the categories laid down in the Directive.

Specifically the Directive requires:

- the collection and treatment of waste water in all agglomerations that have a population equivalent >2000 I.E. (Equivalent Inhabitants);
- secondary treatment of all discharges from agglomerations of population > 2000 I.E., and more advanced treatment for agglomerations of population >10000 I.E. in designated sensitive areas;
- a requirement for pre-authorization of all discharges of urban wastewater into urban wastewater collection systems, the monitoring of the performance of treatment plants and receiving waters, and final the control of sewage sludge disposal and re-use.

The second reference directive is the Directive 2000/60/CE, which establish a framework for Community action on water. The Directive pursues multiple objectives, such as preventing and reducing pollution, promoting sustainable water use, environmental protection, improving the conditions of aquatic ecosystems and mitigating the effects of floods and droughts.

The Italian legislation on water, with the D. Lgs 152/1999 and subsequent amendments, is a comprehensive program to protect water bodies from pollution. This decree incorporates, among other things, the EU Directive 91/271/EEC on urban waste water treatment. In addition to regulate discharges while maintaining concentration limits for various substances contained in wastewater, the decree focuses on the quality of the receiving water body by providing the development of monitoring activities for the quantification of environmental damage caused by the man. The current reference standard is the D. Lgs 152/2006 (Italian environmental code), within which the protection of water bodies and the discipline of discharges is detailed in the Sezione II Titolo III.

The Ministry of Environment sets the limits quality to the discharge of wastewater and defines the general applicability criteria and guidelines.

The technical and administrative framework of the discharge is delegated to Regions, whilst the functions of monitoring, controlling, inspecting and authorizing are the responsibility of the provinces and municipalities. The rules govern 4 different types of waste water waste: urban,

household and similar, industrial and rainwater and run-off. All discharges are regulated according to the objectives of the quality of water bodies and should still meet the limit values laid down in Annex 5 of the Decree. The decree establishes that the Regions, in the exercise of their autonomy, taking into account the maximum permissible loads and the best available techniques, may define emission limit values different than those in Annex 5 to Part III of the Decree, both in maximum allowable concentration and in maximum amount per unit of time relative to each pollutant and for groups or families of related substances. The Regions cannot set values limit less stringent than those of Annex 5.

Discharges from wastewater treatment plants urbane must comply with the emission standards listed in Tables 1.2 and 1.3. In the case of discharge of industrial waste water must comply with the limit values of Table 1.4.

Table 1.2 Emission limits for waste water treatment plants for urban waste water.

Inhabitants served [E.I]	*2.000 – 10.000*		*>10.000*	
Parameters (daily average)	*Concentration*	*% reduction*	*Concentration*	*% reduction*
BOD_5 (without nitrification) [mg/L]	25	70-90 ([5])	25	80
COD [mg/L]	125	75	125	75
Suspended solids mg/L	35	90	35	90

Table 1.3 Limits for emissions for wastewater treatment plants in sensitive areas.

Inhabitants served [E.I]	*10.000 – 100.000*		*>100.000*	
Parameters (daily average)	*Concentration*	*% reduction*	*Concentration*	*% reduction*
Total Phosphorous [P mg/L]	2	80	1	80
Total Nitrogen [N mg/L]	15	70-80	10	70-80

Table 1.4 Emission limits for sewers and surface waters.

Substances	*Units*	*Discharge in superficial water bodies*	*Discharge in public sewage*
pH	-	5.5 - 9.5	5.5 - 9.5
Color	-	Not perceptible with 1:20 dilution	Not perceptible with 1:40 dilution
Odor	-	It may not cause harassment	It may not cause harassment
Course materials	-	Absents	Absents
Total suspended solids	mg/L	80	200
BOD_5	mg/L	40	250
COD	mg/L	160	500
Aluminum	mg/L	1	2
Arsenic	mg/L	0.5	0.5
Barium	mg/L	20	-
Boron	mg/L	2	4
Cadmium	mg/L	0.02	0.02
Total chromium	mg/L	2	4
Chromium VI	mg/L	0.2	0.2
Iron	mg/L	2	4
Manganese	mg/L	2	4
Mercury	mg/L	0.005	0.005
Nickel	mg/L	2	4
Lead	mg/L	0.2	0.3
Cupper	mg/L	0.1	0.4
Selenium	mg/L	0.03	0.03
Tin	mg/L	10	
Zinc	mg/L	0.5	1
Total Cyanide	mg/L	0.5	1
Active Free Chloride	mg/L	0.2	0.3
Sulfur (come S)	mg/L	1	2
Sulfite (come SO_2)	mg/L	1	2
Sulfate (come SO_3) (3)	mg/L	1000	1000
Chlorides	mg/L	1200	1200
Fluorides	mg/L	6	12
Total Phosporous	mg/L	10	10
Ammonia (N-NH_3)	mg/L	15	30
Nitrous Nitrogen (N-NO_2)	mg/L	0.6	0.6
Nitric Nitrogen (N-NO_3)	mg/L	20	30
Grease and oils	mg/L	20	40
Total hydrocarbons	mg/L	5	10
Phenols	mg/L	0.5	1
Aldehydes	mg/L	1	2
Aromatic organic solvents	mg/L	0.2	0.4
Nitrogenous organic solvents	mg/L	0.1	0.2
Total surfactants	mg/L	2	4
Phosphorus pesticides	mg/L	0.10	
Total pesticides	mg/L	0.05	0.05
- aldrin	mg/L	0.01	0.01
- dieldrin	mg/L	0.01	0.01
- endrin	mg/L	0.002	0.002
- isodrin	mg/L	0.002	0.002
Chlorinated solvents	mg/L	1	1

1.1.2 WASTEWATER TREATMENT PLANT PROCESSES AND FACILITIES

Wastewater treatment plant processes are usually macro-divided in three categories:

- Primary treatments
- Secondary treatments
- Tertiary treatments

1.1.2.1 Primary treatments

Primary treatments include a series of physical or physical-chemical processes that are a preliminary step for the following biological remediation. Their purposes are eliminating all constituents that can break or ruin the subsequent facilities and avoid excessive nutrient loadings.

Equalization

Flow equalization is a preliminary step which aims to reduce the operational problems due to daily flowrate and pollutant loadings variations. Since each of the following process is designed on the highest loading and/or flowrate that reaches the plant, by equalizing them the size and the cost of the downstream facilities will be reduced. Two possible configurations can be implemented (Figure 1.1):

1. in-line equalization: in this case all the flowrate passes through the equalization basin; the aim of this configuration is to reduce the pollutant peaks;
2. off-line equalization: with this configuration, the flowrate exceeding a predetermined value is diverged to the equalization basin. This method is usually applied in order to capture the first-flux from combined collection systems.

The best location of equalization facilities has to be analyzed in each case, since it depends on land availability and characteristics; however the best position is after the primary clarifier, thus to cause fewer problems of solids settlements, as shown in figure 1.1.

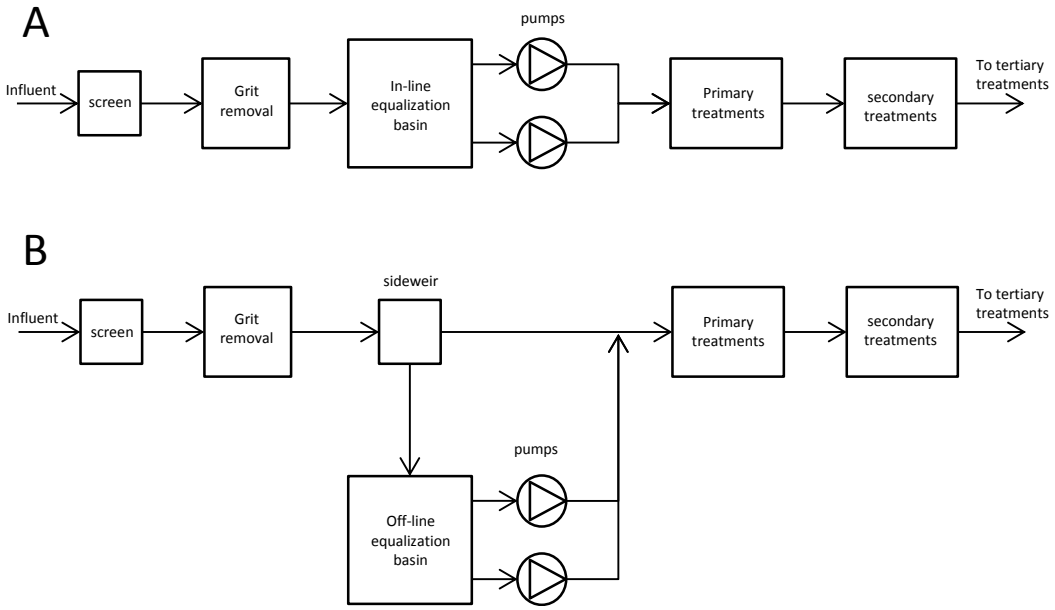

Figure 1.1 Typical wastewater treatment plant flow diagram incorporating flow equalization; A: in-line; B: off-line. Derived from Metcalf & Eddy (2004).

Screening

Generally, the first unit of a wastewater treatment plants is a screening facility. A screen is a device with uniform openings, used to retain solids contained by the influent wastewater.
The main aim of screening is to remove coarse material from the flow stream that could damage the process equipment downstream, reduce overall treatment process reliability and effectiveness, or contaminate waterways (Metcalf & Eddy 2004).
In wastewater treatment, coarse screens are used to protect pumps, valves, pipelines, and other appurtenances from damage or clogging by rags and large objects. Coarse screen are not installed if the sewage line is equipped with grinders.

Grit removal

Removal of grit from wastewater is accomplished in grit chambers or using the centrifugal separation of solids. Grit chambers are tanks designed to remove grit, which is formed by sand, cinders, or other heavy solids materials that have sinking velocities, or specific gravities, substantially greater than those of the organic putrescible solids found in wastewater.
Grit chambers are most commonly located after the bar screen and before the pumping station, in order to reduce pumps strain.

Grit chambers are provided to:

- protect moving mechanical equipment from abrasion and accompanying abnormal wear;
- reduce formation of heavy deposits in pipelines, channels and conduits;
- reduce the frequency of digester cleaning caused by excessive accumulations of grit.

There are three general types of grit chambers:

- horizontal-flow type;
- aerated type;
- vortex type.

Aerated type grit chamber play also an important role in pre-aerating wastewater, which can improve biological treatment yield.

Pumping station

Pumping stations are usually required to head losses and to avoid excess costs of hydraulic works due to tanks buring. Pumps are usually placed after screening and grit removal to avoid breakage and clogging problems. Two main types of pumps are generally used for wastewater treatment plants:

- centrifugal pumps, designed to operate with wastewater rich of solids;
- screw pumps.

Primary sedimentation

The objective of primary sedimentation is to remove readily settleable solids and floating material and thus reducing the suspended solids content. Primary sedimentation tank can remove up to 80% of total suspended solids and achieve a BOD reduction up to 60% if well designed. The purpose of sedimentation is to remove a substantial portion of organic solids to reduce organic loadings to secondary treatments. In some treatment plants they are not used since they reduce too much the organic and nutrient loading, reducing the pre-denitrification yield. There are two main kinds of primary sedimentation tanks:

- Rectangular tanks.
- Circular tanks.

1.1.2.2 Secondary treatments

Secondary treatments are a series of treatments that exploit biological processes, occurring in controlled environmental conditions, for depleting organic matter and nutrient loadings. Therefore the aim of these processes is to convert this organic and inorganic substances in energy and bacteria biomass, that will be subsequently removed from the water stream by means of a secondary clarifier.
Several configurations can be used, with or without nitrogen and phosphorous biological removal. For treatment plants that discharge in sensitive areas nitrogen removal must be provided. Usually phosphorous removal is not achieved with biological process, but with chemical coagulation, since it is less expensive and easier to control.
Below, the most common configuration, called pre-denitrification is exposed. It is composed by three main facilities: pre-denitrification tank, oxidation tank and secondary clarifier. The whole process works in continuous mode. This configuration requires a high amount of mixed liquor recirculation from aerated to anoxic tank in order to permit denitrification to occur.

Oxidation

Oxidation of organic matter occurs in an artificially aerated tank. Bacteria use organic substances as electron donor and oxygen as electron acceptor for their metabolism. Biomass concentration is maintained at a desired value by biomass sludge recirculation from the secondary clarifier. Air or pure oxygen are diffused from the bottom of the tank usually with a series of disk sparger which ensure the maximum gas-liquid transfer and act also as a mixer. The biomass oxygen demand can be estimated with empirical formulas that consider the amount of organic matter loading, gas-liquid transfer coefficients and tank geometry. If nitrogen removal is requested, the oxidation basin acts also as nitrification tank. In fact, environmental conditions (residence time and air supply) are varied to permit the developing of a nitrificant bacteria fraction that can use ammonia and nitrites as electron donor and oxygen as electron acceptor, to make nitrates:

$$\mathrm{NH_4^+} + {}^3\!/_2\, O_2 \rightarrow NO_2^- + 2H^+ + H_2O \qquad \text{(Eq. 1.1)}$$

$$NO_2^- + {}^1\!/_2\, O_2 \rightarrow NO_3^- \qquad \text{(Eq. 1.2)}$$

Reaction 1.1 and 1.2 are consecutive; the second one is usually faster than the first one, so virtually there is no nitrites net production.
These reaction require additional amount of oxygen, that must be provided, and higher residence time (therefore also higher tank volumes).

Pre-denitrification

In this step, facultative heterotrophic bacteria use nitrates and nitrites molecules to assimilate biodegradable organics. This is the reason why denitrification tank is usually set before oxidation tank: denitrification reactions need high amount of organic substances to occur; if denitrification is set after oxidation, organic substances have been already consumed and the process fails. The design of oxidation basin to leave a certain amount of organics for subsequent denitrification has been proved to be a failing strategies since organic loading is subject to daily and seasonal variations, so that a correct design and process control is almost impossible.
The denitrification process occurs only in anoxic conditions and involves a reduction step from nitrate to nitrogen gas, as reported in eq. 1.3.

$$NO_3^- \rightarrow NO_2^- \rightarrow NO \rightarrow N_2O \rightarrow N_2 \qquad \text{(Eq. 1.3)}$$

Since anoxic conditions are fundamental, the recirculation stream must contain the lowest oxygen content possible: this is achieved by maintaining low dissolved oxygen in the oxidation basin (usually, less that 2 mgO_2/l).
Denitrification tanks are generally made of squared or rectangular ponds with depths greater than 3-4 m, equipped with submersible mixers or agitators that keep the tank in agitation to prevent the buildup of sludge without causing a significant transfer of oxygen.
The advantages of nitrification-denitrification process are (Metcalf & Eddy 2004):

- reduction of NO_3 concentration in the effluent;
- reduction of rising sludge in secondary sedimentation tanks due to nitrification process occurring there;
- reduction of oxygen requirements, as organics are removed using also NO_3.

On the other hand the disadvantages are:

- higher capital costs due to higher volume requirements;

- increased plant complexity due to recirculation of mixed liquor from the aerobic to the anoxic tank;
- higher energy consumption related to mix liquor recirculation pumping.

Secondary sedimentation

Secondary sedimentation exploits the force of gravity to separate water from the solid biomass characterized by a higher specific weight (thanks to its flocculating capacities), and therefore able to settle on the bottom of a tank in a time of several hours. Part of the accumulated sludge is recirculated to the biological basin in order to keep the biomass concentration at the desired value (3-7 g/l). Particular attention must be taken for secondary clarifier design, since its failure will cause the failure of the entire process.
The conditions in the biological reactor affect the settling and clarification characteristics of the sludge. As a result, the functions of the biological process and that of the secondary settling tank interact upon each other and the design of one cannot be undertaken independently of the other. Particular attention have to be paid to avoid the formation on anoxic sludge and the subsequent formation of nitrogen bubbles that raise, carrying sludge upwards and releasing odorous compounds.
If total Phosphorous concentration is still too high, it can be removed with chemical processes involving its adsorption on sludge particles. This process is usually mediated with chemicals.

1.1.2.3 Tertiary treatments

Tertiary treatments involve a series of physical or chemical processes to reduce total suspended solids and bacteria concentration.

Filtration

Surface filtration involves the removal of particulates suspended in a liquid, by mechanical sieving achieved passing the liquid through a thin septum, which is the filtering material. Surface filtration has been used to remove the residual suspended solids from secondary effluents and from stabilization pond effluents.
This step is fundamental only if UV disinfection is used, since it guarantees that no self-shading effects will occur there.
Several types of filtration can be implemented, but the most used are sand filtration and disk filters.

Disinfection

This step is fundamental to reduce the pathogens and coliforms concentration. Several systems can be implemented:

- chlorination, which is the most widely used disinfectant. It can be applied in the form of sodium hypochlorite, chlorine dioxide, chlorine liquid or gas. With chlorination processes chloramine compounds, which are toxic, can be formed;
- ozonation, which uses ozone (O_3), a highly effective compound against bacteria and viruses. This process requires high capital costs and is difficult to control since ozone molecules are unstable;
- UV disinfection, which exploits the bactericidal action of UV rays, emitted by means of mercury vapor lamps. The UV rays are strongly effective against bacteria, spores, viruses, fungi. Its main advantage is that it does not create unwanted chemicals.

Sludge line

During wastewater processes three types of sludge can be produced:

- primary sludge: it is produced by settleable solids removed from raw wastewater in primary clarifiers; it is characterized by high putrescibility and good dewaterability when compared to biological sludge; its total suspended solids content is usually in the range 2-7% (Metcalf & Eddy 2004);
- secondary sludge (or excess sludge): it is produced by biological secondary processes and contains microorganisms grown on biodegradable matter, endogenous residues and inert solids not removed in the primary settling (if a primary settler is present) or entering with the raw wastewater (if primary settler is not present); total suspended solids content in secondary sludge is in the range 0.5-1.5% (Metcalf & Eddy 2004);
- chemical sludges: produced by the precipitation of specific substances (i.e. phosphorus) or suspended solids. It is present only if chemical coagulation is used.

The aims of the sludge line are recovering energy or materials from sludge or decreasing its volume and biodegradability for further disposal in landfills.
Sludge line is usually composed of three subsequential processes: thickening (or dewatering), stabilization and final dehydration.

Thickening

In this step sludge is concentered and dewatered by means of physical processes. Reduction of water content can be achieved with different facilities:

- dynamic thickener: this thickener is usually used also as an equalization basin for mixing primary and secondary sludge;
- centrifuge;
- filterpress.

If sludge is treated with a wet anaerobic digestion process, sludge thickening is not necessary.
The excess water from this step of treatment must be recirculated in the wastewater treatment plant since it contains high amounts of organic matter.

Stabilization

Sludge stabilization can be accomplished with aerobic or anaerobic digestion. The latter is usually preferred since it produce a certain recovery of energy, in form of electricity and/or heat.
Anaerobic digestion exploits metabolism of anaerobic bacteria that degrades organic substances, converting them in biogas, a mixture of CO_2, CH_4, H_2 and other compounds. Methane can be burned in biogas engine to produce heat and electricity. Preliminary gas treatments are necessary since the biogas contains high levels of humidity and hydrogen sulfide.
The final product of anaerobic digestion is a well stabilized material, poor in organic fraction and with lower solids content than the initial sludge.
Sludge can be treated alone, or it can be added to putrescible matter, for example coming from separate collection of urban solid waste (co-digestion).

Dehydration

In order to decrease the disposal costs of sludge, water content have to be decreased. A mechanical dehydration is performed by means of empty filter, filter press, press tape and centrifuge.

1.1.3 ISSUES RELATED TO COMMON WASTEWATER TREATMENT PROCESSES

One of the most important problems related to wastewater treatment is the high energy demand of the process (table 1.5): pre-denitrification units require high amount of mixed liquor recirculation (recirculation flowrate can increase of 7 times the average daily flowrate), which is accomplished with high consuming centrifuge pumps.

Besides, anoxic tank have to be mixed to avoid settling of sludge and air have to be fed to oxidation tank: all these facilities require high capital and operational costs. The main aim of wastewater plants is to meet water quality standards, therefore they are usually designed to meet certain effluent requirements, without major energy considerations. As an example, in the US alone WWTPs consume about 2% of the total amount of electricity generated. In fact, WWTPs represent the single largest cost to local governments with up to 33% of their total budget, and their energy consumption is expected to increase by 30–40% in the next 20–30 years (Rojas & Zhelev 2012). After labour, electricity is the largest operating cost associated with wastewater treatment, with 25–40% of the total. In the most common type of WWTP, the activated sludge plant, about 50% of this energy is used for aeration purposes (Metcalf & Eddy 2004).

Besides, plants that implement biological treatment for nutrients removal and filtration use from 30 to 50 % more electricity for aeration, pumping, and solids processing than conventional activated sludge units (Burton 1996).

Table 1.5 Average sewage energy consumption for treatment [kWh/m^3] in different countries (Hernandez-Sancho et al. 2011).

U.S.A	Netherlands	Singapore	Switzerland	Germany	U.K.	Australia	Spain
0.45	0.36	0.56	0.52	0.67	0.64	0.39	0.53

Together with these economic problems, wastewater treatment plants should face also environmental issues: oxidation processes, biogas burning, and indirect energy consumption cause the release of greenhouse gases in the atmospheres.

The main gases emitted by plants are carbon dioxide, methane and N_2O: carbon dioxide is produced by the metabolism of aerobic bacteria in oxidation tanks. It was estimated that treatment plants in the U.S.A. cause the release of 12.7 million of cubic meters of CO_2 per year (Woertz et al. 2009)

Methane is produced by anaerobic fermentation of organic matter in denitrification basin and it is estimated that 9% of global methane emissions are due to wastewater treatment plants (Gupta & S. Singh 2012).

Nitrous oxide is one of the by-products of denitrification reactions; it is considered a gas with one of the highest Greenhouse potential. Gupta & Singh (2012) estimated that 3% of global nitrous oxide emissions are due to wastewater treatment plants.
Technologies for sequestering and treating these gases already exist but their implementation would lead to enormous increase in capital and process costs.

1.1.4 URINE SEPARATION

A large fraction of nutrients found in urban wastewaters comes from human urine, which contributes for 80% of Total Nitrogen and 50% of Total Phosphorous, even if it represents less than 1% of the total wastewater flowrate (T. A. Larsen et al. 2009). Furthermore, urine contains trace elements (for example Cu, Zn, Mo, Mn) necessary for bacterial metabolism and is usually poor in hazardous compounds and heavy metals that can inhibit biological processes (Chang et al., 2013).
Separation of urine from the main wastewater stream could be a way to recover nutrients, to improve the effluent quality and increase the capacity of existing activated sludge wastewater treatment plants (Mbaya et al. n.d.). Typical fresh human urine compostition is reported in table 1.6.

Table 1.6 Fresh human urine composition. Derived from (Mbaya et al. n.d.).

Parameter	Value	Unit
Dilution	1	-
pH	6.2	-
N_{tot}	8830	g/m^3
NH_4^++NH_3	463	g/m^3
NO_3^-+NO_2^-	-	g/m^3
P_{tot}	800-2000	g/m^3
COD	-	g/m^3
K	2737	g/m^3
S	1315	g/m^3
Na	3450	g/m^3
Cl	4970	g/m^3
Ca	233	g/m^3
Mg	119	g/m^3
Mn	0.019	g/m^3
B	0.97	g/m^3

Benefits of source separation of human urine can be summarized as follows:

- reduction of wastewater treatment costs. The nitrification process implemented in treatment plants is designed on the ammonia peak loads, i.e. the worst possible condition. The reduction of this peak due to urine separation at the source would increase the stability and reliability of the nitrification process and therefore allow also a smaller plant size, thus leading to lower capital and operating costs.

  Besides, if influent TKN/COD ratio can be reduced enough, the denitrification-nitrification process can be totally avoided. The degree of urine separation that have to be achieved not to require denitrification-nitrification in wastewater treatment plant depends mostly on the diet of the community (Mbaya et al. n.d.);
- reduction in water consumption: separate urine collection reduces the flush water usage, resulting in lower wastewater generation and therefore also in a lower water consumption.

Source separation techniques are known and used from 70s, but it is only from 90s that they are considered a sustainable alternative to existing wastewater collection and treatment systems for urban and industrialized areas.

Urine separation at the source can be accomplished with appropriate designed toilets (NoMix), which were developed in Sweden in 70s; modern versions of these facilities improves hygienic handling of dry feces (Figure 1.2)

Figure 1.2 Example of NoMix toilet (nomixtoilets.com).

Despite the advantages illustrated above, urine separation technologies presents a series of unsolved problems (M Maurer et al. 2006):

- dilution: the present practice for neutralizing nutrient loadings of source-separated urine require its dilution with large amount of waters (T. A. Larsen et al. 2009). A possible solution is to exploit grey water or overflow streams from sewer sideweirs;
- the modern wastewater management system comprises a series of interdependent actor and facilities, which are extremely difficult and expensive to change;
- transport: transport of source-separated urine to the treatment facility is still an unsolved problem. In some pilot projects, multiple piping systems are tested; besides on-site treatment could be performed, to avoid transportation on urine.

1.2 MICROALGAE AND BIODIESEL PRODUCTION

Microalgae are eukaryotic or prokaryotic photosynthetic organisms, with unicellular or simple multicellular structure, with dimensions ranging from 1 to 10 µm. It is estimated that more than 50000 species of microalgae exist, but only around 30000 species have been yet identified and studied (Mata et al., 2010). Microalgae can grow both in fresh and salt water, and also some terrestrial species are known.

These microorganism are able to convert carbon dioxide into cell biomass, in term of lipids, fatty acids, food and high-value bioactive chemicals, with sunlight-driven metabolism. Besides, microalgae can be useful in bioremediation applications and as nitrogen fixing biofertilizer (Chisti, 2007). Many species can be induced to accumulate consistent quantities of lipid, contributing to obtain a high final oil yield, by controlling environmental parameters, such as carbon dioxide supply, nutrients concentration and lightning conditions. Average lipid content varies significantly from 1 to 70% (some species can reach 90% in particular conditions) therefore the choice of algal strain is fundamental for the entire process feasibility (Mata et al., 2010).

Microalgae growth in batch conditions is characterized by 5 main steps (Fig. 1.3):

1. lag phase: here the algae adapt physiologically to their new environment. Lag phase duration is variable, depending of difference of the environmental conditions such as temperature, nutrient concentration and light conditions. At this stage there is a high nutrients consumption due to algae fast metabolism, while cells concentration increases slowly (or does not increases at all);

2. exponential growth: after adaptation, microalgae start to growth at the highest rate (they can double the biomass in few hours). Exponential growth last until environmental factors are not limiting. For example, nutrient depletions or light attenuation due to self-shading effect of the new biomass can be limiting factors;
3. stationary phase: at a certain point, when one or more factors become limiting, cells number remain constant;
4. death phase: at this step, substrates vital for cells growth are totally absent and this leads to cells death (cells concentration decreases).

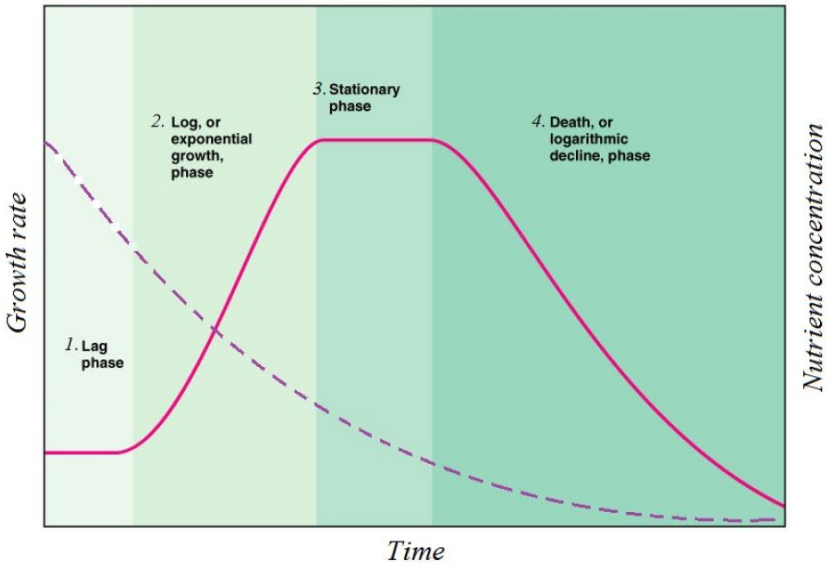

Figure 1.3 Schematic representation of the microalgal growth in batch cultures (continuous line), and the nutrients uptake (dashed line).

1.2.1 THE BIOREFINERY CONCEPT

The microalgal biorefinery concept reflects the concept of a petroleum refinery: it uses every available component of the raw material (in this case biomass) to produce valuable products, with a net energy production. The intensive exploitation of the biomass should decreases the overall process cost. In figure 1.4 an example of biorefinery approach for microalgae is reported.
As said before, microalgae, fixing carbon dioxide and depleting nutrients from the growth medium, produce highly saturated lipids, suitable for biodiesel production through trans-esterification processes (Rawat et al. 2013). In addition, some microalgae species produce valuable by-products: proteins, biopolymers, carotenoids, pigments and anti-oxidant substances that can be used for cosmetic or pharmaceutical purposes (Yen et al. 2011).

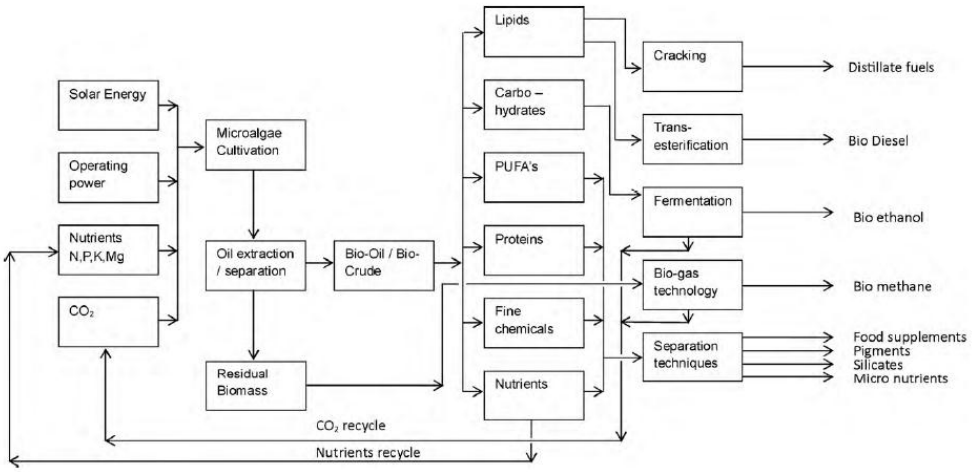

Figure 1.4 Schematic representation of a proposed microalgae biorefinery (J. Singh & Gu 2010).

However, the most interesting aspect remains the possibility of biofuels production; in addition to biodiesel, several types of different renewable fuels can be produced starting from microalgal biomass: bioethanol, methane and hydrogen are some possible alternatives. Although limited reports on bioethanol are available, a number of advantages has been reported in the production of bioethanol from algae. Fermentation process involves less intake of energy and is much simpler in comparison of biodiesel production system. In addition, CO_2 produced as by-product from the process can be recycled for microalgae growth, thus reducing the greenhouse gases emissions. However, the technology for the commercial production of bioethanol from microalgae is yet under development and has to be further investigated (J. Singh & Gu 2010); in addition, contrarily to biodiesel, bioethanol can be used in internal combustion engines only in small percentages without a costly upgrade for the engine.

Methane can be produced simultaneously to bioethanol through the fermentation process, but still no commercial production has been implemented (J. Singh & Gu 2010). Concerning hydrogen production from microalgae, it occurs only in peculiar environmental conditions, such as sulfur deprivation and oxygen absence, which are conditions hard to keep in large scale industrial facilities (Zhang et al. 2002).

Current researches are focusing on biodiesel production, which it could play an important role in the transportation sector in the short-medium period, without the necessity of costly systems upgrading. Besides, biodiesel has a higher calorific value respect to bioethanol (37.3 MJ/kg and 26.7 MJ/kg respectively) (Lam & K. T. Lee 2012).

1.2.2 SELECTION OF ALGAL STRAIN

Many authors report that a critical point of biofuel production optimization setup from microalgae is the choice of the most suitable algal strain. In fact, thousands of microalgae species exist, but only few of these were analyzed for lipid content and biomass production (Table 1.7); published biofuel studies have focused on less than 20 species taken from culture collections and of these publications, 70% are not comparative studies but they focus only on one specific species (Larkum et al. 2012). One reason of this trend is that it is much easier to operate with well know species, rather than starting from microalgae with completely unknown characteristics. Besides, it seems that examining new strains would not lead to higher productivity performances, since this aspect is mainly governed by external environmental conditions rather than by the strain. Another challenge is the possibility of culture endemic indigenous strain, i.e. a microalgae consortium found in the natural environment where facilities would be installed. In fact, these strains are already adapted to the local environmental conditions, therefore they should give better performances in case of open pond systems.

Table 1.7 Lipids contents and lipids productivity of 30 microalgal strains (J. Singh & Gu 2010).

Algal group	Microalgae strains	Habitat	Lipid content (% biomass)	Lipid productivity (mg/l/d)
Diatoms	*Chaetoceros muelleri F&M-M43*	Marine	33.6	21.8
	Chaetoceros calcitrans CS 178	Marine	39.8	17.6
	P. tricornutum F&M-M 40	Marine	18.7	44.8
	Skeletonoma costatum CS 181	Marine	21	17.4
	Skeletonoma sp. CS 252	Marine	31.8	27.3
	Thalassioria pseudonana CS 173	Marine	20.6	17.4
	Chlorella sp. F&M-M48	Freshwater	18.7	42.1
	Chlorella sorokiniana IAM-212	Freshwater	19.3	44.7
	Chlorella vulgaris CCAP 211/11b	Freshwater	19.2	32.6
	C. vulgaris F&M-M49	Freshwater	18.4	36.9
Green algae	*Chlorococcum sp. UMACC 112*	Freshwater	19.3	53.7
	Scenedemus quadricauda	Freshwater	18.4	35.1
	Scenedemus F&M-M19	Freshwater	19.6	40.8
	Scenedemus sp. DM	Freshwater	21.1	53.9
	T. suecica F&M-M33	Marine	8.5	27
	Tetraselmis sp. F&M-M34	Marine	14.7	43.4
	T. suecica F&M-M35	Marine	12.9	36.4
	Ellipsoidion sp. F&M-M31	Marine	27.4	47.3
	Monodus subterraneus UTEX 151	Freshwater	16.1	30.4
	Nannochloropsis sp. *CS 246*	Marine	29.2	49.7
Eustigmatophytes	*Nannochloropsis* sp. *F&M-M26*	Marine	29.6	61
	Nannochloropsis sp. *F&M-M27*	Marine	24.4	48.2
	Nannochloropsis sp. *F&M-M24*	Marine	30.9	54.8
	Nannochloropsis sp. *F&M-M29*	Marine	21.6	37.6
	Nannochloropsis sp. *F&M-M28*	Marine	35.7	60.9
	Isochrysis sp. (T-ISO) CS 177	Marine	22.4	37.7
	Isochrysis sp. F&M-M37	Marine	27.4	37.8
Prymnesiophytes	*Pavlova salina CS 49*	Marine	30.9	49.4
	Pavlova lutheri CS 182	Marine	35.5	50.2
Red algae	*Porphyridium cruentum*	Marine	9.5	34.8

In summary, the main aspects that have to be considered in this step are:

- species growth rate and productivity;
- quantity and quality of lipid produced;
- settling and processing characteristics;
- possibility of exploiting secondary valuable chemicals;

- resistance to changing in environmental conditions like temperature, nutrient load, light conditions.

1.2.3 BIOMASS CULTIVATION

Microalgae can grow in three different conditions:

1. phototrophic;
2. heterotrophic;
3. mixotrophic.

The first one uses light as energy source and carbon dioxide as carbon source. The second uses complex organic compounds as energy and carbon source. Regarding mixotrophic conditions, microalgae can grow in phototrophic and heterotrophic conditions at the same time, depending on carbon source concentration and light availability (Mata et al. 2010).
Presently, only phototrophic culture method is implemented in commercial scale.
A correct design of the culture system is fundamental for the overall process yield and sustainability, since it permits to maximize productivity and quality of microalgal biomass. The following criteria should be carefully analyzed :

- effective illumination area of the culture reactor;
- optimal gas-liquid transfer in case of carbon dioxide supply;
- easy operability of the microalgal reactor, i.e. maintenance, disinfection, cleaning;
- low contamination level (in case of single microalgal strain usage);
- minimal land area requirement;
- low capital and maintenance cost of the whole system.

Microalgae cultivation can occur in closed or open facilities (Figure 1.5). Open ponds systems are the most common solutions implemented nowadays since they require lower capital and process costs than closed photobioreactors. Usually they are limited to liquid depth of 20-30 cm in order to avoid shading effects. The settling of the biomass is avoided through a paddle wheel. Even if open ponds are less expensive, they are characterized by low efficiency since some environmental factors cannot be controlled: water loss due to evaporation, changes in temperature and CO_2 limited transfers are the most common problems (Rawat et al, 2013). Closed photobioreactors usually guarantee higher performances since environmental conditions are strictly controlled. Typical configurations used are vertical flat panel reactor, annular reactors or plastic bags used in batch mode and tubular reactors.

Besides, they permit single-species cultures of microalgae hence it is possible to avoid competition between species, they are designed to maximize light absorption and gas transfer, thus giving higher productivity, and finally, knowing microalgae behavior at different conditions, quality and quantity of lipids can be maximized.

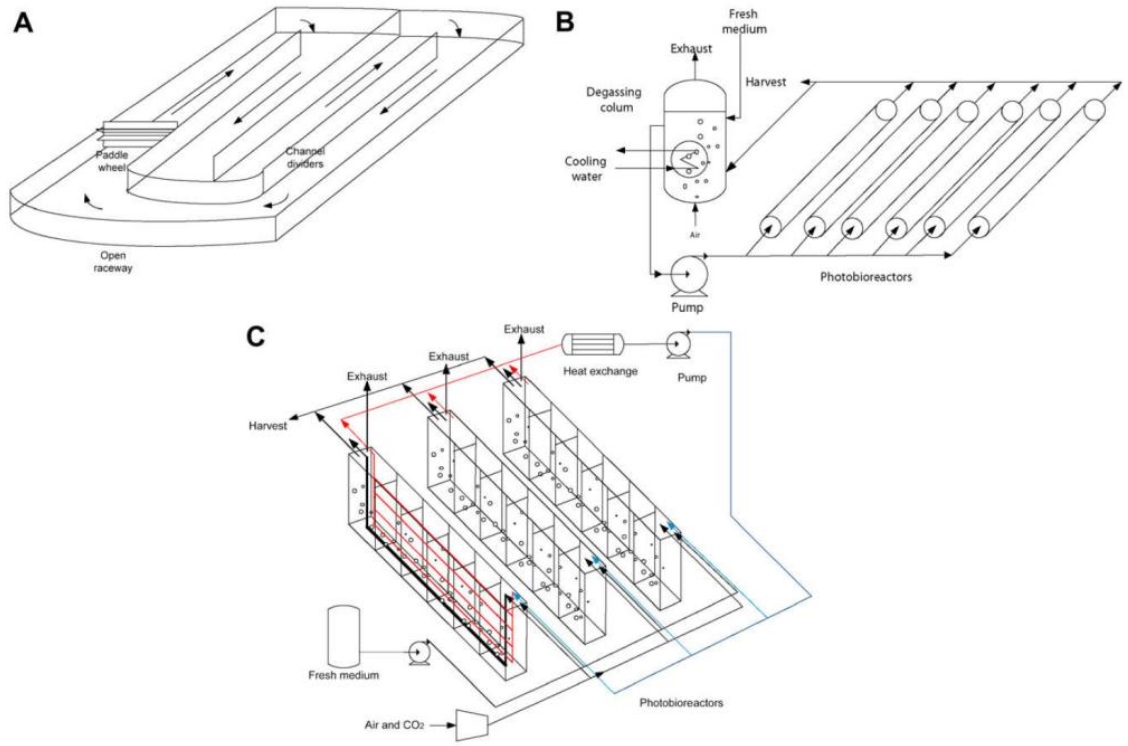

Figure 1.5 Schematic representation of (A) raceway ponds, (B) tubular horizontal photobioreactor and (C) flat-panel photobioreactor.

1.2.4 BIOMASS HARVESTING

The separation of microalgal biomass from the culture media is necessary to biomass downstream processing operations. This step is considered to be one of the most problematic and challenging due to the small size of microalgal cells, and it can contribute up to 30% of the total process costs (Rawat et al, 2013). There are several unit operations involved:

- filtration. Improved filtration is necessary since conventional filtration techniques are insufficient for microalgal biomass recovery.
- centrifugation. This method is usually problematic due to the high power consumption of centrifuges, even if they ensure a rapid and effective biomass separation.
- gravity sedimentation. It is the most common method implemented for large volumes of water, since it is the cheapest.

- chemical flocculation. Multivalent cations or polymers are used to improve sedimentation characteristics of the biomass.

A standard harvesting method for microalgal biomass has not been developed yet and this is still an active field of research (Mata et al. 2010).

1.2.5 ISSUES RELATED TO BIOFUEL PRODUCTION WITH MICROALGAE

Many authors have highlighted that the environmental and economic benefits (Lardon et al., 2009) of microalgae utilization are not always clear and effective when passing from laboratory to large scale. For these reasons nowadays there is no commercial plant producing and processing microalgae biomass into biofuels yet (Lam & K. T. Lee 2012). The major open problems related to microalgae biomass production are:

- photobioreactor design (Jorquera et al., 2010);
- dewatering and biomass drying (Sander & Murthy 2010);
- lipid extraction (A. L. Stephenson et al., 2010);
- nutrients source.

Regarding photobioreactor design, current research is focusing on improving biomass productivity and quality in closed systems, in order to decrease the net cost of the plant. If capital and processing cost remain at the present level, open pond systems will be the only economically feasible solution.
Regarding nutrient source, the cultivation of microalgae at the industrial scale for biofuels production requires a large amount of nutrients, typically nitrogen in the form of nitrate or ammonia and phosphorous in the form of orthophosphates. Usually, nutrients are supplied to biomass through the addition of chemical fertilizers, which are expensive and definitely not sustainable (Lam & K. T. Lee 2012).

1.3 TREATING WASTEWATER WITH MICROALGAE

The idea of treating wastewaters with microalgae goes back to the 50s, as early studies were carried out by Oswald et al. (1953), but it is only in the last decade that researches have focused of this field, because of the problem of energy sources and the need of finding more sustainable solutions for fuel production. Modern wastewater treatments, in fact, are characterized by high energy demands and only a small portion of this energy can be recovered by means of anaerobic

digestion of the excess sludge. Besides, the final product of the denitrification process currently used is atmospheric nitrogen (N_2), which is a useless compounds, thus leading to an additional waste of energy.

Integrating the microalgae biomass production and the wastewater treatment, economic and environmental advantages can be achieved (Lam & Lee 2012), such as the recovery of nutrients, no need of fresh/saline water, CO_2 emissions saving.

1.3.1 BIOLOGICAL OXYGENATION

The ability of algae to produce oxygen by photosynthesis is vital to the ecology of the water environment: microalgae use dissolved CO_2 and a part of nutrients dissolved in wastewater (nitrogen and phosphorous) to grow, and release oxygen as a byproduct. Aerobic bacteria can use this readily available oxygen in order to consume the organic matter present in wastewater and create CO_2 as byproduct. In turn this CO_2 can be used by microalgae for photosynthesis, closing this biological circle (Figure 1.6).

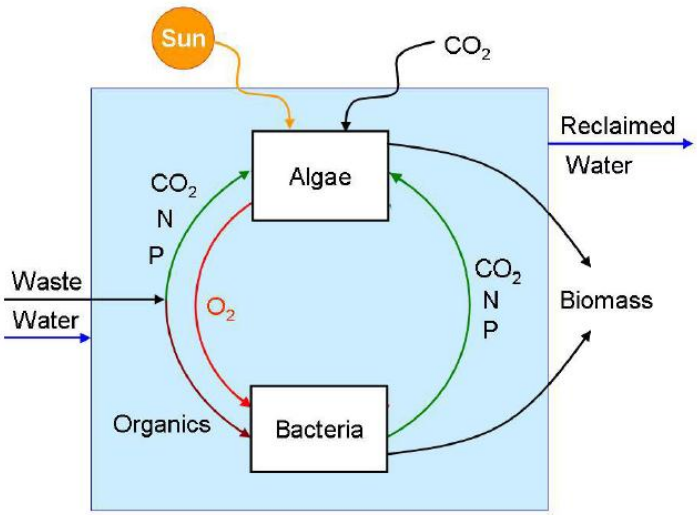

Figure 1.6 Simplified algal-bacterial interactions in wastewater treatment ponds (Woertz et al. 2009).

Recent studies pointed out that microalgae metabolism can lead to high concentration of dissolved oxygen, with values up to 8 mg/l of O_2 (Su et al. 2012).

The oxygen produced by microalgae should be more readily available than that supplied with the common air sparging systems: if microalgae reactor is placed before the activated sludge process, the air demand of this latter can be substantially reduced, thus allowing to additional energy and money savings. In fact, current air supply systems are characterized by low transfer efficiency: usually, only 5% of gas transfer is achieved in 1 meter of oxidation tank.

1.3.2 GREENHOUSE GASES

Coupling wastewater treatment with microalgae biomass production can lead to a substantial environmental improvements: the energy saved using microalgae for nutrients removal, the aeration of the mixed liquor, and the reduction of the greenhouse gases overall emissions: in fact microalgal biomass production and utilization for biofuel synthesis offers potentials for greenhouse gas avoidance since it reduce the needs of fossil fuel extraction and burn.
Elevated CO_2 levels coming from typical power plants could be supplied to microalgal cultures to enhance the biomass production thus allowing an effective GHG reduction.

1.3.3 OTHER ADVANTAGES

Significant concentrations of heavy metals and toxic organic compounds can be detected in municipal wastewater. Microalgae are efficient sorbers of heavy metals: the bioaccumulation of metals in microalgae may become a feasible and cheaper method for remediating wastewater contaminated with metals. Microalgal metal sequestering processes are driven by different mechanisms, which are dependent on the species, the metal ion considered, the solution conditions and whether the algal cells are living or not (Abdel-Raouf et al. 2012).
Besides, it was observed that the environmental factors (first of all the increase of pH of the solution during microalgal photosynthesis), which are favorable for algal growth, become unsuitable for the survival of coliform bacteria and pathogenic organisms usually found in wastewaters, such as *Salmonella*, *Shigella*, viruses and protozoa (Abdel-Raouf et al. 2012). In high-rate ponds, Shelef et al. (1977) reported a reduction of 99% in total coliform bacteria thanks to the high pH and residence time.

1.4 SCOPE OF THE THESIS

The objective of the present thesis work is to investigate experimentally the possibility of treating urban wastewater with microalgae; specifically, the species *Chlorella protothecoides* 33.80 (from SAS Goettingen) has been tested, starting from a previous thesis work that identified this strain as the most suitable for urban wastewater treatment.
Batch experiments have been carried out in order to measure the microalgae growth rate constant and the nutrient consumption at different temperatures, simulating the annual temperature trend of the influent wastewater at Camposampiero (PD) plant.
A further batch experiment has been performed to develop and characterize the native-microalgae consortium found in urban wastewater from Camposampiero plant.

*C. prototheco*ides has been also cultured in continuous flow experiments at constant illumination to evaluate the biomass productivity at different residence times and the nutrient depletion capacities; results of these experiments have been integrated with those of a previous thesis (Morandini 2012).

Continuous flow experiments simulating October day/night light cycles were performed in order to evaluate *C. prototheco*ides behavior in this more realistic conditions.

Moreover, the possibility of applying microalgae biomass production to source-separated urine has been tested through batch experiments.

Finally, experiments results have been exploited to develop three possible wastewater treatment process integrated with microalgae biomass production.

2 MATERIALS AND METHODS

2.1 MICROALGAE

Previous screening experiments permitted to select *Chlorella protothecoides 33.80* (from SAG Goettingen) as the best microalgae species for urban wastewater treatment, thanks to its high growth rate (about 1 d^{-1}) and its shortest lag phase (Morandini 2012). This species can grow in fresh water and in both autotrophic and heterotrophic environments. Its lipid content varies significantly according to growing environment and can reach, in autotrophic conditions, up to 23% of its total dry weight (Cheng et al. 2012).
Consequently, in this thesis work *C. protothecoides* was used for all batch and continuous flow experiments.

2.2 WASTEWATER

Screening experiments were carried out in order to select the most suitable wastewater type for microalgal growth. In particular, urban wastewater from Camposampiero (PD) treatment plant and mixed urban/industrial wastewater from Montecchio Maggiore (VI), both at different points of treatment (after primary treatments and at discharge) were tested (Morandini 2012). These experiments pointed out that treated wastewater has a too low nutrient load to support microalgae growth; besides, there were little differences in final cell concentration between Padua and Vicenza primary treated wastewaters.
For these reasons, primary treated wastewaters from Camposampiero treatment plant were used for all batch and continuous flow experiments.
In some continuous flow experiments, wastewater was preliminary filtered with blotting paper and laboratory paper, in order to avoid tubes clogging.

2.3 SYNTHETIC URINE

The medium of urine experiments is synthetic human urine according to real human urine (Mayrovitz & Sims 2001). Several synthetic urine recipes were evaluated. The choice was based on the pH of the recipe: in fact, some synthetic urine presents an unsuitable pH for microalgae cultivation. For these reasons, the synthetic urine chosen has a pH of 7.8.
The urine formulation is reported in table 2.1. The constituents are expressed in grams per liter of sterile water.

Table 2.1 Composition of one liter of synthetic human urine, according to Mayrovitz et al. (2001).

Composition	Quantity [g/l]
Urea	25
Sodium Chloride	9
Disodium hydrogen orthophosphate, anhydrous	2.5
Ammonium chloride	3
Creatinine	2
Sodium Sulfite, hydrate	3

Bi-distilled water was used for urine production. After the solution was prepared, it has been sterilized in autoclave for 30 minutes at 120°C.

2.4 ANALYTICAL METHODS

2.4.1 MEASUREMENTS OF BIOMASS CONCENTRATION

Microalgae concentration was determined by means of 3 different procedures:

1. cell concentration;
2. optical Density (OD);
3. dry weight.

Usually, cells concentration and OD measures were performed on the same sample, with different dilution factors.

2.4.1.1 Cell concentration

Cell concentration was measured according to this standardized procedure:

1. a sample (1.5-2ml) of microalgal solution was taken using BD Falcon™ Express™ Pipet-Aid®;
2. the sample was diluted with a dilution factor ranging from 20 to 200;
3. cell counting was performed by a microscope using a Burker Counting Chamber. Only 3 of the 9 squares were counted, and then an average value was calculated.

Burker Counting Chamber is a glass slide 7.5x3.5 cm wide and 4 mm deep. The chamber is composed of two cells 1/10mm deep, each one divided in 9 squares of 1 mm side and divided by a triple line. Each square is further divided in 16 smaller squares, divided by double lines (Figure 2.1).

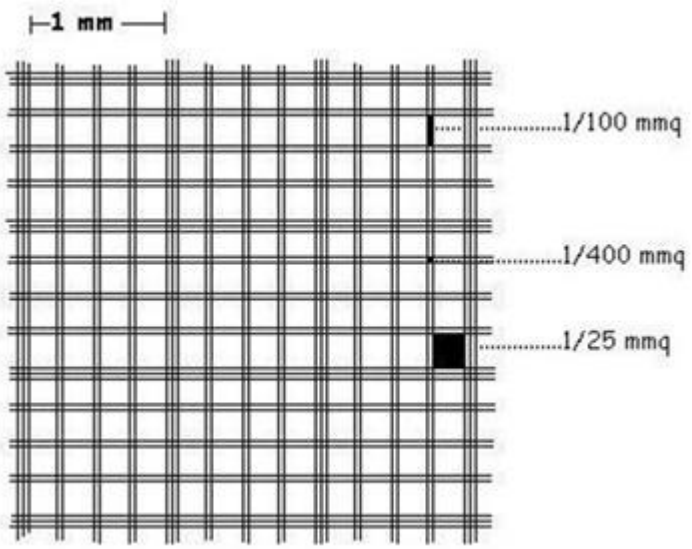

Figure 2.1 Structure of the Burker Counting Chamber reticulate.

2.4.1.2 Optical density (OD)

Microalgal concentrations can be estimated using this standardized procedure:

1. a sample (1.5-2ml) of microalgal solution was taken using BD Falcon™ Express™ Pipet-Aid®;
2. the absorbance of the sample at a wavelength of 750 nm, placed in a cuvette with path length l = 1cm, was measured using Spectronic Unicam UV- 500 UV-visible spectrometer. At this wavelength chlorophyll does not absorb photons and light attenuation is uniquely due to scattering phenomena, i.e., to cells and suspended solids concentration. Using this instrument the absorbance has to range between 0,1 to 1. The sample has to be diluted when the upper limit is exceeded (a dilution factor from 1 to 10 was used); the absorbance, also called optical density (OD), obtained by spectrophotometer was directly linked to cells concentrations by the Lambert-Beer law:

$$A_{750} = \varepsilon l c \qquad \text{(Eq. 2.1)}$$

where:

- A_{750} sample absorbance at λ= 750 nm, $A_{750} = {}^{I}/_{I_0}$ [-]
- l path length [cm]

- ε extinction coefficient [cm^2/cell]
- c cells concentration [cell/ml]

Results of these measurements are plotted in figure 2.2, where the relationship between microalgal concentration and OD_{750} is reported. The figure clearly shows that the relationship was linear but it shows also a certain dependence on temperature and a high variability (low R^2 value). This variability can be due to wastewater suspended solid content (TSS) which can influence the sample OD_{750}, especially at low biomass concentration, when scattering due to TSS is greater than that due to biomass.

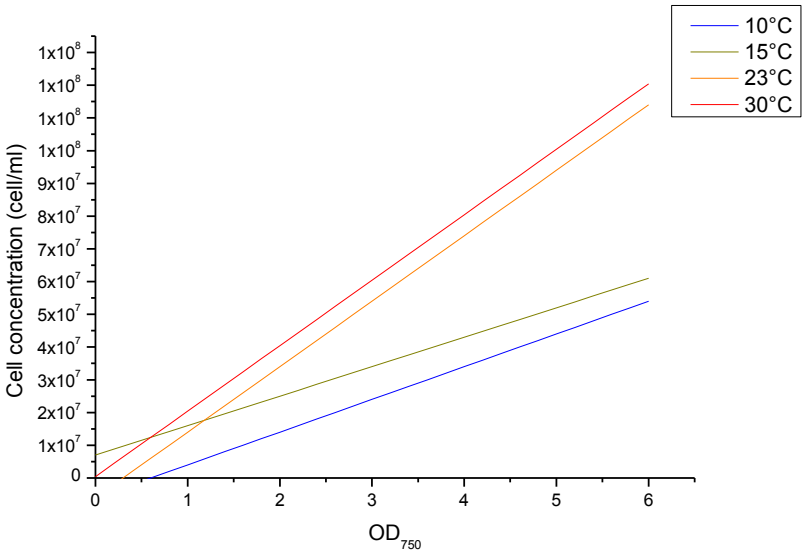

Figure 2.2 Cell concentration vs OD_{750}. Each straight line is the linear fitting results of temperature screening batch experiments reported in paragraph 3.3.

Equations associated to the linear fitting straight lines in figure 2.2 are reported in table 2.2.

Table 2.2 Cell concentration and OD_{750} relationships at different temperatures.

Temperature	cell/ml-OD_{750} relationship	R^2
10°C	y = 1E+07x - 6E+06	0.9527
15°C	y = 9E+06x + 7E+06	0.9428
23°C	y = 2E+07x - 6E+06	0.9581
30°C	y = 2E+07x + 414260	0.9848

2.4.1.3 Dry weight

The dry weight of microalgal biomass (DW) represents the amount of microalgae per unit of volume better than the cell concentration. The analytical procedure used in order to evaluate the biomass growth in terms of dry weight is summarized as follows:

1. a sample of 3 ml or 5 ml of microalgal suspension was collected using BD Falcon™ Express™ Pipet-Aid®;
2. a biomass filter (Sartorius Stedim biotech cellulose nitrate filter pore size 0,2 µm or Whatman NC 20 Membrane filters pore size 0,2 µm) was placed in the oven for 20 minutes to remove the absorbed humidity and then weighted with Atilon Acculab Sartorius Group microbalance with instrument sensitivity of $1 \cdot 10^{-4}$ g. This value represents the tare;
3. the biomass filter was placed in a suitable filtering flask and a known volume of sample was spilled on the filter with a micropipette (Gilson Pipetman P1000): the liquid fraction flows through while microalgal biomass was retained;
4. the filter was placed in the oven at 80° C for 2 hours. In this step all the sample humidity evaporates;
5. the filter was weighted. This value represents the gross weight.

The dry weight was calculated according to

$$DW = \frac{gross\ weight - tare}{volume} \left[\frac{g}{l}\right] \quad \text{(Eq. 2.2)}$$

2.4.2 MEASUREMENT OF BACTERIA CONCENTRATION

Bacteria concentration was measured in terms of CFU/ml (Colony-Forming Unity) following a standardized procedure.

1. a sample (1,5-2ml) of microalgal solution was taken using BD Falcon™ Express™ Pipet-Aid®;
2. the sample was diluted several times in sterile conditions (working under biological safety hood ASALAIR Vertical 700 laminar flow);
3. a precise volume (typically 20 µl) was spread on a Petri plate by means of a sterile disposable spatula;
4. the Petri plate was incubated for 24 hours at 37°C in an incubator (BINDER);

5. eventually a manual counting of CFU was performed.

Starting from the CFU value of each plate, bacteria concentration in the microalgal solution can be calculated with equation 2.3.

$$CFU/ml = \frac{CFU_{Plate}}{V*1000} * D \quad \text{(Eq. 2.3)}$$

where:

- CFU/ml CFU value present in a milliliter of the starting microalgal solution
- CFU_{Plate} CFU value counted on the plate
- V sample volume spread on the plate [µl]
- 1000 transformation factor from µl to ml
- D dilution factor

2.4.3 MEASUREMENT OF POLLUTANTS CONCENTRATION

Nutrients measured in this thesis work were ammonia, orthophosphates, nitrates and COD using standard methods for wastewaters (APHA-AWWA-WEF. 1992). Samples preparation follows this procedure:

1. sampling of tipically 10ml of microalgal culture using BD Falcon™ Express™ Pipet-Aid®;
2. filtering of samples by means of Sartorius Stedim biotech Minisart® with a pore size of 0,2 µm or VWR INTERNATIONAL Sterile syringe filter 0,2 µm;
3. dilution of the sample to achieve a final pollutant concentration within the sensitivity range of the analytical method.

Sample filtering was necessary for correct application of the procedure, but it is important to notice that this permits to evaluate only dissolved nutrients concentration.

2.4.3.1 Chemical Oxygen Demand (COD)

COD was measured using a Sigma COD determination kit (Sigma-Aldrich®). This method is based on the oxidation of organic and inorganic substances by the dichromate ion, whose concentration is quantified by a spectrophotometer. The procedure involves incubation at 148°C for 2 hours. Interferences of chloride ions are avoided thanks to the presence of mercury sulphate, while sulfuric acid acts as a catalyst. The calibration line (Figure 2.3) was determined

with solutions at known COD value, obtained dosing potassium hydrogen phthalate in bi-distilled water. Comparing figure 2.3 with figures 2.4, 2.5 and 2.6 it can be noticed that the slope of the calibration lines is opposite: in fact, the COD kit is made-up with vials containing pre-dosed potassium dichromate; this method measure the quantity of remaining dichromate in the vials after the reaction with organic substances, while all the other methods measure the quantity of reaction products formed.

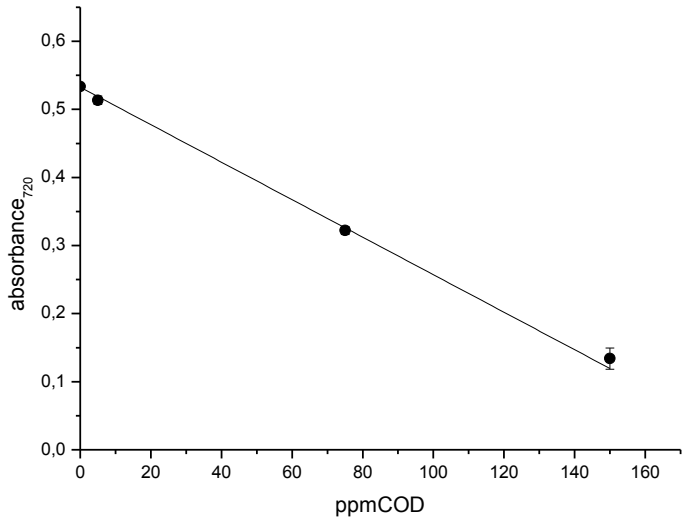

Figure 2.3 COD kit calibration curve.

Equation associated to calibration line is:

$$abs = -0.0027ppm + 0.5283 \qquad R^2 = 0.9991 \qquad \text{(Eq. 2.4)}$$

2.4.3.2 Ammonia

Ammonia Nitrogen was measured by means of 2 kits with pre-dosed reagents:

1. the first kit is distributed by Carlo Erba Reagenti. It is based on a colorimetric reaction between Nessler reagent (Potassium tetraiodomercurate) and ammonia, according to the reaction described by equation 2.5.

$$2K_2[HgI4] + NH_3 + 3KOH \rightarrow [Hg_2ONH_2]I + 7KI + 2H_2O \qquad \text{(Eq. 2.5)}$$

   Ammonium ions present in wastewater are previously converted to ammonia form by hydroxides contained in reagents. This reaction leads to a dense yellow/orange color. The absorbance of the sample due to the colorimetric reaction was measured by means

of Spectronic Unicam UV-500 UV-visible spectrometer at a wavelength of 445 nm. The calibration line (Figure 2.4) was determined based on solutions at known ammonia concentrations, prepared with ammonium chloride;

2. the second kit is HYDROCHECK SPECTRATEST Ammonia. It is based on the same colorimetric reaction (Eq. 2.5) reported for the first kit. The calibration line (Figure 2.4) was determined with solutions at known ammonia concentrations, prepared with ammonium chloride.

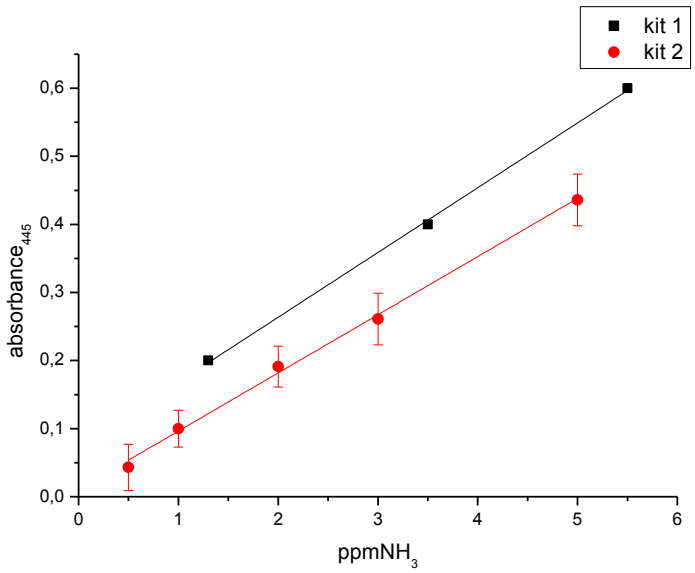

Figure 2.4 Ammonia kit calibration curves.

Equations associated to calibration lines are:

1. $abs = 0.0952ppm + 0.0733 \qquad R^2 = 0.9992$ (Eq. 2.6)
2. $abs = 0.0857ppm + 0.0090 \qquad R^2 = 0.9974$ (Eq. 2.7)

2.4.3.3 Orthophosphates

Orthophosphates were analyzed with 2 different procedures. Analysis on continuous flow experiments were carried out by a kit with pre-dosed reagents, but the kit showed a low accuracy, therefore an analytical procedure based on self-preparation of reagents was implemented and used in temperature screening experiments with batch reactors.

According to the first procedure, orthophosphates were measured by means of HYDROCHECK SPECTRATEST Phosphates low range kit. The colorimetric reaction creates a blue colored complex between the orthophosphates ion and molybdenum under reducing conditions. The method was a variation of the classical Tschopp test. The absorbance of the sample due to the

colorimetric reaction was measured by means of Spectronic Unicam UV-500 UV-visible spectrometer at a wavelength of 720 nm.

The calibration line (Figure 2.5) was evaluated by means of known orthophosphates standard solutions prepared with potassium dihydrogen phosphate.

In the second procedure, orthophosphates were measured by means of an analytical method described in Nova Thalassia vol. 11 (1990), modified in order to be applied to a sample of 2.5 ml.

The mixed reagent was prepared immediately before the analysis (since it become unstable in 3-4 hours), mixing predetermined quantities of stock solutions and ascorbic acid solution. The latter must be prepared the same day of the analysis, as it become unstable in 24 hours, while stock solutions can be stored for months. The composition of each solution is:

- sulphuric acid 5N: prepared diluting 35 ml of 96%$_{p/p}$ of sulphuric acid in 250 ml of milliQ water;
- potassium antimonyl tartrate: 0.34 g of potassium antimonyl tartrate was dissolved in 250 ml of milliQ water;
- ammonium molybdate: 7.5 g of ammonium molybdate tetrahydrate was dissolved in 250 ml of milliQ water;
- ascorbic acid: 1.35 g of ascorbic acid was dissolved in 25 ml of milliQ water.

The final composition of the mixed reagent is reported in table 2.3.

Table 2.3 Mixed reagent final composition.

SOLUTION	VOLUME [ml]
Sulphuric acid 5N	25
Potassium antimonyl tartrate	5
Ammonium molybdate	10
Ascorbic acid	10

For the analysis, 0.25 ml of mixed reagent was added to each sample and the absorbance was measured after 5 minutes.

Colorimetric reaction is the same explained in the previous procedure. The calibration line was evaluated by means of known orthophosphates standard solutions prepared with potassium dihydrogen phosphate. The absorbance of the sample due to the colorimetric reaction was measured spectrophotometrically at a wavelength of 705 nm. This procedure show a higher accuracy, as can be easily noticed looking at the slope of the calibration line, even if the sensibility range is smaller: 0,1-3 ppm instead of 1-5 ppm.

Calibration lines of the two procedures are reported in figure 2.5.

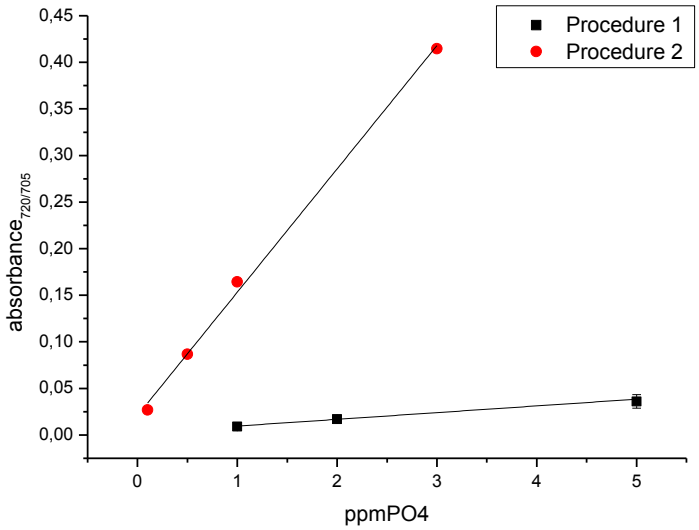

Figure 2.5 Phosphates calibration curves.

Equations associated to calibration lines are:

1. $abs = 0.0067ppm + 0.0026 \qquad R^2 = 0.9965$ (Eq. 2.8)
2. $abs = 0.1324ppm + 0.0210 \qquad R^2 = 0.9979$ (Eq. 2.9)

2.4.3.4 Nitrates

Nitrates were measured by means of Idrimetre St. Carlo Erba Reagenti. The colorimetric reaction firstly reduces nitrate to nitrite, which, by reacting with sulfanilic acid, produces diazo. The reaction between diazonium salt and gentisc acid (2.5 dihydroxibenzonic acid) produces the azo dye. The absorbance of the sample was measured spectrophotometrically at a wavelength of 445 nm. The calibration line (Figure 2.6) was evaluated by means of known nitrate concentration standard solutions prepared with $NaNO_3$.

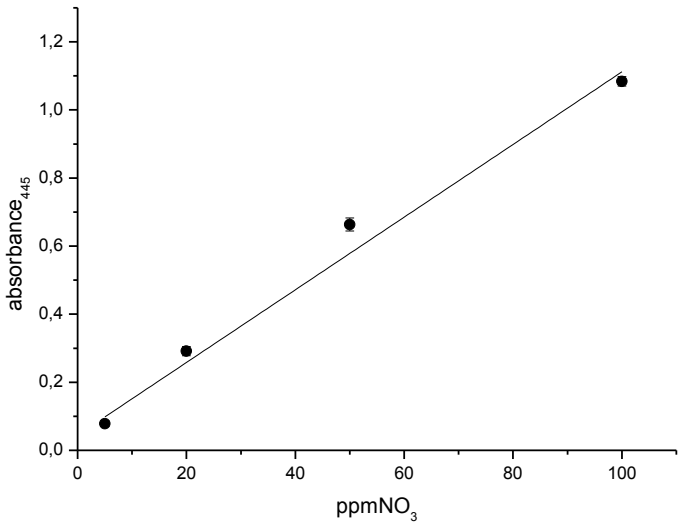

Figure 2.6 Nitrates kit calibration curve.

Equation associated to calibration line is:

$$abs = 0.0105ppm + 0.0711 \qquad R^2 = 0.9862 \tag{Eq. 2.10}$$

2.5 EXPERIMENTAL SETUP

The setup of each experiment is now described, with reference to reactor type, culture medium, illumination system and air supply system.

2.5.1 LABORATORY FACILITIES

All laboratory experiments were carried out in thermostatic incubators where temperature can be adjusted within an error of ±1°C. In each incubator 8 air supply lines are present. Usually, a mixture air/CO_2 at 5% CO_2 volume concentration was used. The plant (Figure 2.7) is powered by a cylinder of air and a cylinder of CO_2. In each cylinder there are two manometers, that give the values of inner cylinder pressure and delivery pressure. The latter one can be adjusted through a pressure reducer. Each cylinder is equipped also with an on-off valve which allow the opening (or the closure) of the cylinder. Outlet gases are sent to two volumetric flowmeters, which allow to control each gas flowrate, thus determining the volumetric ratio of the gas to be fed to the reactor. Gases from the two flowmeters are mixed through a "T" junction; mixed gases are then sent to the 8 terminal lines inside the incubator. Each terminal line is equipped with an on-off valve and a regulation valve which permits to adjust the flux of the gas through each reactor.

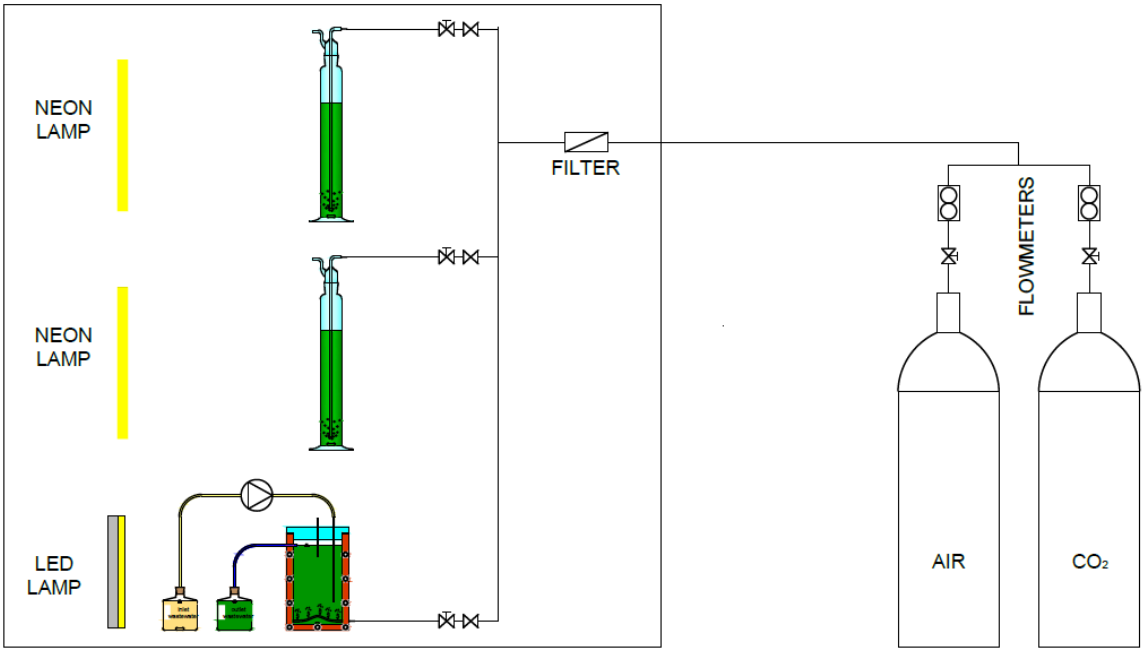

Figure 2.7 Schematic representation of the laboratory plant.

2.5.2 URINE BATCH EXPERIMENTS

Urine experiments were performed in Quickfit® Drechsel Bottles with a volume of 250 ml and a diameter of 5 cm, as shown in figure 2.8.

Experiments were carried out in sterile conditions; for screening experiments microalgae inoculum was added without centrifugation, while in the following experiments inoculum was centrifuged for 6 minutes at 5100 rpm in order to separate microalgae from BG11 medium. Microalgae specie used was *C. prototothecoides*, previously grown in a bottle with BG11 medium.

Two types of air supply system were used: for experiments with CO_2 supply, bottles were continuously bubbled with air enriched with CO_2. The total flow rate was 1 l/h. For experiments without CO_2 supply, atmospheric air was bubbled by means of a compressor.

The bottles were continuously mixed by both a magnetic stirrer and air bubbling and they were placed inside an incubator (Frigomeccanica Andreaus) where temperature was maintained constant at 23°C (±1°C).

Light sources used were white neon lamps (OSRAM). The bottles where placed at a distance from the lamp so that light intensity hitting the bottle was 150 µE/(m^2*s), as measured with a radiometer (DELTA OHM HD 2102.1).

For screening experiment, one bottle was used for each dilution rate; the following experiments were carried out in two replicas with the same set up, and results reported are an average from analysis on each replica.

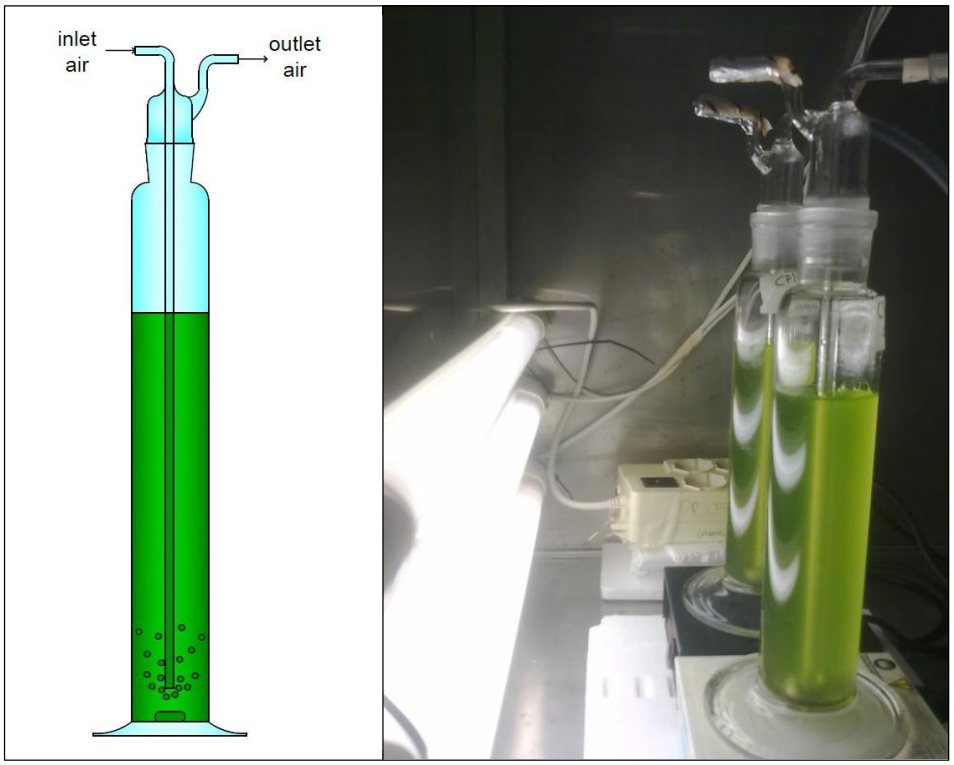

Figure 2.8 Drechsler glass bottle system sketch up and photo.

2.5.3 WASTEWATER BATCH WITHOUT INOCULUM

Also this experiment was carried out in Drechsler glass bottle (Figure 2.8). No inoculum was added to the bottle. Bottle air supply, light and temperature conditions were the same as the urine batch experiments.

2.5.4 TEMPERATURE SCREENING BATCH EXPERIMENTS

Temperature screening experiments were all carried out in two replicas: experiments under constant light intensity were performed in bottles while experiments under day/night light cycle were performed in vertical flat panel photobioreactor (see 2.5.5), operated in batch mode. *C. protothecoides* species was inoculated after centrifugation for 6 minutes at 5100 rpm.

Air supply and mixing conditions are the same as for the urine batch experiments.

Experiments were carried out in an incubator (Frigomeccanica Andreaus), where temperature could be adjusted at the desired values. A monitoring campaign for determining the actual temperature inside the incubator was performed, resulting that temperature setup had to be one degree lower than the desired temperature (For example, in order to keep an actual temperature of 30°C, the incubator had to be set to 29°C); temperature was monitored daily with a mercury thermometer.

For experiments at constant light conditions, light sources used were white neon lamps (OSRAM). The bottles where placed at a distance so that the light intensity hitting the panel was 150 µE/(m^2*s).

For experiments under day/night light conditions, the daily sun cycle was simulated by means of a LED lamp system (PHOTON SYSTEMS INSTRUMENTS, lamp n°2), linked to a digital controller (PHOTON SYSTEMS INSTRUMENTS - Light Controller LC 100). The sin function (Figure 2.9) was used to simulate the daily solar irradiation curve.

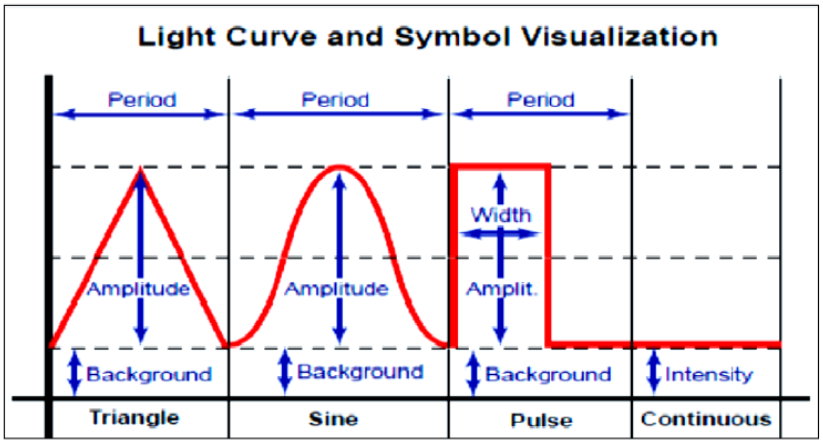

Figure 2.9 Light functions available in the controller.

October sun cycle in Padua was simulated starting from data available online (PVGIS© European Communities 2007). As the controller used, did not permit a light period longer than 9 hours, the first and last hours of illumination were simulated with white neon lamps (OSRAM), whose on/off cycle was governed by a mechanical timer. In figure 2.10 real and simulated sun cycles are reported. The result is quite satisfactory.

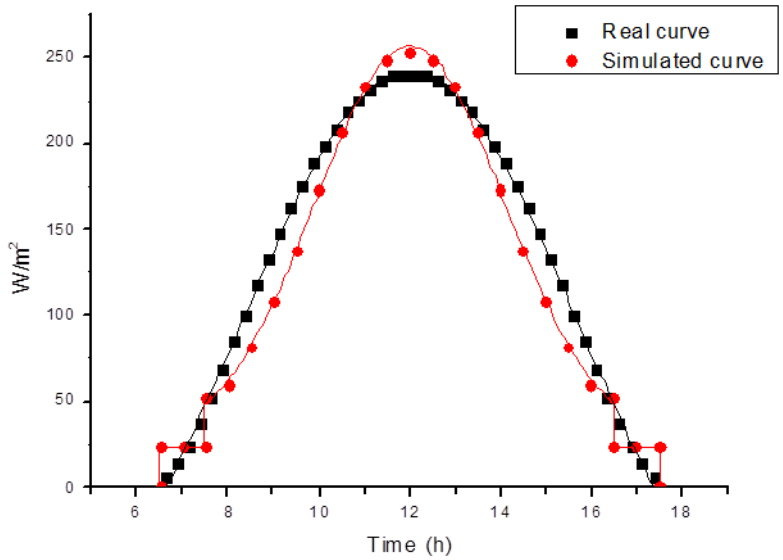

Figure 2.10 LED lamp n°2 calibration curve confronted with real sun daily irradiation in Padua in October.

2.5.5 CONTINUOUS FLOW EXPERIMENTS

Continuous flow experiments were carried out in a vertical flat panel photobioreactor (Figures 2.11 and 2.12). This photobioreactor is made of two transparent polycarbonate sheets glued at a "U" support. The support thickness affects the reactor volume and the light path length. The reactor was continuously mixed by means of both a magnetic micro-stirrer and gas bubbling. The reactor was continuously bubbled with industrial air enriched with CO_2 through a rubber tube placed at the bottom. The air/CO_2 mixture was 95/5 by volume and the total flow rate was 0.5 l/h. Previous studies (Facca 2013) permitted to assess that this reactor can be considered a CSTR type with a good approximation, in fact the dead volume was estimated to be 10% of the total volume. The system was placed inside an incubator (Frigomeccanica Andreaus) whose temperature was maintained constant at 23°C (±1°C). *C. protothecoides* is the only fresh water microalgae used in these experiments.

Reactor was operated in batch conditions: *C. protothecoides* was inoculated in the reactor with 200 ml of non-sterilized wastewater at the beginning of each run.

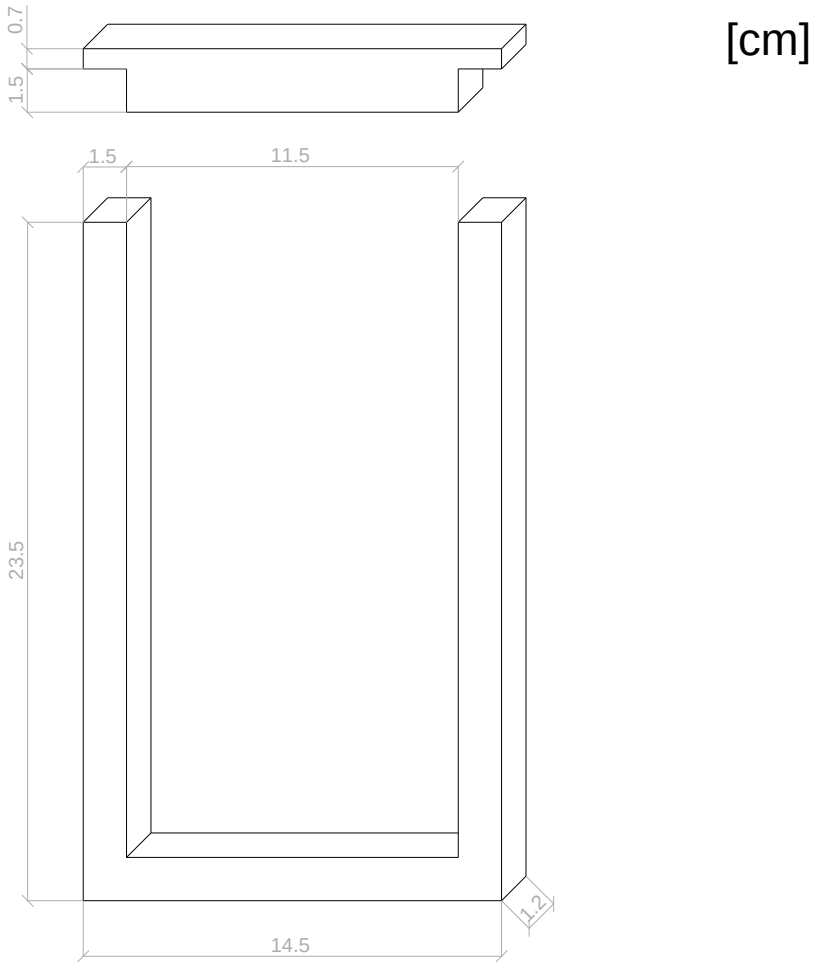

Figure 2.11 Geometry and dimensions of the vertical flat panel photobioreactor used.

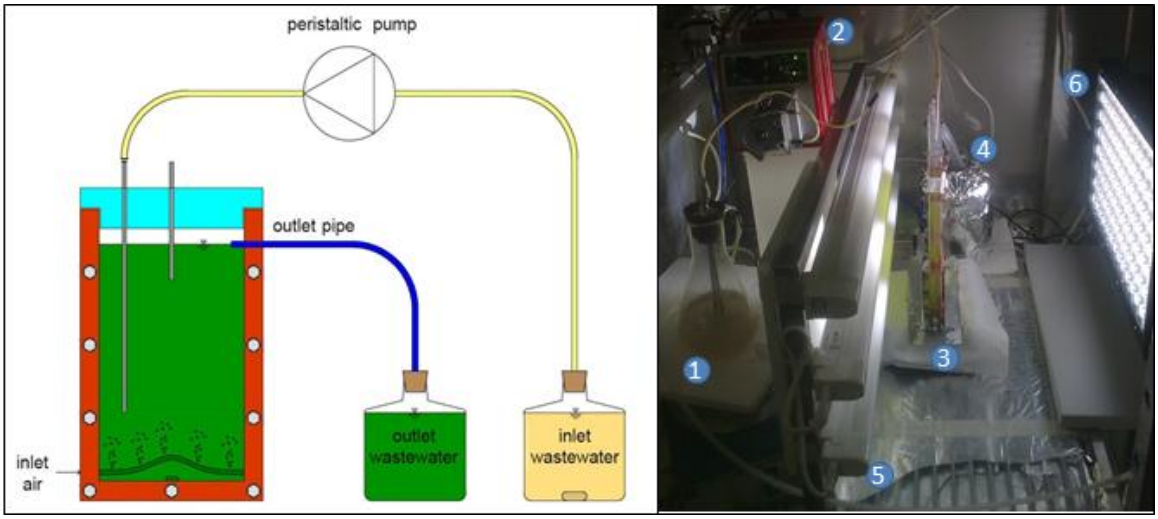

Figure 2.12 On left: schematic representation of a continuous flow system setup. On right: photo of a continuous flow experiment running at day/night light condition (1. inlet wastewater; 2. Pump; 3. Reactor; 4. Outlet wastewater; 5. Neon lamps; 6. LED lamp).

Once the desired cell concentration was reached, the operation was switched to continuous mode. Accordingly, the reactor was fed with wastewater through a peristaltic pump (Watson Marlow pumps 120S). Inlet wastewater storage tank was continuously mixed with a magnetic stirrer. The liquid level in the reactor was controlled with an overflow plastic tube placed close to the top.

For experiments under constant light conditions, light sources were white neon lamps and the panels where placed at a distance where light intensity reaching them was 100 µE/(m^2*s).

For experiments under day/night light conditions, the daily sun cycle was simulated by means of a LED lamps (PHOTON SYSTEMS INSTRUMENTS, lamp n°1) linked to a digital controller. October sun cycle in Padua was simulated starting from data available online (PVGIS© European Communities 2007). As the controller used did not permit a light period longer than 9 hours, the first and last hours of light were simulated with white neon lamps. In figure 2.13 real and simulated sun cycle are reported.

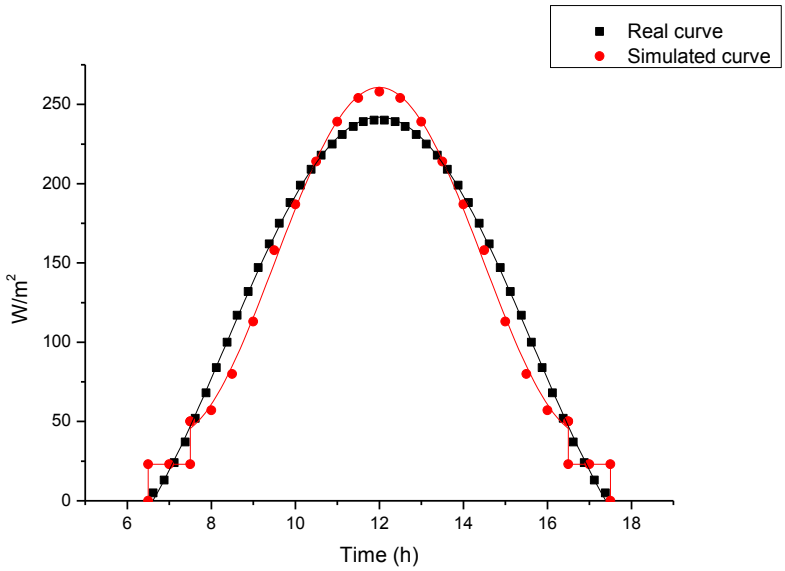

Figure 2.13 LED lamp n°1 calibration curve confronted with real sun daily irradiation in Padua in October.

3 RESULTS AND DISCUSSION

3.1 SYNTHETIC URINE BATCHES

Synthetic human urine is characterized by a very high nutrient content, which can have inhibition effects on microalgae growth, therefore a dilution with water is necessary. Of course, higher dilutions can limit *C. protothecoides* growth and need too much water for a real scale process.

First of all a dilution screening was performed in order to analyze the growth of *C. protothecoides* at different dilutions. 10-diluted urine was initially chosen thanks to its highest growth rate but in subsequent experiments *C. protothecoides* did not grown at all, therefore an additional batch experiment with air not enriched in CO_2 was performed in order to asses if CO_2 was a limiting factor for microalgae growth in synthetic human urine. Besides, urine 100-diluted (following 100-d) was tested.

3.1.1 DILUTION SCREENING

A dilution screening was performed over different dilution factors from 1 to 200; biomass concentration was monitored through OD_{750} analysis for 3 days. OD_{750} measurements for each dilution factor are reported in table 3.1.

Table 3.1 OD_{750} measurements at different dilution factor (D). Data refers to batch system with the same set up.

Day	OD_{750}					
	200-D	**50-D**	**10-D**	**2-D**	**1.25-D**	**1-D**
0	0.575	0.536	0.537	0.526	0.731	0.574
1	0.661	0.651	0.703	0.410	0.469	0.430
3	0.698	0.666	0.992	0.228	0.259	0.241

Figure 3.1 shows the results of the screening experiments. The two bottles with medium urine 200-d and 50-d did not show a significant growth after 3 days probably due to poor nutrient content. In the cultures 2-d, 1.25-d and 1-d the growth was stopped after the first day due to high concentration of NH_4-N.

Only 10-d urine displayed a significant growth. Then the following experiments were focalized on this dilution ratio only.

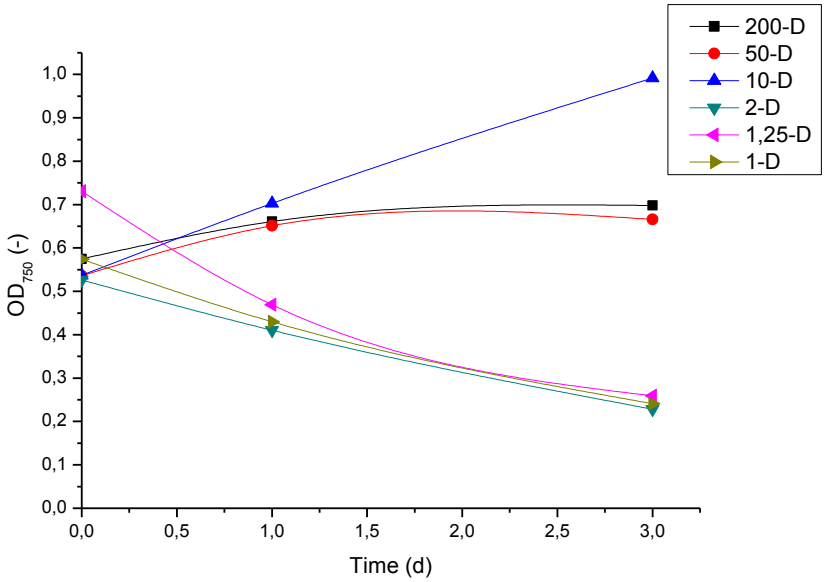

Figure 3.1 OD_{750} trend ad different dilution ratio in synthetic human urine.

3.1.2 EXPERIMENT 1: 10-DILUTED URINE

Results of this first run are discordant with screening experiments. According to what is reported in table 3.2 and in figure 3.2 it can be clearly seen from OD_{750} and cells counting that there is no growth at all.

Table 3.2 OD_{750} and cells concentration at 10-d urine. Values are an average from two replicas with the same set up.

Time [d]	OD_{750} [-]	St. dev. [-]	Cell. conc. [10^6 cells/ml]	St. dev. [10^6 cells/ml]
0	0.530	0.000	10.11	-
1	1.048	0.119	15.70	1.74
2	1.333	0.007	15.70	0.99
3	0.839	0.021	9.83	0.24
4	0.554	0.007	10.02	0.68
7	0.948	0.060	-	-
9	1.106	0.105	12.83	3.06

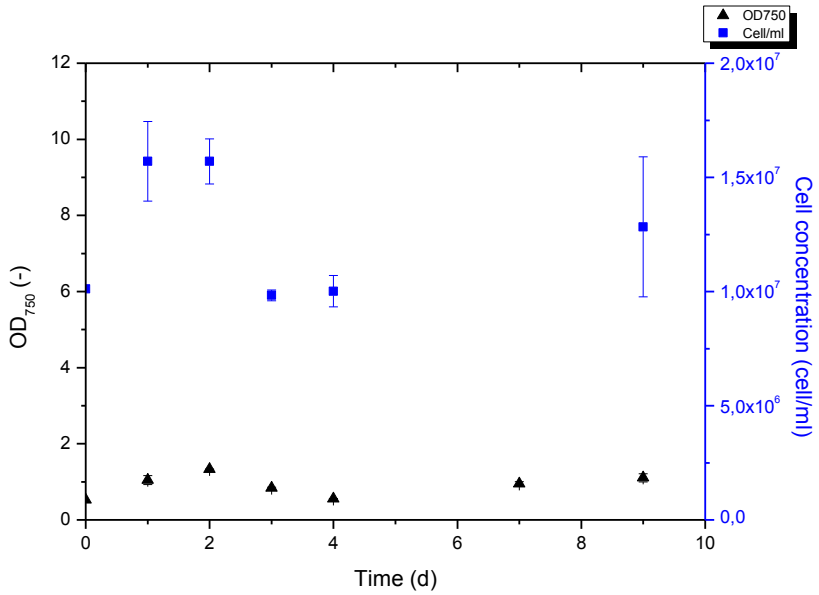

Figure 3.2 OD_{750} and cells concentration trend for *C. protothecoides* in 10-d synthetic human urine.

3.1.3 ESPERIMENT 2: 10-DILUTED URINE WITHOUT CO_2 SUPPLY

The previous batch experiment showed a discrepancy with screening experiments. Since CO_2 was not supplied in screening experiments, a batch system with 10-d synthetic human urine with only atmospheric air supply was performed, in order to assess whether the CO_2 was a limiting factor or not. Results are reported in table 3.3.

Table 3.3 OD_{750} and cells counting at 10-d urine. Values are an average from two replicas with the same set up.

Time [d]	OD_{750} [-]	St. dev. [-]	Cell. conc. [10^6 cells/ml]	St. dev. [10^6 cells/ml]
0	0.537	0.000	11.47	-
1	0.579	0.042	14.16	0.76
4	0.963	0.144	16.23	1.23
5	1.109	0.168	17.12	0.45
6	1.227	0.229	17.47	0.15
7	1.251	0.204	18.13	0.99
11	0.954	0.011	13.70	2.11
12	0.833	0.103	16.57	3.06

Also in this case, no growth was detected (Figure 3.3).

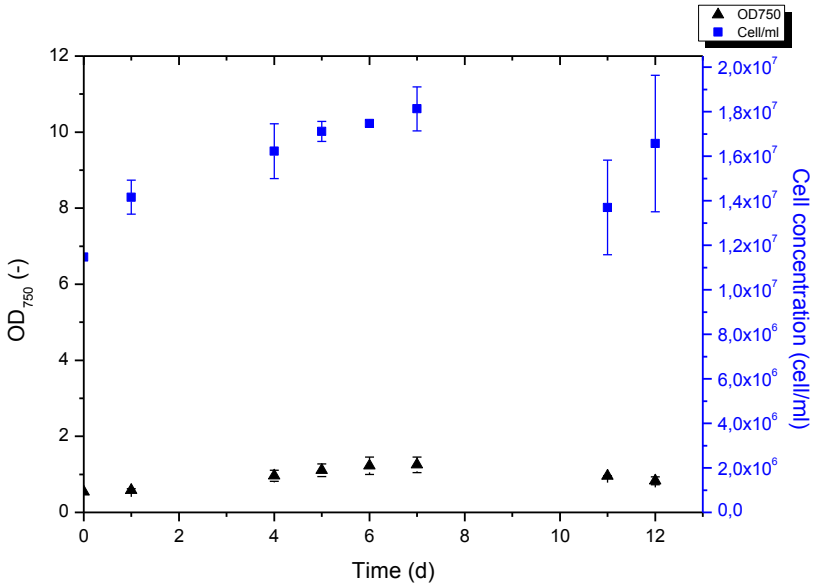

Figure 3.3 OD_{750} and cells concentration trend for *C. prototheco*ides in 10-d synthetic human urine diluted without CO_2 supply.

It was concluded that CO_2 cannot be considered as a limiting factor for the growth of *C. prototheco*ides in synthetic human urine.

3.1.4 EXPERIMENT 3: 100-DILUTED URINE

As a last attempt to grow *C. prototheco*ides in urine based medium, the nutrient concentration was further reduced, and a batch experiment with synthetic human urine 100-d with bi-distilled water was performed.

Results are summarized in table 3.4 and in figure 3.4.

Table 3.4 OD_{750} and cells concentration at 100-d urine. Values are an average from two replicas with the same set up.

Time [d]	OD_{750} [-]	St. dev. [-]	Cell. conc. [10^6 cells/ml]	St. dev. [10^6 cells/ml]
0	0.430	0.000	7.00	-
1	0.710	0.004	9.17	0.42
2	0.689	0.025	11.35	2.29
3	0.594	0.033	8.82	0.50
4	0.588	0.040	8.52	0.54

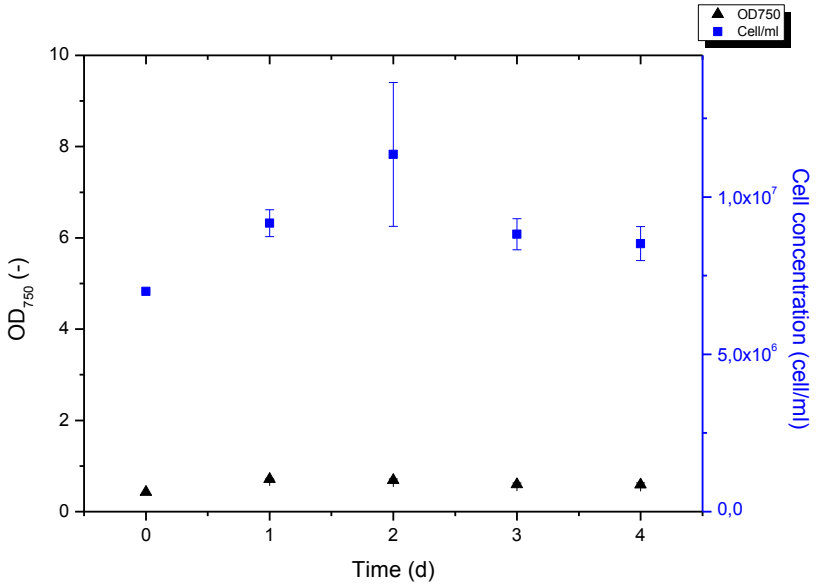

Figure 3.4 OD_{750} and cells concentration trend for *C. prototheco*ides in 100-d synthetic human urine diluted.

Even with this high dilution no growth of *C. prototheco*ides was observed. It was concluded that nutrients were not the reason for that.

The quite absolute absence of growth in experiments with 10-d and 1-d urine could be explained by the absence of micronutrients in the synthetic human urine used (for example, Mg which is fundamental for chlorophyll molecule synthesis). Growth in screening experiments (see 3.1.1) was probably possible thanks to micronutrients inoculated together with *C. prototheco*ides; in fact, for screening a different inoculum procedure was used, which did not include algae centrifugation, so a certain amount of nutrient and micronutrient was likely to be added to the system. It is noteworthy that our results disagree with similar experiments found in the literature, where other species of microalgae were successfully grown in diluted synthetic human urine (even with low growth rate constants between 0.1-0.3 d^{-1}, showing high nutrient removal capacity (C. Yang et al.,2008 and Y. Chang, 2012).

Therefore, for further analysis on *C. prototheco*ides growth, a preliminary study for assessing the correct synthetic human urine formula suitable for this microalga should be performed.

3.2 BATCH EXPERIMENT IN WASTEWATER WITHOUT MICROALGAE INOCULUM

Optical microscope analysis of primary wastewater from Camposampiero plant permitted to identify the presence of some microalgae cells inside the medium, though their concentration was very low (about 11000 cell/ml). Since wastewater was just sampled from the plant and did not contact any microalgae in the laboratory, we concluded that they were native microalgae of the wastewater.

So, a batch experiment with no microalgae inoculum was carried out with the aim to develop those native microalgae. Cells concentration was monitored each day until stationary phase was reached. Results are reported in table 3.5.

Table 3.5 Cells counting and natural logarithm for wastewater batch without inoculum.

Time [d]	Cell. conc. [10^6 cells/ml]	St. dev. [10^6 cells/ml]	Ln(cell/ml)	St. dev. ln(cell/ml)
0	0.06	0.01	10.964	0.203
7	0.34	0.03	12.724	0.098
8	1.56	0.34	14.247	0.221
9	4.40	0.78	15.289	0.178
10	14.33	4.48	16.453	0.318
14	21.17	2.59	16.864	0.123
15	25.50	1.65	17.053	0.065
16	26.83	1.18	17.105	0.044

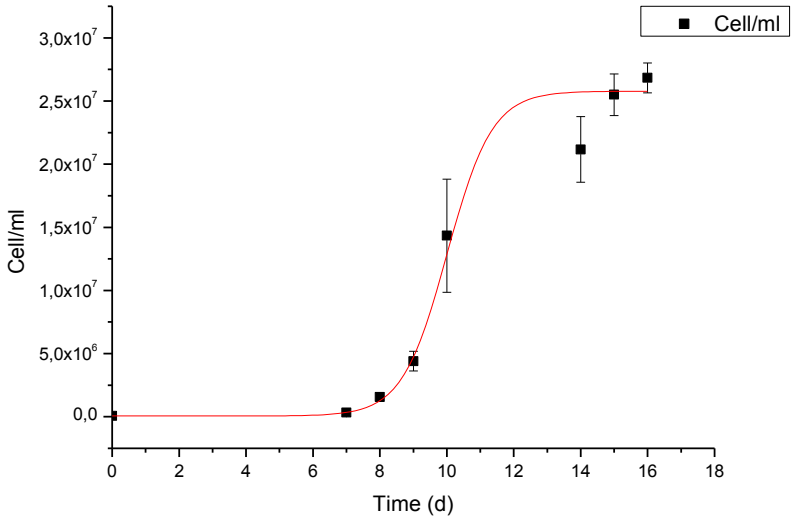

Figure 3.5 Growth curve of native wastewater microalgae consortium.

Figure 3.5 shows that native microalgae have a long lag phase, about 7 days, after which a fast exponential growth starts. Some reactor photos are reported just to show the evident changing in turbidity and color as shown in figure 3.6.

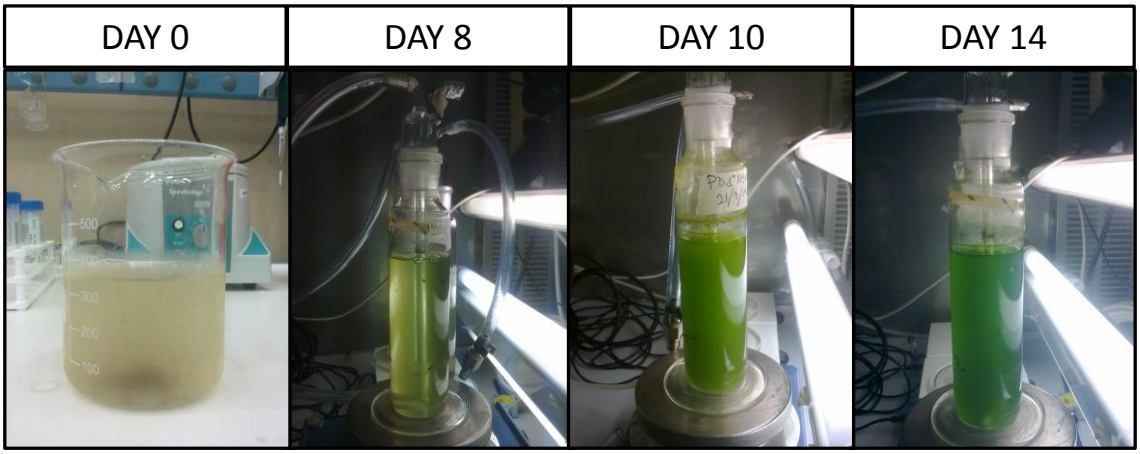

Figure 3.6 Color and turbidity variation over days in batch experiments without algae inoculum.

The kinetic growth constant can be evaluated by plotting the natural logarithm of cell concentration over time. From the slope of the straight line it was obtained $k = 1.275 \pm 0.062\ d^{-1}$ for these unknown species.

Native microalgae growth rate is slightly higher than for *C. prototheco*ides ($k_{CP,23°C}$=1.157 d^{-1}), but further experiments would be needed to draw a conclusion, as starting conditions are too different: batch experiments with *C. prototheco*ides always started with a cell concentration of about 10÷20x10^6 cells/ml.

In order to characterize this microalgae consortium, a sample from the last point of the curve was analyzed in the Biology Department of Padua University.

The sample is currently under analysis: native microalgae strains are going to be isolated and identified, but it takes longer than expected since the correct culture medium have to be found for their growing.

3.3 TEMPERATURE SCREENING BATCH EXPERIMENTS

During the year, the wastewaters in the treatment plants are characterized by a significant temperature changes, depending on geographical position and climate. Wastewater temperature is usually higher than that of the water supply thanks to the addition of feces, urine and warmer water from household appliances. Besides, water specific heat leaves wastewaters warmer than local air during cold periods and colder in warm periods (Metcalf & Eddy, 2004), so that their temperatures usually range from 10°C to 30°C (5°C can be reached at high altitude). As temperature has a strong influence on biological processes, it is important to evaluate its effects on *C. prototheco*ides growth rate and nutrients removal.

Accordingly, process design procedures should be based on the worst possible conditions.

3.3.1 TEMPERATURE RANGE SELECTION

For this study, data from Camposampiero plant were obtained in order to select the more representative temperatures for testing. Wastewater inlet temperatures at Camposampiero plant over the year are reported in figure 3.7.

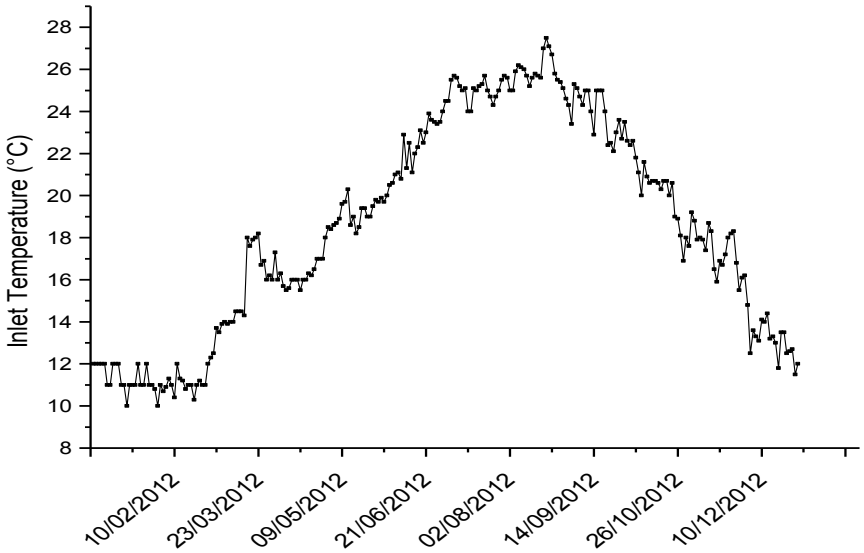

Figure 3.7 Inlet wastewater temperature at Camposampiero plant. Data from ETRA s.p.a.

As it can be seen the values range from 10 to 27°C. Therefore temperatures chosen for the experiments are 10,15,23 and 30°C.

The temperature of 23°C was selected in order to have a comparison with other experiments performed in laboratory, since this is the common temperature used. Experiments at 15°C and 23°C were carried out both under constant and night/day illumination conditions. In each run, OD_{750}, cells concentration, dry weight and nutrients concentration were monitored once a day for 10 and 15°C curves and twice a day for 23 and 30°C curves.

3.3.2 EXPERIMENTS AT CONSTANT LIGHT INTENSITY

In table 3.6 the results of experiments at 10,15,23 and 30°C in constant light conditions are summarized. They are calculated as an average of stationary phase data.

Table 3.6 Results of temperature screening batches at constant light conditions.

Temperature [°C]	Final cells concentration [10^6cell/ml]	Final dry weight [g/l]	Final cell density [pg/cell]
10	18.08±0.95	0.458±0.168	25.4±9.4
15	66.42±4.52	1.250±0.165	18.1±2.7
23	134.17±11.31	1.033±0.047	7.7±0.4
30	146.00±9.81	0.933±0.047	6.7±0.3

As a comparison, the 4 curves are reported together in figure 3.9; temperature effects are clearly visible, both in lag phase duration and in the specific growth rate.

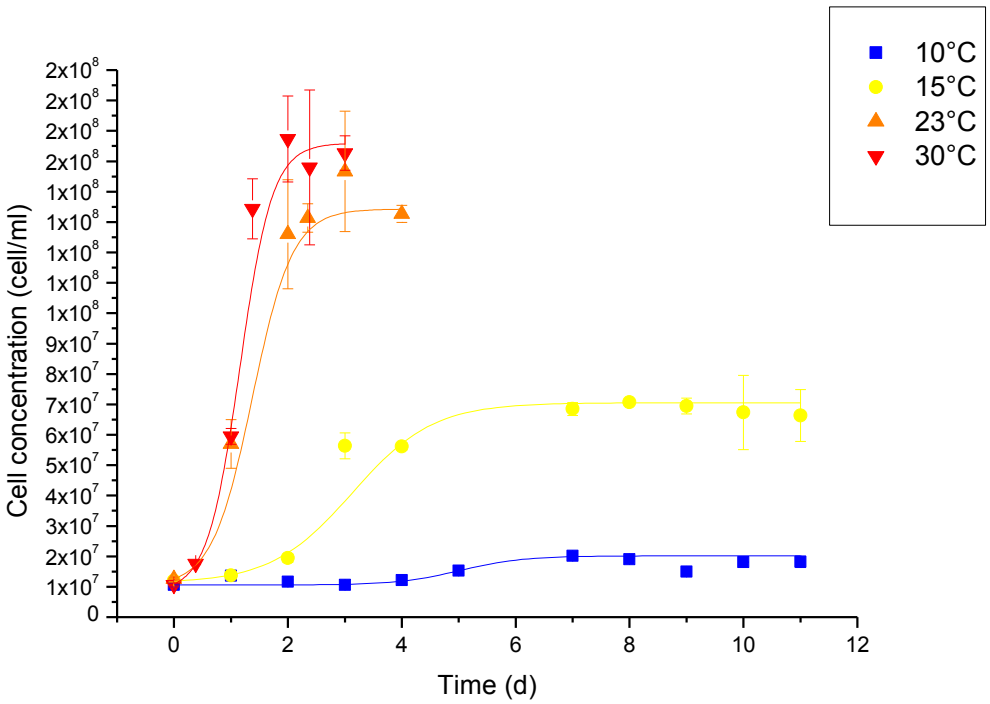

Figure 3.8 *C. protothecoides* growth curves at 10,15,23 and 30°C.

In order to evaluate *C. protothecoides* growth rates at different temperatures the natural logarithm of cell concentration was plotted against time. Results of curve fitting are reported in table 3.7. In the range between 10°C and 30°C an increase in temperature lead to a remarkable increase in *C. protothecoides* growth rate constant.

Table 3.7 Growth rate and lag phase comparison at 10,15,23 and 30°C.

Temperature [°C]	Growth rate [d^{-1}]	Lag phase [d]
10	0.161±0.006	3
15	0.692±0.204	1
23	1.345±0.238	0
30	1.911±0.143	0

Plotting kinetic growth rates against temperature a linear relationship can be found, as shown in figure 3.10.

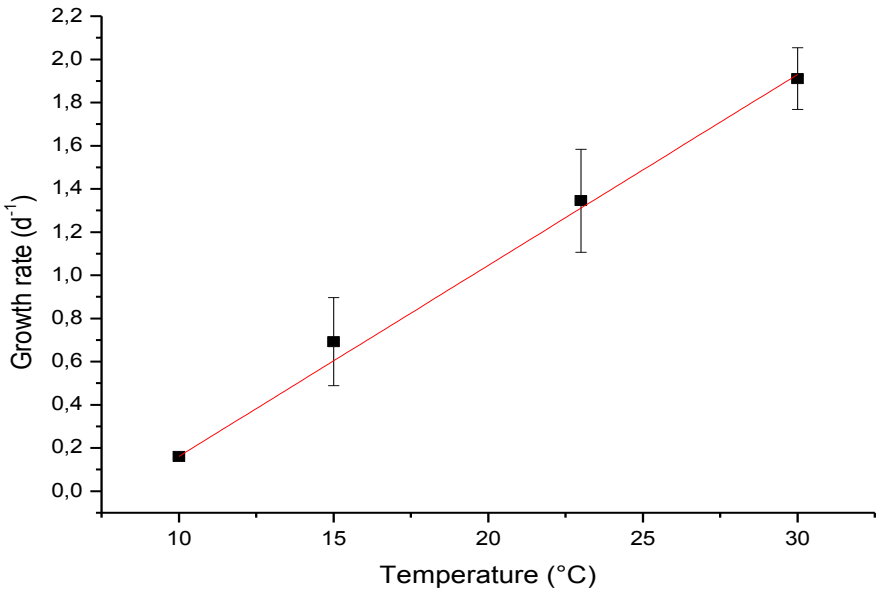

Figure 3.9 *C. protothecoides* growth rate at 10,15,23,30°C.

The correlation straight line equation is:

$$k(T) = 0.08844T - 0.7233 \qquad \text{(Eq. 3.1)}$$

where k is *C. protothecoides* growth rate [d^{-1}] at the medium temperature T [°C]

This equation can be applied only in the range 10-30°C.

It is interesting to observe the effect of temperature on the final dry weight and on the cell density, as shown in figure 3.10.

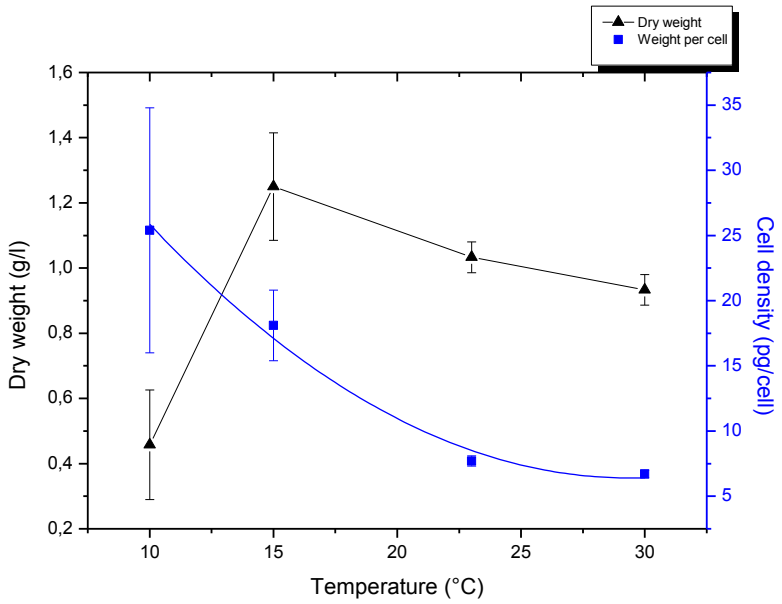

Figure 3.10 Final dry weight and cell density for *C. protothecoides* at 10,15,23 and 30°C.

For dry weight, a peak can be found at 15°C, besides it tends to slightly decrease with increasing temperature, while at 10°C its value is quite low.

Looking at the cell densities: increasing temperature leads to an exponential decrease of density, which might influence the lipid contend and the settling properties.

This behavior can be described by a nonlinear curve fitting, leading to the equation:

$$\rho = 51.097 - 3.042 * T + 0.052 * T^2 \qquad \text{(Eq. 3.2)}$$

Where ρ is the cell density [pg/cell] at temperature T [°C].

Results of cell density measurements are coherent with literature: several authors (Sharma et al. 2012; de Castro Araújo & Garcia 2005) reported a variation in cell composition at different temperatures, which lead also to a different cell density. Further experiments with lipid, proteins and carbohydrates analysis are necessary to verify this hypothesis.

Phosphates and ammonia concentration were monitored once or twice a day; the removal curves of these nutrients are reported in figures 3.11 and 3.12.

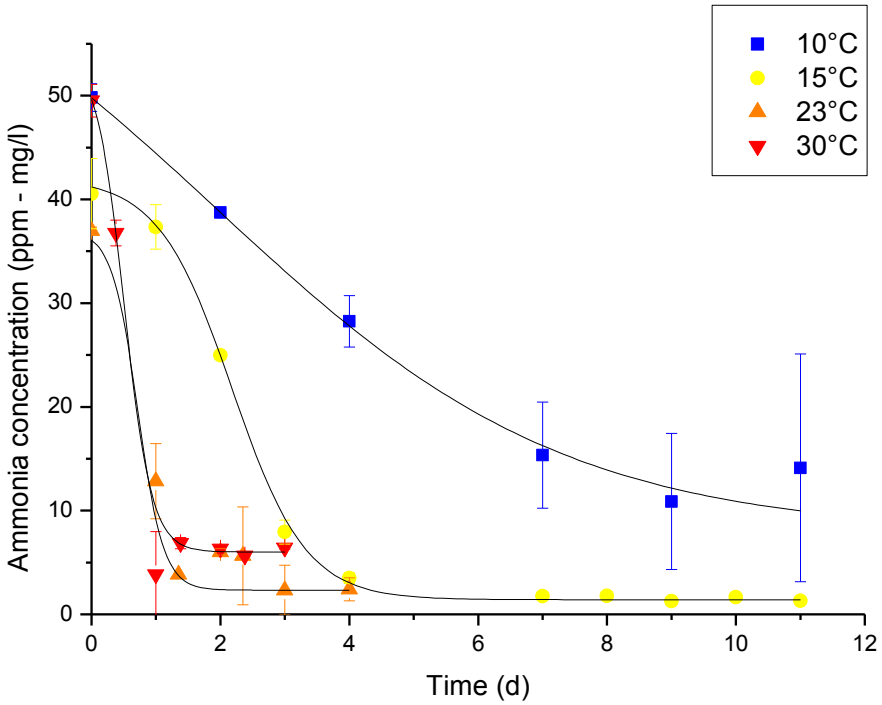

Figure 3.11 Ammonia concentration in batch cultures of *C. prototheocoides* at 10,15,23 and 30°C.

Ammonia depletion curves agree with the growth curves at the corresponding temperature. When exponential growth ends, ammonia concentrations reach values below 5 ppm, except for experiment at 10°C.

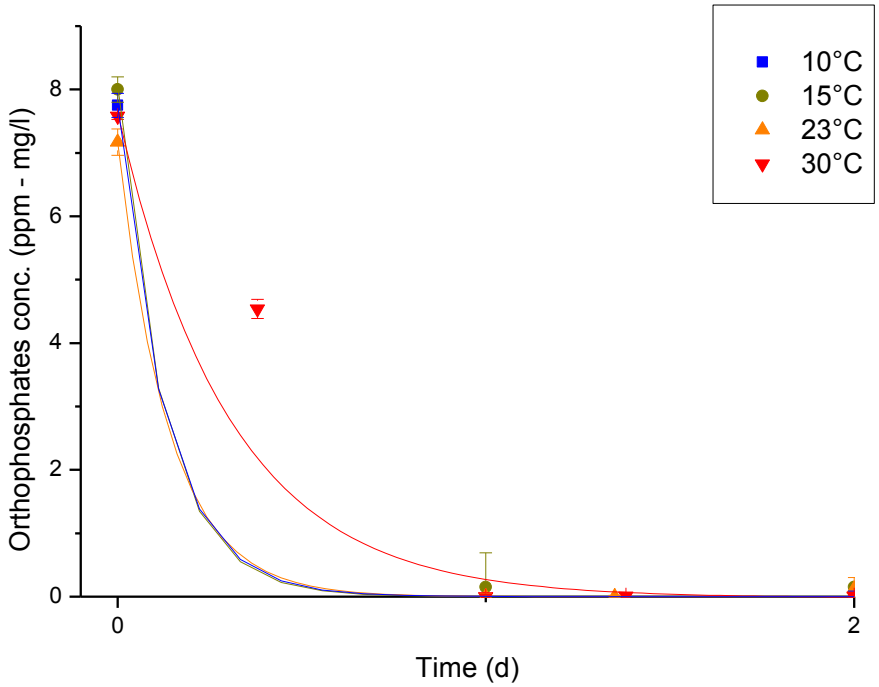

Figure 3.12 Orthophosphates concentration in batch cultures of *C. prototheocoides* at 10,15,23 and 30°C.

Concerning phosphorous, *C. prototheocoides* show a high removal rate at all the temperatures tested, always leading to very low concentration (<0.1 ppm) after one day, even if the

exponential growth starts later on. Therefore it can be supposed that *C. protothecoides* is able to adsorb and/or accumulate phosphate molecules in the cell, and build up a reservoir which can make them readily available during the exponential growth.

3.3.3 EXPERIMENTS AT DAY/NIGHT LIGHT CONDITIONS

At 15°C and 23°C experiments were carried out also under day/night light cycles, in order to simulate *C. protothecoides* growth behavior with real sunlight conditions.

The ones of October in Padua were tested.

OD_{750}, cell concentration, dry weight and nutrients concentration were monitored twice a day: samples were collected at the end of both the dark and light period in order to give information on *C. protothecoides* behavior during both night and day.

As a comparison, the two curves are reported in figure 3.13 together with growth curves at 15 and 23°C with constant illumination:

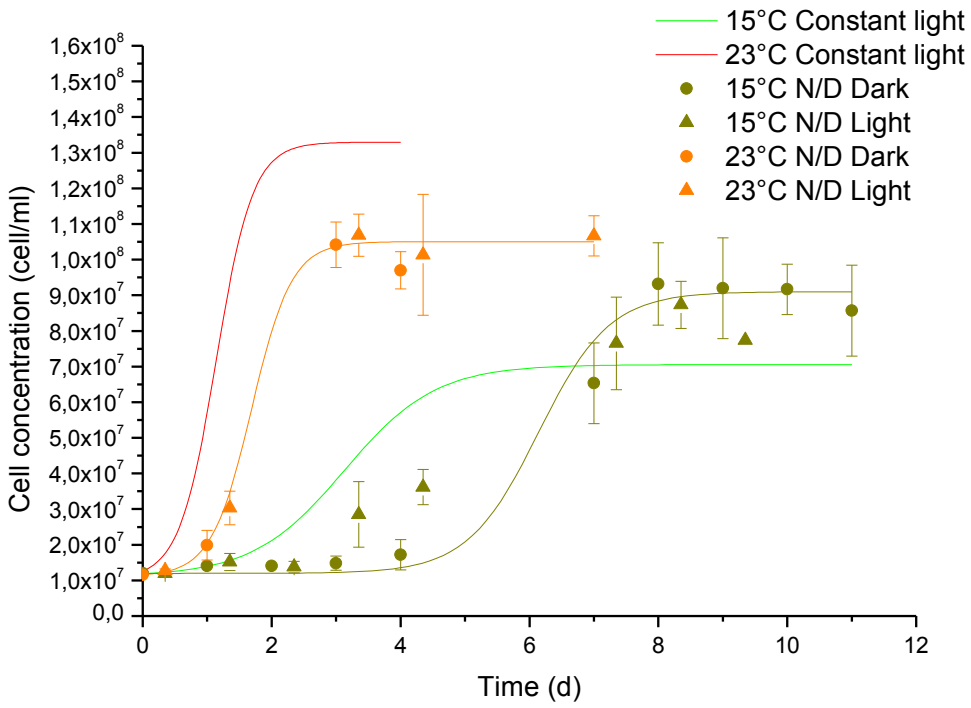

Figure 3.13 *C. protothecoides* growth curves at 10,15,23 and 30°C.

From figure 3.13, a longer lag phase can be noticed for both experiments (3 days at 15°C and) one day at 23°C.

Besides, the final cell concentration is lower at 23°C and higher at 15°C, respect to the respective values found at constant illumination (see 3.3.2) and the cell concentration is different in the

light and dark periods: in dark period a higher cell concentration is registered against light period, as shown in figure 3.13.

Results of the growth rate constant for these experiments are calculated and reported in table 3.8.

Table 3.8 Growth rate and lag phase comparison at 15 and 23°C.

Temperature [°C]	Light conditions	Growth rate [d^{-1}]	Lag phase [d]
15	Day/night	0.426±0.022	4
15	Constant	0.692±0.204	1
23	Day/night	0.789±0.046	1
23	Constant	1.345±0.238	0

A decrease of *C. protothecoides* growth rate with respect to constant light can be noticed from table 3.8 both at 15 (-38%) and 23°C (-41%), while there is an increasing in both lag phases.

Final dry weight and cell densities measurements are reported below (Table 3.9).

Table 3.9 Dry weight and cell density for 15 and 23°C at day/night light conditions.

Temperature	Light period		Dark period		Average	
	Dry weight	Cell density	Dry weight	Cell density	Dry weight	Cell density
[°C]	[g/l]	[pg/cell]	[g/l]	[pg/cell]	[g/l]	[pg/cell]
15	0.694±0.024	8.23±0.56	0.800±0.031	9.05±0.81	0.759±0.029	8.72±0.71
23	1.000±0.008	9.74±1.88	1.192±0.035	11.91±0.54	1.096±0.077	10.83±1.21

From table 3.9, a difference in both dry weight and cell density is evidenced; after light period there is a lower dry weight and cell density in both experiments. Besides, average values of cell density show a high difference between constant illumination and day/night light cycles. In the following figure (Figure 3.14), a comparison between day/night and constant light illumination results is reported.

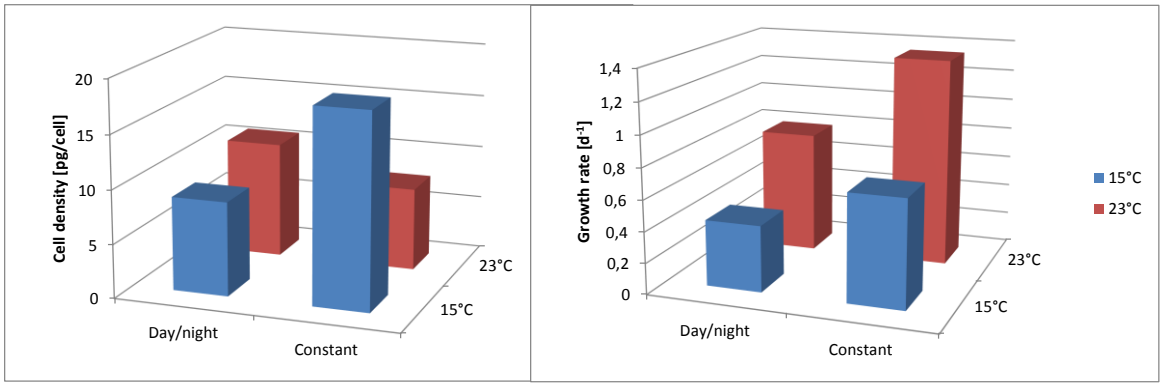

Figure 3.14 Growth rate and cell density comparison at 15 and 23°C for day/night and constant light conditions.

Ammonia and phosphates concentration during the growth are plotted in figure 3.15 and 3.16.

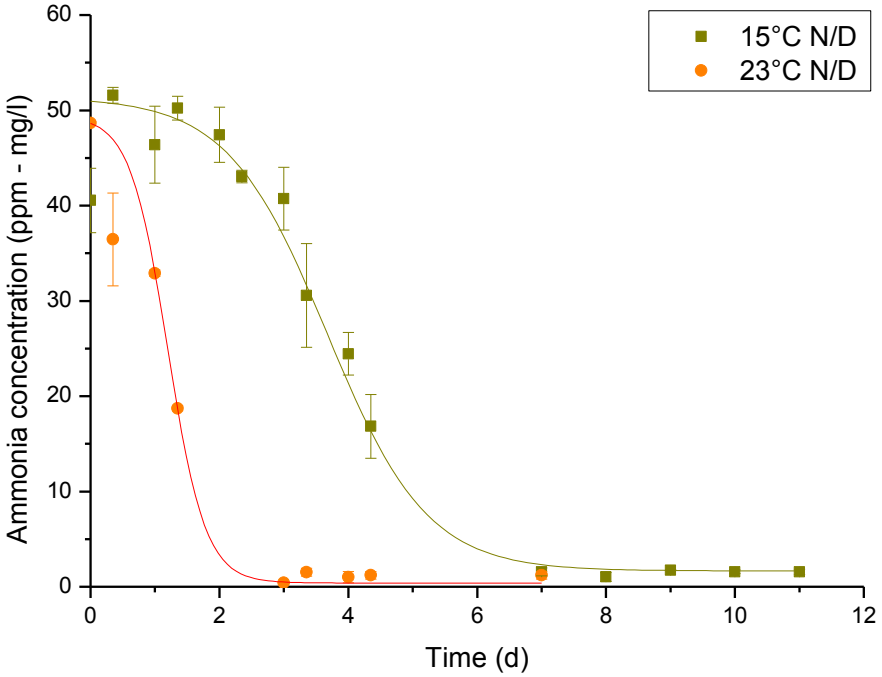

Figure 3.15 Ammonia concentration in batch cultures of *C. protothecoides* at 15 and 23°C at day/night light conditions.

Also in day/night cycles, as for experiments at constant illumination, ammonia depletion curves agree with the growth curves at the corresponding temperature. When exponential growth ends, ammonia concentrations reach values below 5 ppm.

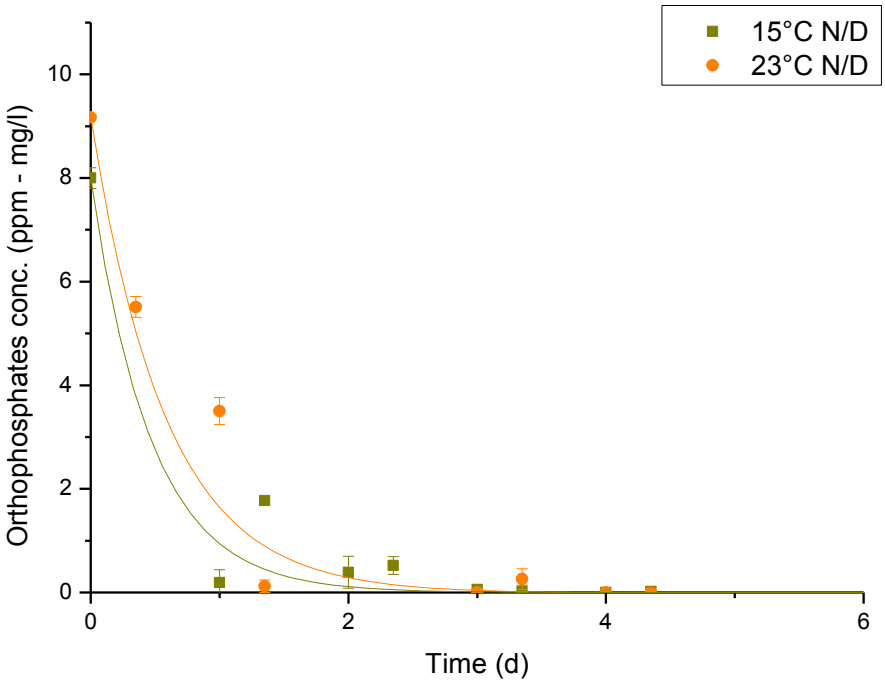

Figure 3.16 Orthophosphates concentration in batch cultures of *C. protothecoides* at 15 and 23°C at day/night light conditions.

Concerning phosphorous removal, in experiments at day/night cycles, the removal rate is lower respect to experiments at corresponding temperatures in constant illumination; however, also in these cases, phosphorous concentration reaches very low values (<0.1 ppm) before the end of the exponential growth phase, confirming that also at these illumination condition microalgae seems to be able to adsorb and/or accumulate orthophosphates molecules.

3.4 CONTINUOUS FLOW EXPERIMENTS

A set of continuous flow experiments was carried out in order to test *C. protothecoides* behavior in these more realistic conditions: moreover once steady-state operation is reached, all the variable values will be constant, thus allowing all growth under constant conditions. The reactor is started in batch mode and valves are opened only after a high cell concentration is achieved, thus to avoid the occurring of wash out. Continuous flow experiments were carried out both at constant (100 μE/(m^2*s)) and day/night (October) light conditions.

3.4.1 CONSTANT LIGHT CONDITIONS

Continuous experiments at constant light conditions were carried out in order to verify biomass concentration and biomass productivity dependence on resident time, as suggested in other studies (Ruiz et al., 2012). Also the nutrients removal capacity was tested; nitrates and nitrites were not monitored since they were not present in the wastewater fed to the reactor.
Reactor residence times used in these experiments were:

1. 0.79 d
2. 0.64 d

Our results will be compared with data obtained by Morandini (2012).

3.4.1.1 Experiment 1: τ=0.79d

In this first experiment, filtered wastewater was used in order to avoid tube clogging. Peristaltic pump flowrate was set to 312.5 ml/d, thus resulting in a residence time (τ) of 0.79 d. Experiment started in batch mode at higher light intensity (150 μE/(m^2*s)). At day 3, at a cell concentration of 125E+06 cell/ml, it was switched to continuous mode and at day 6 light intensity was reduced to 100 μE/(m^2*s), thus to reproduce the same environmental conditions maintained in

experiments carried out by Morandini (2012). OD_{750}, cell concentration, dry weight and nutrient concentration were monitored daily.

Cells concentration values are reported in figure 3.17. The steady-state condition was achieved in few days with an average value of 103E+06 cell/ml.

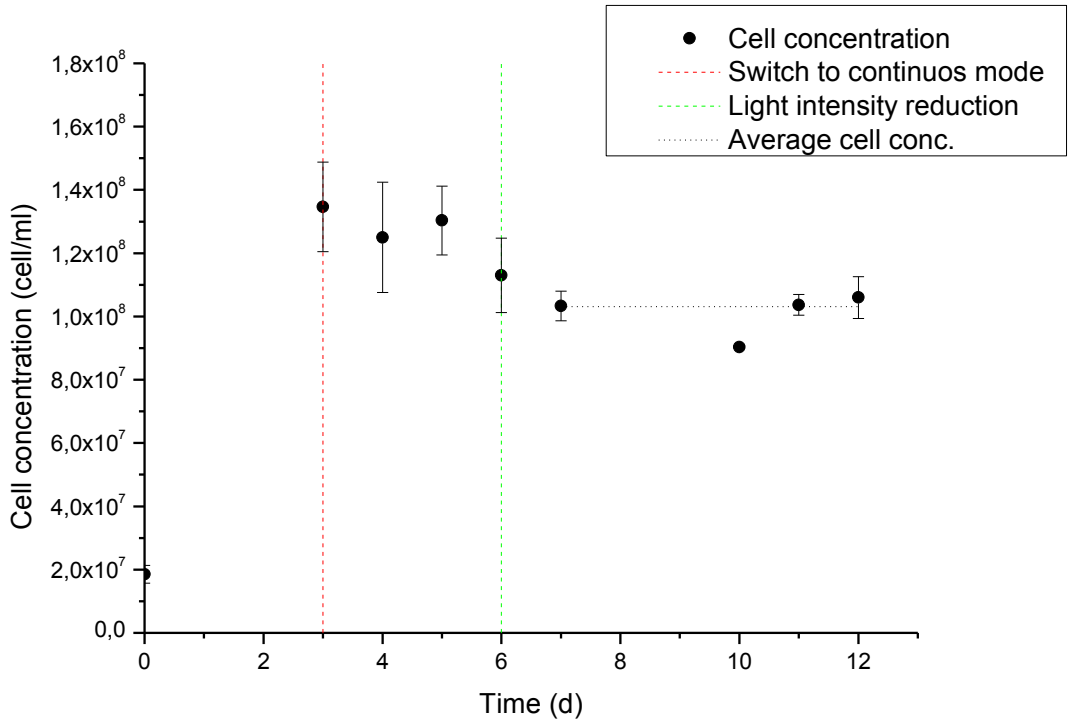

Figure 3.17 Cell concentration of *C. prototheco*ides at continuous experiment 1.

For biomass concentration, a value of 0.468 g/l was found, calculated as an average of daily measures at steady-state operation. From this value, biomass productivity can be calculated through this formula:

$$P = \frac{X}{\tau} \qquad \text{(Eq. 3.3)}$$

where

- P is biomass productivity [g/(l*d)
- X is biomass concentration [g/l]
- τ is the residence time [d]

Biomass productivity at 0.79 d of residence time was 0.596 g/(l*d).

Concerning nutrient removal, inlet ammonia total inorganic nitrogen (N_{in}) and total phosphorous (P_{in}) were respectively 41.01 ppm and 5.32 ppm. Outlet average measured concentration were 0.94 ppm for nitrogen (N_{out}) and 0.91 ppm for phosphorous (P_{out}) resulting in a removal percentage of 97.70% and 82.85% respectively. Results of nutrients analysis for steady state conditions are shown in figure 3.18.

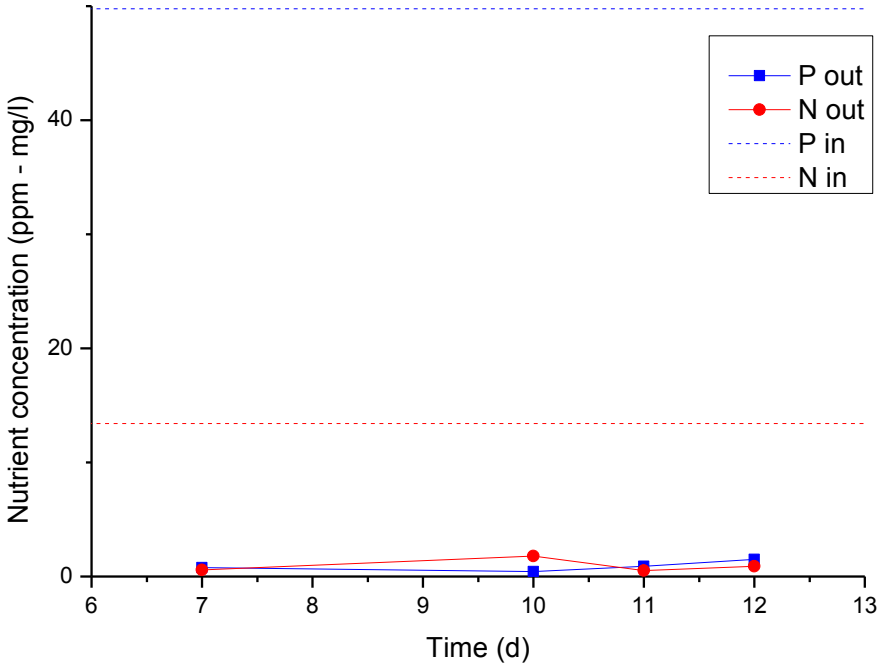

Figure 3.18 Inlet and outlet nutrient concentration at continuous experiment 1.

Values of operating variables and results are summarized in table 3.10.

Table 3.10 Experiment 1 running parameters and results.

Data	Value	Unit
Inlet flow	312.5	ml/d
Residence time	0.79	d
Inner biomass concentration	0.468	g/l
Cells concentration	103E+06	cell/ml
Biomass productivity	0.596	g/(l*d)
Total inorganic Nin	41.01	mg/l
Total Pin	5.32	mg/l
Nin/Pin	7.71	-
Total inorganic Nout	0.94	mg/l
Total Pout	0.91	mg/l
Total inorganic N removal	97.70	%
Total P removal	82.85	%
ΔN/ΔP	9.09	-

3.4.1.2 Experiment 2: τ=0.64d

The second experiment started from the previous one without interrupting the reactor operation and restarting from a batch mode.

Residence time was decreased to 0.64d, by changing the pump flowrate to 390 ml/d. Steady state conditions were reached one day after this stepchange, reaching an average cell concentration of 81E+06 cells/ml (Figure 3.19).

Biomass concentration was found 0.307 g/l, resulting in a biomass productivity of 0.478 g/(l*d).

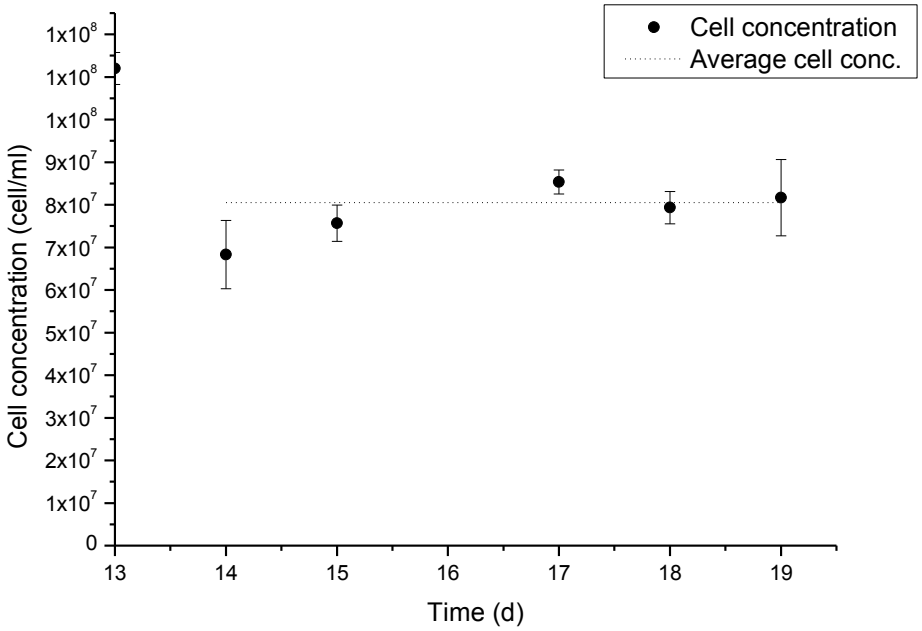

Figure 3.19 Cell concentration of *C. prototheco*ides at continuous experiment 2.

Concerning nutrient removal, inlet ammonia total inorganic nitrogen (N_{in}) and total phosphorous (P_{in}) were respectively 41.01 ppm and 5.32 ppm. Outlet average measured concentration were 11.50 ppm for nitrogen (N_{out}) and 0.76 ppm for phosphorous (P_{out}) resulting in a removal percentage respectively of 97.70% and 82.85% respectively. Results of nutrients analysis for steady state conditions are reported in figure 3.20.

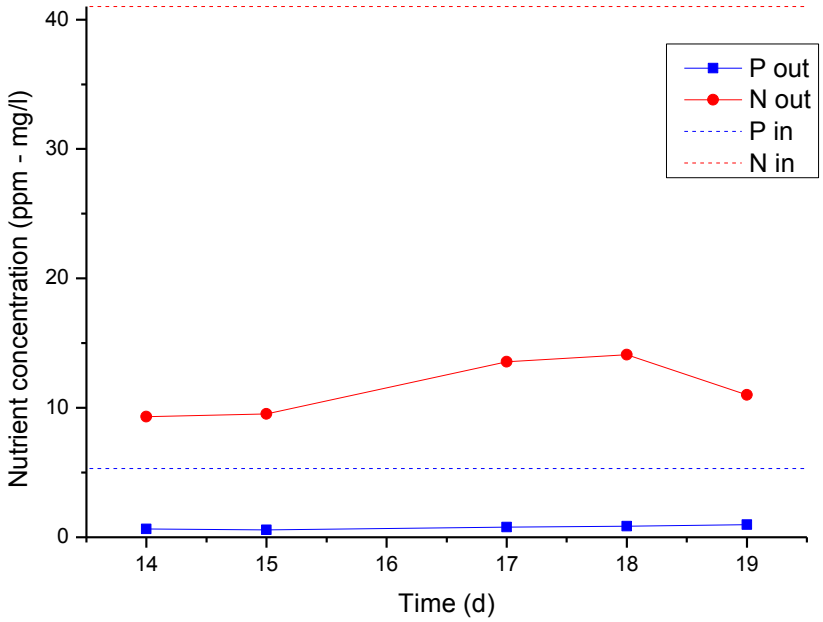

Figure 3.20 Inlet and outlet nutrient concentration at continuous experiment 2.

Values of operating variables and results are summarized in table 3.11.

Table 3.11 Experiment 2 running parameters and results.

Data	Value	Unit
Inlet flow	390	ml/d
Residence time	0.64	d
Inner biomass concentration	0.307	g/l
Cells concentration	81E+06	cell/ml
Biomass productivity	0.478	g/(l*d)
Total inorganic Nin	41.01	mg/l
Total Pin	5.32	mg/l
Nin/Pin	7.71	-
Total inorganic Nout	11.50	mg/l
Total Pout	0.76	mg/l
Total inorganic N removal	71.96	%
Total P removal	85.66	%
ΔN/ΔP	6.74	-

3.4.1.3 Continuous experiments discussion

The data obtained in experiments 1 and 2 can be compared with results of similar experiments performed by Morandini (2012) at different residence times, with the same wastewater type and light intensity. In table 3.12 results of Morandini's experiments are summarized.

Table 3.12 Morandini (2012) experiments' running parameters and results.

Data	Value			Unit
Inlet flow	247,09	198	126,83	ml/d
Residence time	1.01	1.263	1.97	d
Inner biomass concentration	0.54	0.64	0.80	g/l
Cells concentration	66.9E+06	124E+06	117E+06	cell/ml
Biomass productivity	0.53	0.51	0.41	g/(l*d)
Total inorganic Nin	54.81	54.81	54.81	mg/l
Total Pin	3.08	3.08	3.08	mg/l
Nin/Pin	1.78	1.78	1.78	-
Total inorganic Nout	8.44	10.78	11.03	mg/l
Total Pout	0.68	0.26	0.26	mg/l
Total inorganic N removal	84.59	80.33	79.87	%
Total P removal	77.85	91.62	91.62	%
ΔN/ΔP	19.35	15.61	15.53	-

Biomass concentration and productivity are now compared with results of experiments 1 and 2, in order to evaluate the effect of residence time.

Biomass concentration

In table 3.13 data of biomass concentration at different residence time are reported.

Table 3.13 Biomass concentration at different residence time.

Residence time (τ) [d]	Biomass concentration [g/l]	Reference
0.64	0.307	-
0.79	0.468	-
1.01	0.54	Morandini (2012)
1.26	0.64	Morandini (2012)
1.97	0.80	Morandini (2012)

Plotting these results (Figure 3.21) it can be observed that biomass concentration increases with increasing residence time.

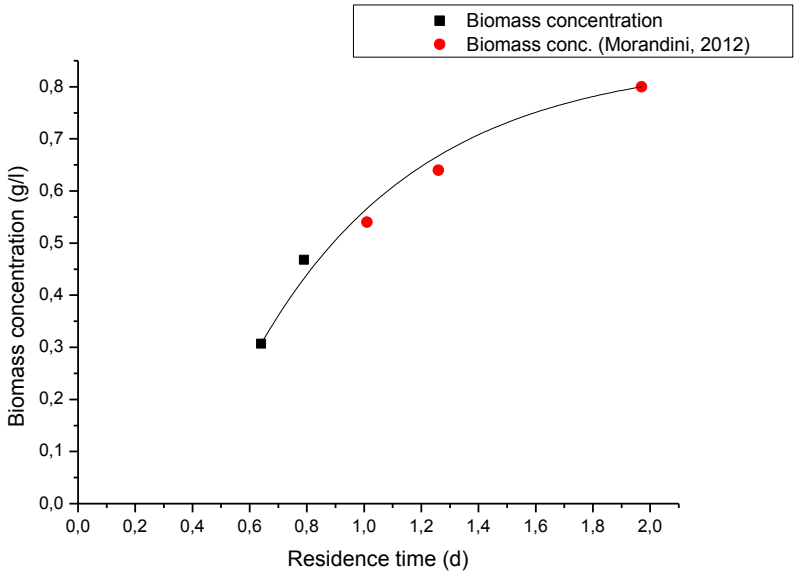

Figure 3.21 Biomass concentration at different residence time.

The points reported in figure 3.21 are fitted with a non-linear curve, whose equation is

$$C_x = -0.166 * e^{-\tau/0.577} + 0.855 \qquad \text{(Eq. 3.4)}$$

where C_x is the biomass concentration [g/l] at residence time τ [d].

Biomass Productivity

In the table 3.14 data of biomass productivity, calculated with eq. 3.3, are reported.

Table 3.14 Biomass productivity at different residence time.

Residence time (τ) [d]	Biomass productivity [g/(l*d)]	Reference
0.64	0.478	-
0.79	0.596	-
1.01	0.53	Morandini (2012)
1.26	0.51	Morandini (2012)
1.97	0.41	Morandini (2012)

A plot of these data (Figure 3.22) suggests that biomass productivity has a peak around a residence time of 0.79 d. This trend confirms literature results (Ruiz et al., 2012).

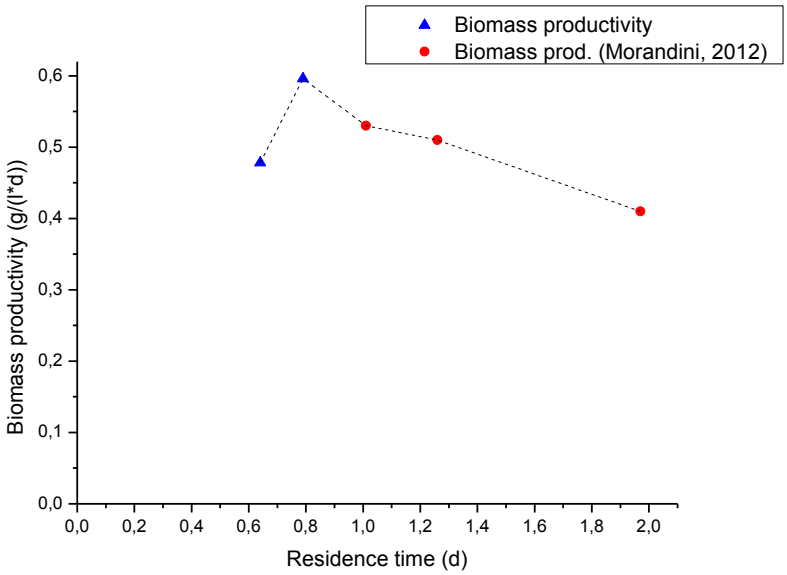

Figure 3.22 Biomass productivity at different residence time.

3.4.2 DAY/NIGHT LIGHT CONDITIONS

Day/night light conditions were tested in order to investigate *C. protothecoides* behavior in a more realistic environment. Sunlight cycle for October in Padua was simulated. OD_{750}, cell concentration, dry weight and nutrient concentration were monitored once a day. Samples were collected at 7:30, respect to the simulated day/night cycle.

3.4.2.1 Filtered wastewater

In this experiment wastewater was previously filtered with laboratory paper in order to avoid tubes clogging. A flowrate of 128 ml/d was set, thus leading to a residence time (τ) of 1.98d. The reactor started in batch mode and valves were opened after 6 days when a cell concentration of 110E+06 cells/ml was reached. Stationary phase was observed after 5 days and maintained for further 20 days without problems. In figure 3.23 the data collected are shown, in terms of both cell and mass concentration.

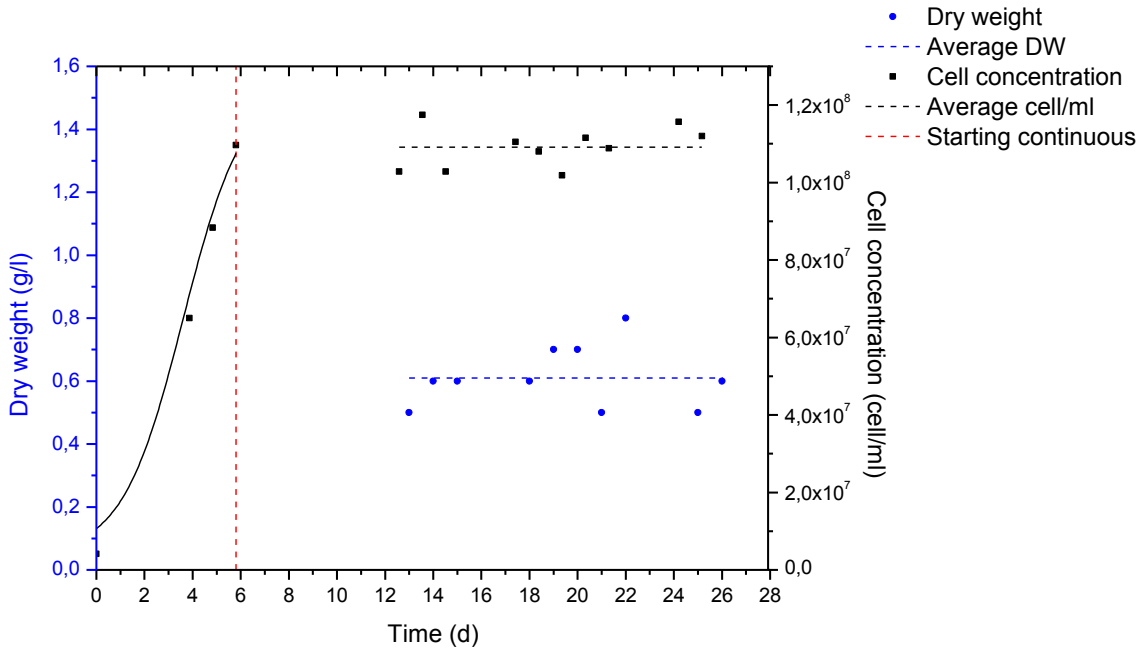

Figure 3.23 Cell concentration and dry weight for *C. protothecoides* in day/night light conditions at τ=1.98d.

Starting from an average outlet concentration of 0.6 g/l the biomass productivity calculated with eq. 3.3 was 0.300 g/(l*d).

In table 3.15 results of day/night experiments are compared to those at constant light for the same residence time (Morandini 2012).

Table 3.15 Comparison between different light conditions.

Light conditions	Biomass Productivity [g/l*d]	Daily total radiation [MJ/d]	Reference
Day/night	0.300	0.112	-
Constant	0.410	0.040	Morandini (2012)

From table 3.15 it can be concluded that biomass productivity in day/night cycles is lower by almost 25% than under constant light conditions, even if the total daily irradiation is higher (more than double). This results can be due to a higher microalgae activity in constant light conditions or to the respiration penalty in the dark; however, as this data refers to samples collected after the dark period, we decided to perform further investigation by additional experiments (Cap. 3.4.2.2).

In order to investigate *C. protothecoides* nutrient and COD removal capacities Nitrates, Ammonia, Phosphates and COD concentration were analyzed daily.

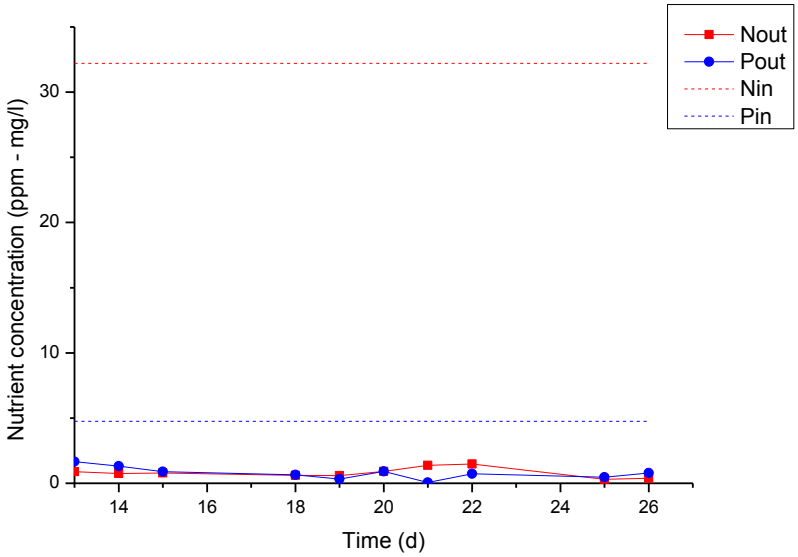

Figure 3.24 Nutrient outlet and inlet concentration in stationary phase in day/night light conditions with τ=1.98d.

Regarding nitrates, they were not detected in the outflow; since they are not present also in inlet wastewater, it can be concluded that there is no net nitrate production by the microalgae+bacteria consortium inside the reactor. Total inorganic nitrogen (N_{out}) reaches an average outflow value of 0.81 ppm, from a starting concentration of 32.21 ppm, with a 97% reduction; total phosphorous (P_{out}) outflow average concentration is 0.78 ppm, starting from 4.76 ppm, with a reduction of 86%. In table 3.16, outflow nutrient concentrations are compared with law limits for urban wastewater. For nitrogen comparison, it was supposed that with 2 days of residence time all organic nitrogen is hydrolyzed to ammonia and nitrates concentration is negligible, so TKN is equal to total inorganic nitrogen.

Table 3.16 Comparison between outlet nutrient concentration and Italian law limits from d. lgs. 152/06.

	Outlet concentration [ppm]	Law limit [ppm]	% abatement
TKN	0.81 mgN/l	15 mgN/l	97
TP	0.78 mgP/l	2 mgP/l	86

Soluble COD was analyzed daily in order to evaluate if microalgae/bacteria consortium can reduce its value in this conditions; results are reported in figure 3.25.

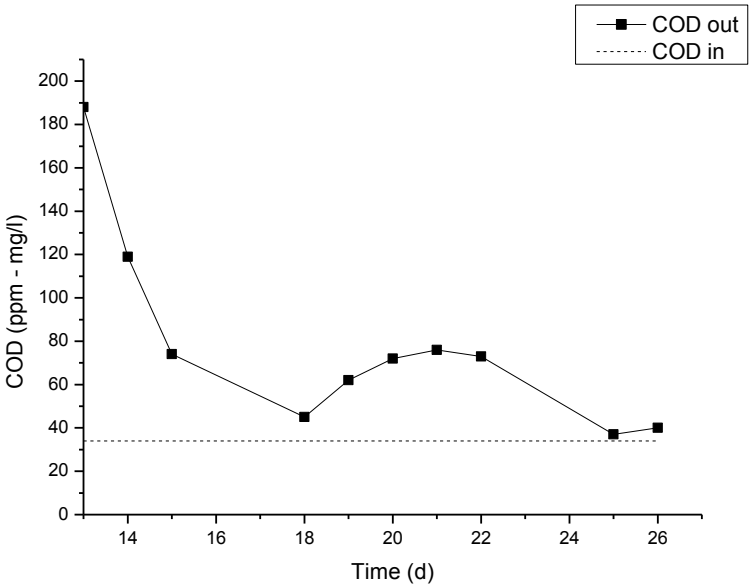

Figure 3.25 COD inlet and outlet concentration in stationary phase in day/night light conditions at with τ=1.98d.

From figure 3.25 it is clear that COD is not reduced by microalgae treatment, indeed a higher concentration respect to the inlet was detected. COD concentration is much higher immediately after the ending of the bathe phase and tends to decrease once steady state in reached, even if the average value is higher than the inlet concentration. The COD values at the beginning of continuous operations can be due to an accumulation of dead cell components during the batch phase, which are eluted at steady state.

The final average value higher that the inlet one can be explained with the hydrolysis of suspended COD in the reactor. In fact the COD kit used for this experiment can detect only soluble COD.

Bacteria concentration was monitored, showing a decrease after the end of the batch phase. In previous experiments (Milani 2013) a bacteria grow rate of 0,6-0,7d^{-1} was observed; this can explain why there is a decreasing in bacteria concentration during the stationary phase; in fact, the dilution rate imposed in the reactor is 0,5 d^{-1}, a value similar to bacteria growth rate, therefore bacteria tend to be eluted from the reactor. Besides, bacteria growth rate is influenced by CO_2 concentration. In figure 3.26 results of bacteria monitoring is plotted together with cell concentration; the batch phase ends at day 6.

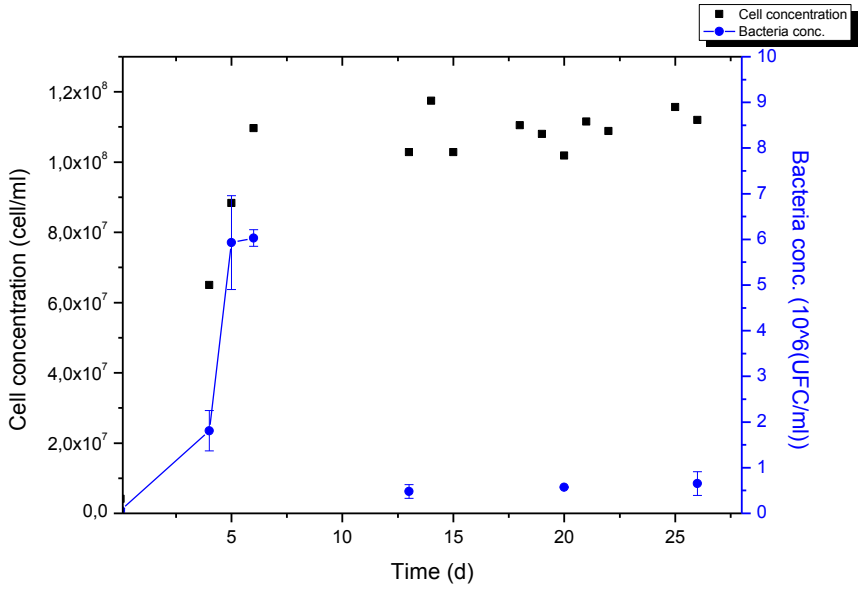

Figure 3.26 Microalgae and bacteria concentration from batch to stationary phase in day/night light conditions at with τ=1.98d.

In table 3.17, main operating variables and results of this experiment are summarized.

Table 3.17 Running parameters and results for continuous flow experiment at τ=1.97d in day/night light cycle.

Data	Value	Unit
Inlet flow	128	ml/d
Residence time	1.98	d
Inner biomass concentration	0.600	g/l
Cells concentration	110E+06	cell/ml
Biomass productivity	0.300	g/(l*d)
Total inorganic Nin	32.21	mg/l
Total Pin	4.76	mg/l
Nin/Pin	6.77	-
Total inorganic Nout	0.81	mg/l
Total Pout	0.78	mg/l
Total inorganic N removal	71.96	%
Total P removal	85.66	%
ΔN/ΔP	7.89	-

3.4.2.2 Unfiltered wastewater

In order to test more realistic inlet wastewater conditions, a continuous flow experiment with unfiltered wastewater was carried out. Wastewater flowrate was set to 133 ml/d, resulting in a residence time (τ) of 1.88 d.

OD_{750}, cells concentration, dry weight and CFU/ml were monitored twice a day, at 7:30 and 16:30 respect to the simulated day/night cycle (see figure 2.10). Experiment started from the steady-state of the previous one, so there is no initial batch phase. Steady-state conditions were reached after 5 days from the change.

Results of cells concentration and dry weight are reported in figure 3.27.

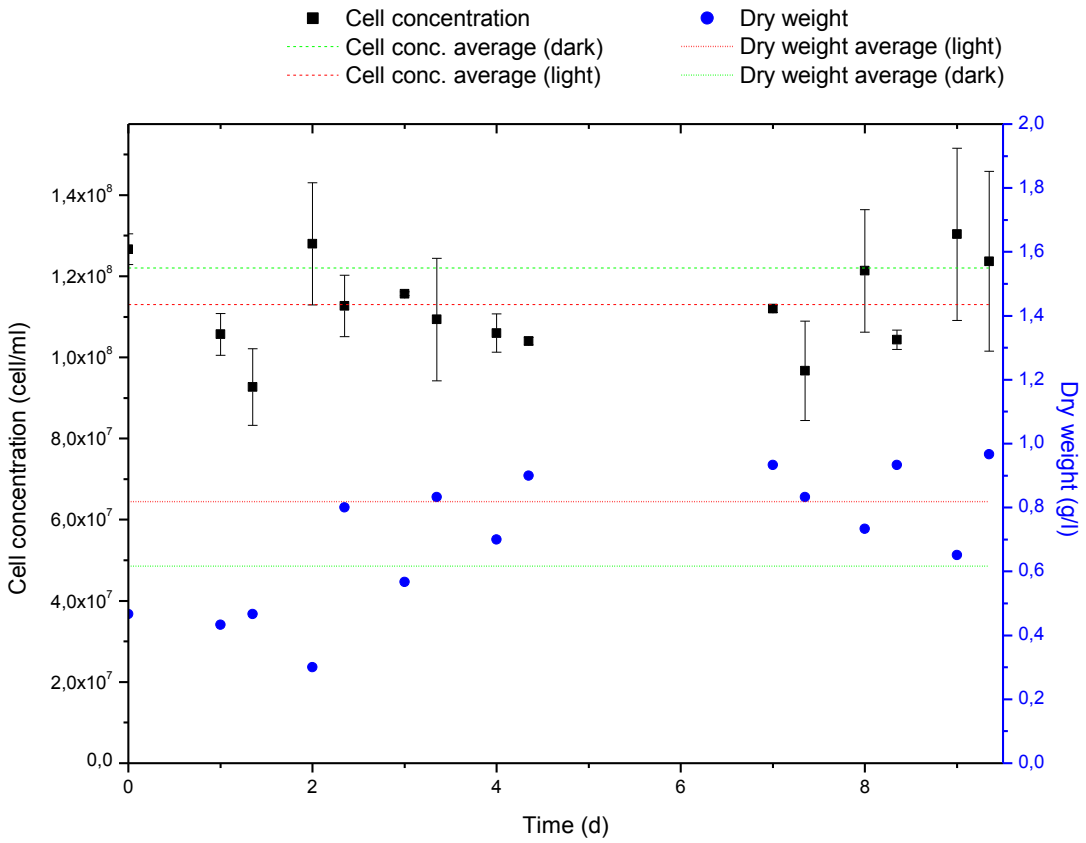

Figure 3.27 Cell concentration and dry weight in stationary phase in day/night light conditions with τ=1.88d.

From figure 3.27, there is a clear effect of dark and light period on both cell concentration and dry weight; right after the dark a lower dry weight is measured (-33%), which leads to a lower productivity. Average data of cell concentration and dry weight for light and dark period are summarized in table 3.18.

Table 3.18 Cell concentration, dry weight and biomass productivity comparison between dark and light period.

	Cell concentration [cell/mL]	Dry weight [g/l]	Productivity [g/l*d]
Dark period	117E+06	0.617	0.328
Light period	106E+06	0.819	0.436
Difference % (respect to dark period)	-9.24	32,8	32.8

Dry weight difference between light and dark periods is coherent with results of other studies (Ogbonna et al., 1996) for the microalgae species *Chlorella pyrenoidosa*, now called *C. protothecoides* (Zeng et al., 2009).

Besides, biomass productivity over light period result higher than productivity at the same residence time in constant light conditions (Morandini 2012).

Bacteria concentration was monitored in order to evaluate if there is a difference between dark and light period; results are plotted in figure 3.28.

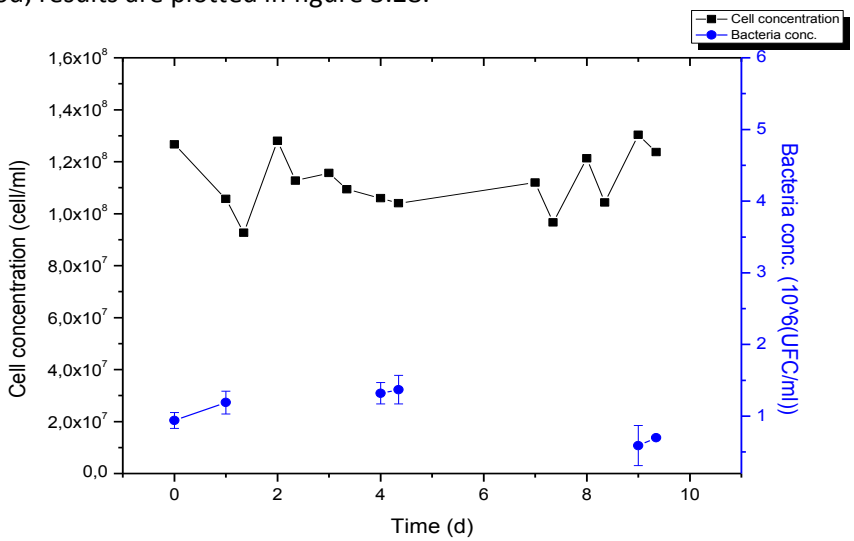

Figure 3.28 Microalgae and bacteria concentration in stationary phase in day/night light conditions with τ=1.88d.

From figure 3.28, it can be seen that also in this case bacteria concentration is quite low, and that there is a little difference after dark and light period, which is within the standard deviation range, so it cannot be concluded that bacteria concentration in influenced by day/night cycles.

3.4.2.3 Continuous flow experiment without CO_2 supply

Inhibition effect of CO_2 for bacterial growth was tested in this experiment, which started from experiment reported in paragraph 3.4.2.2. The CO_2 supply line was closed and all other parameters were kept unchanged. Microalgae and bacteria concentration were monitored twice a day. Results are plotted in figure 3.29.

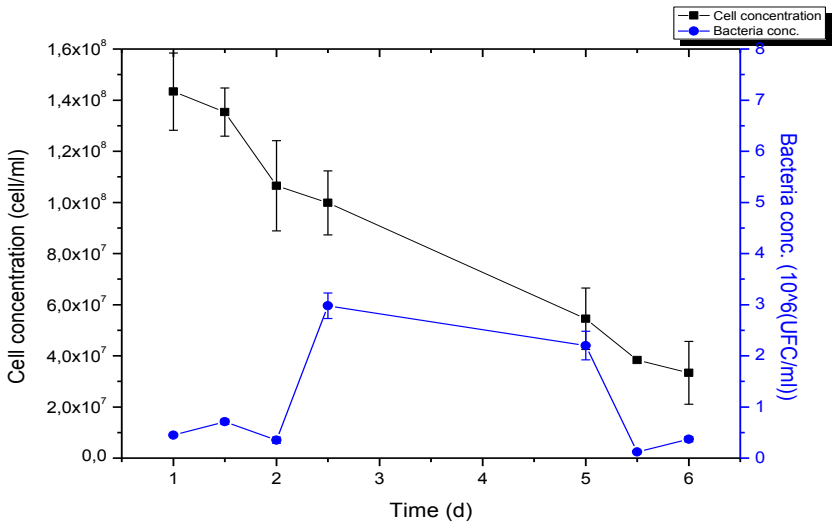

Figure 3.29 Microalgae and bacteria concentration in day/night light conditions with τ=1.88d, without CO_2 supply.

After CO_2 supply line closing a decreasing in microalgae concentration is observed as expected, while bacteria concentration remained constant; average bacteria concentration (1.02E+06 UFC/ml) is coherent with the average value (1.02E+06 UFC/ml) found in the previous experiment. Since there is no increasing, it can be concluded that CO_2 is not the limiting factor for bacterial growth under the operating conditions used.

4 PROCESS SCHEME PROPOSAL

In this chapter, a combined process with microalgae and conventional activated sludge is proposed, discussing three different configurations. In all cases, the microalgae reactor will remove nutrients, while activated sludge will reduce the organic matter of the wastewater. All processes will be designed in order to achieve an outlet pollutants concentration under the imposed law limits (see 1.1.1).

Our experimental results (see 3.4.2) showed that microalgae cannot deplete COD in their operating conditions, so it will be assumed that the COD concentration is not modified in the microalgal reactor.

4.1 OPTION 1: PRE-MICROALGAL REACTOR

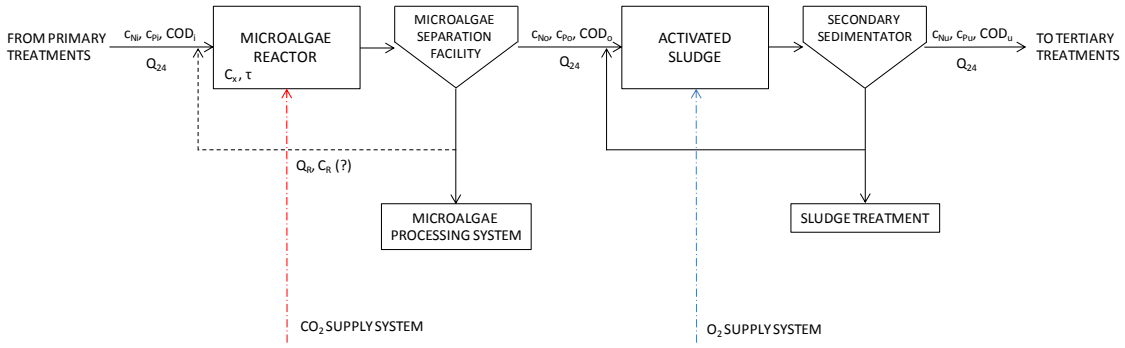

Figure 4.1 Process scheme proposal: microalgae reactor followed by conventional activatel sludge process.

According to the first process scheme proposal (Figure 4.1), a microalgal reactor for nutrient (N and P) removal is followed by a conventional activated sludge process for COD removal. Microalgal reactor would be equipped with a separation facility (centrifuge, decanter or sedimentation tank) and could include also a recirculation line if the requested biomass concentration is not autonomously developed. For microalgal section design it must be taken into account that the activated sludge process requires a certain amount of nutrients for biomass production, therefore nutrients consumption must be limited to avoid the failure of treatment step downstream.

Nutrient and COD loadings vary significantly along the day, so an equalization basin should be provided before algal treatment to normalize nutrients concentration during day, and permit an easier operation of the entire wastewater treatment process.

4.1.1 ACTIVATED SLUDGE NUTRIENT DEMAND

Activated sludge bacteria consortium is characterized by this average elemental composition (Metcalf & Eddy, 2004):

$$BOD: N: P = 100: 5: 1 \quad \text{(Eq. 4.1)}$$

This ratio means that in order to consume 100 mg/l of organic substances (BOD) bacteria needs 5 mg/l of Nitrogen and 1 mg/l of Phosphorous.

Laboratory analysis for primary treated wastewater at Camposampiero (PD) plant show the nutrient and COD concentrations reported in table 4.1.

Table 4.1 Wastewater composition.

	COD	N-NH_3	TP
	[mgCOD/l]	[mgN/l]	[mgP/l]
Primary treated ww.	272	37.99	4.14

Assuming:

$$\frac{BOD}{COD} = 0.5 \quad \text{(Eq. 4.2)}$$

The effective amount of organic matter that can be consumed is:

$$BOD = COD * 0.5 = 272 \frac{mgCOD}{l} * 0.5 \frac{mgBOD}{mgCOD} = 136 \frac{mgBOD}{l} \quad \text{(Eq. 4.3)}$$

In order to deplete this amount of organic matter, these N and P concentration must be provided to the activated sludge reactor:

$$BOD: N: P = 100: 5: 1 = 136: 6.8: 1.36 \quad \text{(Eq. 4.4)}$$

Accordingly, the nutrient concentrations exiting the microalgal reactor ($c_{No,min}$ and $c_{Po,min}$) should be those listed in table 2.2.

Table 4.2 Minimum nutrient concentrations for activated sludge process.

	Nutrient conc. for A.S. process
	[mg/l – ppm]
$C_{No,min}$	6.8
$C_{P,min}$	1.36

4.1.2 MICROALGAL REACTOR DESIGN

Microalgal reactor design will be based on Phosphorous or Nitrogen balances, depending on whichever of these balance is more precautionary for the activated sludge process downstream, coupled with microalgae biomass balance.

4.1.2.1 Design based on nitrogen balance

Table 4.3 Process parameters.

Data	Symbol	Value	Unit	References
Total N concentration inlet	C_{N_i}	37.99	ppm	-
Total P concentration inlet	C_{P_i}	4.14	ppm	-
Total N concentration outlet	$C_{N_{o,min}}$	6.80	ppm	-
Total P concentration outlet	$C_{P_{o,min}}$	1.36	ppm	-
Nitrogen–biomass yield	Y_N	0.098	gN/gBiomass	Morandini (2012)
Phosphorous–biomass yield	Y_P	0.00503	gP/gBiomass	Morandini (2012)
Carbon–biomass yield	Y_C	0.527	gC/gBiomass	Morandini (2012)
Biomass-Nitrogen yield	$Y_{x/N}$	10.204	gBiomass/gN	Morandini (2012)
Biomass-Phosphorous yield	$Y_{x/P}$	198.807	gBiomass/gP	Morandini (2012)
Nitrogen max consumption rate	$\mu_{N,max}$	0.668	gN/(gBiomass*d)	Morandini (2012)
Phosphorous max consumption rate	$\mu_{P,max}$	0.849	gP/(gBiomass*d)	Morandini (2012)
Nitrogen half-saturation constant	k_N	23.4	gN/m^3	Morandini (2012)
Phosphorous half-saturation constant	k_P	28.2	gP/m^3	Morandini (2012)

The amount of nitrogen that has to be consumed is

$$\Delta N = C_{N_i} - C_{N_{o,min}} = 31.19 \ \frac{gN}{m^3} \qquad \text{(Eq. 4.5)}$$

Equation 4.4 takes into account that a certain amount of Nitrogen ($c_{N_{o,min}}$) is necessary for the following activated sludge reactor.

The general nitrogen balance over the microalgae reactor is:

$$A = I - O + R \qquad \text{(Eq. 4.6)}$$

where:

- A is accumulation term [g/d]
- I inlet Nitrogen [g/d]
- O outlet Nitrogen [g/d]
- R Nitrogen consumed by reaction [g/d]

Under the assumptions:

- Steady-state conditions: the accumulation term is equal to zero ($A = 0$)
- Reactor CSTR type: the outlet nitrogen concentration is equal to the inner one.

the nitrogen balance becomes:

$$0 = C_{Ni} - C_{No} + R \quad \text{(Eq. 4.7)}$$

Concerning the reaction term (R):

$$R = -r_N * C_x * \tau \quad \text{(Eq. 4.8)}$$

Where:

- r_N is the Nitrogen specific consumption rate [gN/(gBiomass*d)]
- C_x is inner, and outlet, microalgal biomass concentration [gBiomass/m3]
- τ is reactor residence time [d]

Nitrogen consumption rate is assumed to obey the Monod kinetic:

$$r_N = \frac{\mu_{N,max} * C_{No}}{k_N + C_{No}} \quad \text{(Eq. 4.9)}$$

Where:

- $\mu_{N,max}$ is the maximum Nitrogen specific consumption rate for *C. protothecoides* *[gN/(gBiomass*d)]*
- k_N is the half-saturation constant for *Chlorella protothecoides* [gN/m3]

$\mu_{N,max}$ and k_N are kinetic parameters experimentally determined in previous works (Morandini, 2012). Their values are reported in table 4.3. In figure 4.2 nitrogen specific consumption rate is plotted against nitrogen outlet concentration.

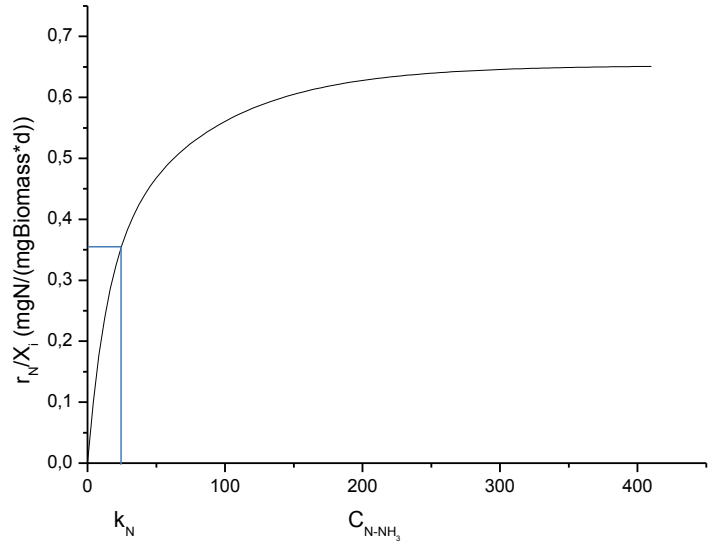

Figure 4.2 N specific consumption rate against N outlet concentration according to Monod model.

In summary, the Nitrogen balance over microalgae reactor is:

$$C_{Ni} - C_{No} - \frac{\mu_{N,max} * C_{No}}{k_N + C_{No}} * C_x * \tau = 0 \qquad \text{(Eq. 4.10)}$$

In this equation, C_x and τ are the system unknowns, while all the other terms are known.

The microalgal biomass balance over the reactor is a second equation that can be solved together with eq. 4.10 to determine C_x and τ.

Assuming steady-state conditions, CSTR reactor and no inlet microalgae biomass (process without recirculation), the biomass balance is:

$$0 = -C_x + r_x * C_x * \tau \qquad \text{(Eq. 4.11)}$$

Where:

- C_x is inner and outlet microalgal biomass concentration [g/m^3]
- r_x is the biomass production rate [d^{-1}]
- τ is reactor residence time [d]

The biomass production rate r_x can be linked to Nitrogen specific production rate through the Biomass/Nitrogen yield ($Y_{x/N}$), in fact:

$$-\frac{dC_x}{dC_N} = Y_{x/N} \qquad \text{(Eq. 4.12)}$$

Dividing the first member by dt and considering that $\frac{dC_N}{dt} = -r_N$:

$$-\frac{\frac{dC_x}{dt}}{\frac{dC_N}{dt}} = Y_{x/_N} \rightarrow \frac{dC_x}{dt} = r_x = Y_{x/_N} * r_N = Y_{x/_N} * \frac{\mu_{N,max} * C_{No}}{k_N + C_{No}} \quad \text{(Eq. 4.13)}$$

Substituting into the biomass balance we have:

$$-1 + Y_{x/_N} * \frac{\mu_{N,max} * C_{No}}{k_N + C_{No}} * \tau = 0 \quad \text{(Eq. 4.14)}$$

Equations 4.9 and 4.14 form a system with 2 equations in 2 unknowns:

$$\begin{cases} C_{Ni} - C_{No} - \frac{\mu_{N,max} * C_{No}}{k_N + C_{No}} * C_x * \tau = 0 \\ -1 + Y_{x/_N} * \frac{\mu_{N,max} * C_{No}}{k_N + C_{No}} * \tau = 0 \end{cases} \quad \text{(Eq. 4.15)}$$

By solving the system, it can be obtained:

$$\begin{cases} \tau = \frac{k_N + C_{No}}{\mu_{N,max} * C_{No}} * \frac{1}{Y_{x/_N}} \\ C_x = (C_{Ni} - C_{No}) * Y_{x/_N} \end{cases} \quad \text{(Eq. 4.16)}$$

With the parameter values reported in table 4.3, we obtain:

$$\begin{cases} \tau = 0.63\ d \\ C_x = 318.27\ g/m^3 \end{cases} \quad \text{(Eq. 4.17)}$$

Now, the phosphorous outlet concentration have to be checked as well, in order to respect the nutrient demand of activated sludge process. Phosporous balance over the system is:

$$C_{Pi} - C_{Po} - \frac{\mu_{P,max} * C_{Po}}{k_P + C_{Po}} * C_x * \tau = 0 \quad \text{(Eq. 4.18)}$$

By substituting the parameter values reported in table 4.3 and nitrogen/mass balance system results, and solving respect to C_{Po} the outlet phosphorous concentration is obtained.

$$C_{Po} = 0.60 \frac{g}{m^3} < C_{Po}, min \quad \text{(Eq. 4.19)}$$

With this design method, outlet phosphorous concentration won't achieve the minimum value needed for activated sludge process. Therefore, the design of the process should be based on Phosporous balance, thus admitting a greater concentration of Nitrogen exiting the reactor.

4.1.2.2 Design based on phosphorous balance

The amount of phosphorous that has to be consumed is

$$\Delta P = \mathrm{C_{P_i}} - \mathrm{C_{P_{o,min}}} = 2.78\ \frac{\mathrm{gP}}{\mathrm{m^3}} \qquad \text{(Eq. 4.20)}$$

Equation 4.4 takes into account that a certain amount of phosphorous ($\mathrm{c_{P_{o,min}}}$) is necessary for the following activated sludge reactor.
Phosphorous consumption rate is assumed to obey at Monod kinetic:

$$r_P = \frac{\mu_{P,max} * C_{Po}}{k_N + C_{Po}} \qquad \text{(Eq. 4.21)}$$

In figure 4.3 phosphorous specific consumption rate is plotted against the phosphorous outlet concentration.

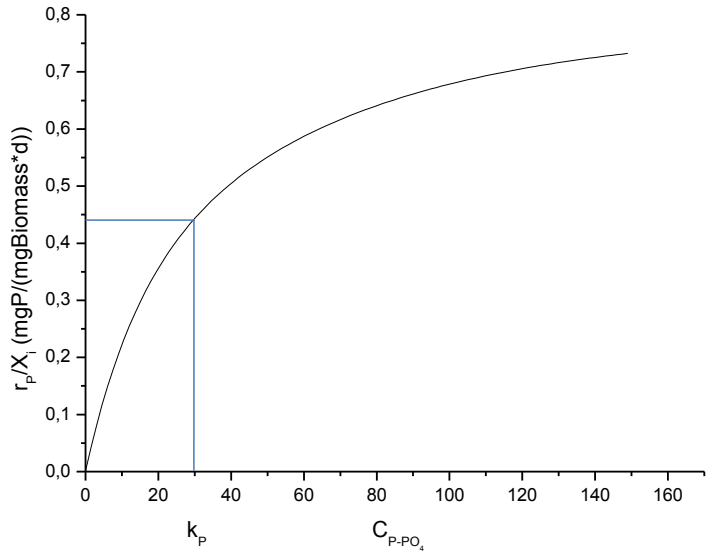

Figure 4.3 P specific consumption rate against P outlet concentration according to Monod model.

The same assumption made for Nitrogen balance can be adopted in Phosporous balance; repeating all equation from 4.5 to 4.16, substituting Phosphorous parameters to Nitrogen, the system with Eq. 4.22 and 4.23 is obtained:

$$\begin{cases} \tau = \dfrac{k_P + C_{Po}}{\mu_{P,max} * C_{Po}} * \dfrac{1}{Y_{x/_P}} & \text{(Eq. 4.22)} \\ C_x = (C_{Pi} - C_{Po}) * Y_{x/_P} & \text{(Eq. 4.23)} \end{cases}$$

Equations 4.22 and 4.23 are solved with parameters reported in table 4.3.

$$\begin{cases} \tau = 0.13\ d \\ C_x = 552.68\ g/m^3 \end{cases} \quad \text{(Eq. 4.24)}$$

Biomass productivity associated to this values of residence time and biomass concentration is:

$$P_x = \frac{C_x}{\tau} = 4291.91 \frac{g}{m^3 * d} \quad \text{(Eq. 4.25)}$$

Nitrogen outlet concentration from the microalgal reactor can be calculated with eq. 4.10.

$$C_{No} = 17.23\ \frac{g}{m^3} > C_{No,min} \quad \text{(Eq. 4.26)}$$

While the nitrogen outlet concentration from the activated sludge process is:

$$C_{Nu} = C_{No} - 6.8 = 10.43 \frac{g}{m^3} \quad \text{(Eq. 4.27)}$$

Which is lower than the law limit imposed by Italian legislation.

Biomass productivity is directly linked to the specific energy irradiation available, i.e. biomass production depends on the incident solar energy:

$$E_r = 20 \frac{MJ}{kg} \quad \text{(Eq. 4.28)}$$

In fact, in order to produce 1kg of biomass 20MJ of energy from solar irradiation are necessary.

For Padua, the annual solar irradiation available is:

$$E_{PD} = 4541 \frac{MJ}{m^2 * y} \quad \text{(Eq. 4.29)}$$

Assuming a photosynthetic efficiency of 0.07, solar energy actually exploitable is:

$$E_{PD,a} = E_{PD} * \eta = 4541 * 0.07 = 317.87 \ \frac{MJ}{m^2 * y} \quad \text{(Eq. 4.30)}$$

The maximum productivity obtainable with the available solar energy in Padua is:

$$P_{m,PD} = \frac{E_{PD,a}}{365 * E_r} = \frac{317.87}{365 * 20} * 1000 = 43.54 \ \frac{g}{m^2 * d} \quad \text{(Eq. 4.31)}$$

From this parameter the reactor height can be calculated:

$$H = \frac{P_{m,PD}}{P_x} \cong 0.01 \ m \quad \text{(Eq. 4.32)}$$

This value is too low, as it would be impossible to manage a reactor with a depth of 1 cm.
Therefore, another design calculation procedure is proposed, based on nitrogen balance, changing the outlet nitrogen concentration;

$$C_{No} = 12 + C_{No,min} = 18.8 \ \frac{\text{gN}}{\text{m}^3} \quad \text{(Eq. 4.33)}$$

Results of these calculations are reported in table 4.4 and figure 4.4.

Table 4.4 Design results for a pre-microalgal reactor.

PARAMETER	VALUE	UNIT
C_{N_o} (imposed)	18.8	gN/m^3
C_{P_o}	1.48	gP/m^3
τ	0.32	d
C_x	195.82	g/m^3
P_x	612.43	g/(m^3*d)
H	0.07	m

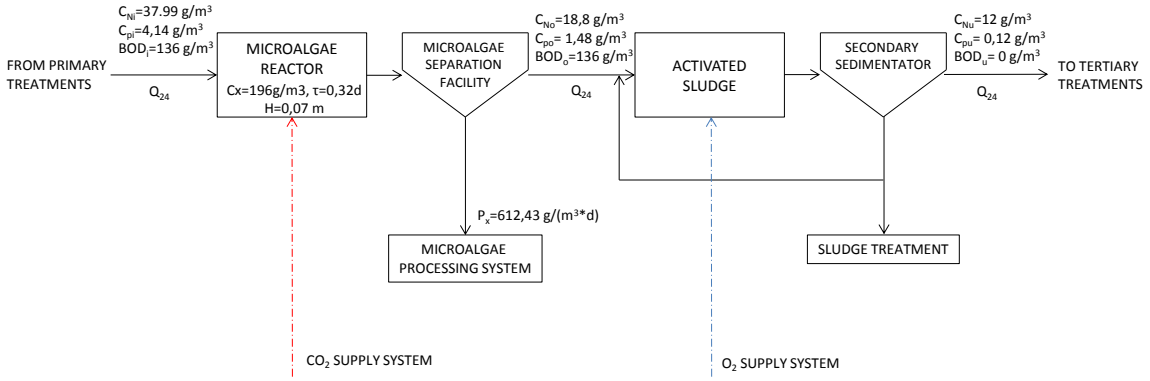

Figure 4.4 Process scheme proposal 1 with design parameters.

Starting from these results, a set of surface areas for the microalgal reactor can be proposed, based on different wastewater treatment plant dimensions, considering a daily water consumption per equivalent inhabitant (E.I.) of 0.3 m^3/(d*E.I.) and an inflow sewer coefficient of 0.8 (i.e. the amount of water consumed that flow into sewer). As an example, the reactor side is calculated and reported, assuming a square shape.

$$Q_{24} = 0.3 * 0.8 * Population\ served \quad \text{(Eq. 4.34)}$$

$$S = \frac{Q_{24} * \tau}{H} = \frac{Q_{24} * \tau}{P_{m,PD}} * P_x = \frac{Q_{24} * C_x}{P_{m,PD}} \quad \text{(Eq. 4.35)}$$

Table 4.5 Microalgal reactor extensions according to different wastewater flowrates.

Population served	Q_{24}	Reactor surface (S)	Reactor side
E.I.	m^3/d	m^2	m
30000	7200	32378	180
60000	14400	64757	254
100000	24000	107928	329
150000	36000	161892	402

From the carbon content of the microalgal cell, the amount of CO_2 that have to be fed to the reactor can be estimated;

$$Q_{air} = \frac{Q_{24} * C_x * Y_C * 3.6}{1.96 * \%_{v/v} * 1000} * \frac{1}{\eta} \quad \text{(Eq. 4.36)}$$

where

- Q_{air} is the total gas flowrate [Nm^3/h]
- Q_{24} is the inlet wastewater flowrate [m^3/h]
- C_x is biomass concentration in the reactor [g/m^3]
- Y_C is the microalgal carbon content = 0.527 [gC/gBiomass] (Morandini, 2012)
- 3.6 is CO_2/C ratio [gCO_2/gC]

- 1.96 CO_2 density at 1 atm and 20°C [g/l]
- $\%_{v/v}$ CO_2 air content, expressed in volumetric percentage
- 1000 transformation factor from l to m^3
- η is the efficiency of gas/liquid transfer with respect to the total amount = 0.05 [-]

Assuming a CO_2 content of 8.1 $\%_{v/v}$, which is the average CO2 fraction in the Padua incinerator plant, the air demand for the set of reactors reported in table 4.5 is calculated and reported in table 4.6.

Table 4.6 Air demand for a set of microalgal reactors.

Population served	Q_{24}	Q_{air}
E.I.	m^3/d	Nm^3/h
30000	7200	13931
60000	14400	27863
100000	24000	46438
150000	36000	69657

The total incinerator plant gas emission is 164969 Nm^3/h, which is enough also for the biggest microalgal reactor proposed.

4.2 OPTION 2: POST-MICROALGAL REACTOR

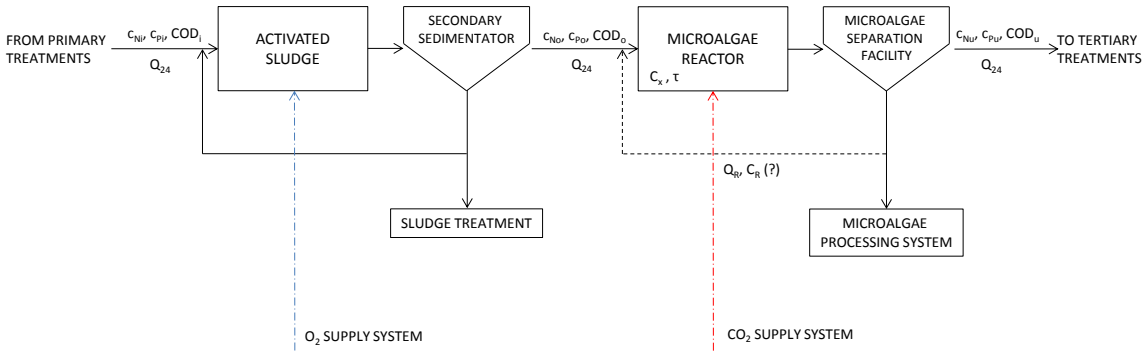

Figure 4.5 Process scheme proposal 2: conventional activatel sludge process followed by microalgae reactor.

In a second scheme proposal (Figure 4.5), a conventional activated sludge process, is followed by a microalgal reactor. In the activated sludge step, organic matter are consumed together with a certain amount of nutrients. In the latter reactor, a further depletion of nutrients is accomplished by means of microalgal biomass production. The main advantage of this configuration is that the activated sludge reactor has all the nutrients available, therefore its operation is easier. On the other hand, there are less nutrients for microalgae production, so the

final biomass productivity and subsequential energy production will be lower with respect to the first option.

The design model is based on the same assumptions made for the first proposal (see 4.1).

Starting from inlet wastewater pollutants concentration reported in table 4.1, the nutrient concentration entering the microalgal reactor are calculated with equation 4.4, thus to take into account that in the activated sludge process upstream, a certain amount of nutrients are depleted by bacteria metabolism. Results are reported in table 4.7; symbols refers to figure 4.5.

Table 4.7 Nutrient concentration before and after the activated sludge treatment step.

PARAMETER	VALUE	UNIT
C_{Ni}	37.99	gN/m^3
C_{Pi}	4.14	gP/m^3
C_{No}	31.19	gN/m^3
C_{Po}	2.78	gP/m^3

Outlet nitrogen and phosphorous concentrations from the microalgal reactor of 5 gN/m^3 and 1 gP/m^3 have to be set, respectively, in order to achieve law requirements; the same design method used for the first process, based on nitrogen balance, can be applied, thus leading to results reported in table 4.8 and figure 4.6

Table 4.8 Design results for a post-microalgal reactor.

PARAMETER	VALUE	UNIT
C_{Nu}	5	gN/m^3
C_{Pu}	1	gP/m^3
τ	0.81	d
C_x	267.24	g/m^3
P_x	330.31	$g/(m^3*d)$
H	0.12	m

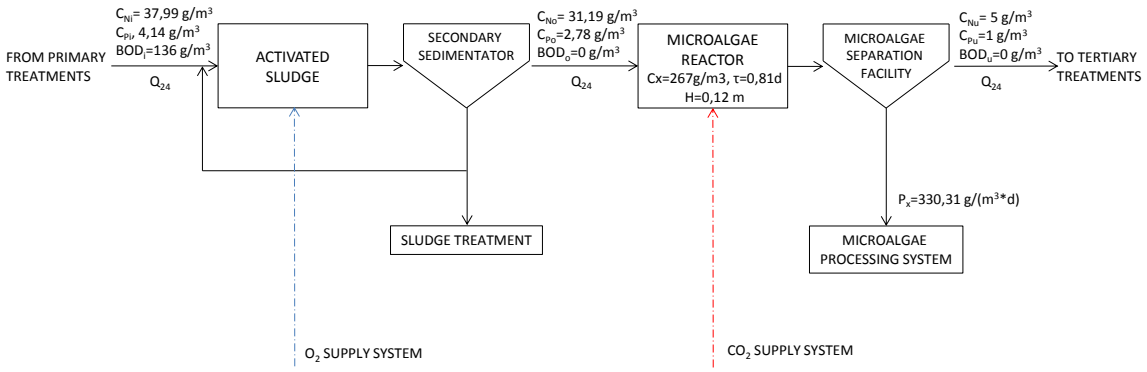

Figure 4.6 Process scheme proposal 2 with design parameters.

Comparing these results with those reported in table 4.4, it can be noticed that the microalgal biomass productivity is almost halved but, on the other hand, discharge nutrients concentrations are more precautionary.

Starting from these results, a set of surface areas for the microalgal reactor can be proposed, based on different wastewater treatment plant dimensions, considering a daily water consumption per equivalent inhabitant of 0.3 m^3/(d*E.I.) and an inflow sewer coefficient of 0.8 (i.e. the amount of water consumed that flow into sewer). As an example, the reactor side is calculated and reported, assuming a square shape. Daily average flowrate (Q_{24}) and reactor surface were calculated with eq. 4.34 and 4.35 respectively.

Besides, for each reactor the corresponding air demand is reported, based on the same assumption reported in paragraph 4.1.

Table 4.9 Microalgal reactor extensions and corresponding air demand, according to different wastewater flowrates.

Population served	Q_{24}	Reactor surface	Reactor side	Q_{air}
E.I.	m^3/d	m^2	m	Nm^3/h
30000	7200	47342	218	19013
60000	14400	94683	308	38026
100000	24000	157806	397	63377
150000	36000	236708	487	95066

4.3 OPTION 3: FLOATING PHOTOBIOREACTOR SOLUTION

4.3.1 FLOATING TUBOLAR PHOTOBIOREACTOR

An alternative process scheme could be implemented in case of no land availability close to the wastewater facility: this solution consists on a series of floating polyethylene tubes, arranged on the oxidation basin of a conventional treatment plant. This particular photobioreactor is mate in polyethilene, permeable to gases, such as CO_2 and O_2, and to fresh water, but impermeable to biomass (both bacteria and microalgae) and dissolved salts. As it can be seen from figure 4.7, the

tube systems floats over the oxidation basin. As it can be seen from figure 4.7, the systems floats over the oxidation basin.

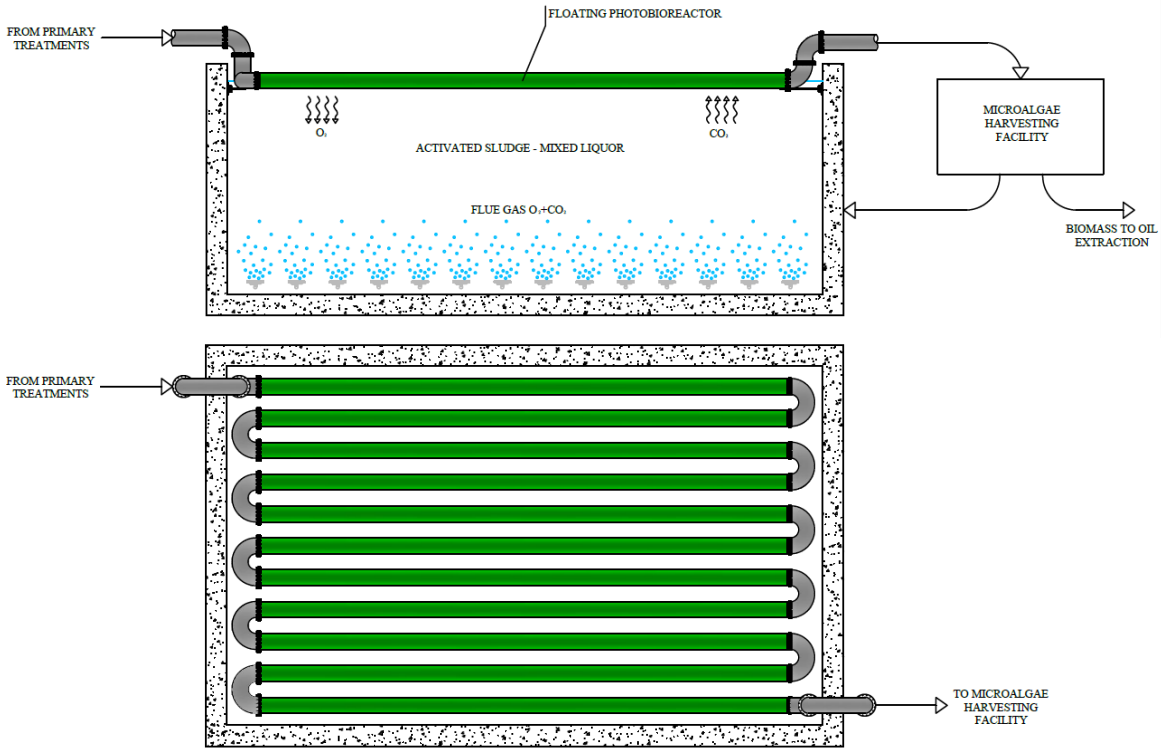

Figure 4.7 Concept representation of a floating mattress photobioreactor.

The wastewater enters the photobioreactor, where microalgae biomass can grow depleting a part of the nutrients content. The height of the mattress should not exceed a value of 0.5 m, thus to avoid self-shading effects (Enzo 2011). The tube path should be designed in order to maximize the photobioreactor volume.

After the photobioreactor, microalgae are harvested by means of a gravity clarifier (with or without chemicals adding) or by means of centrifuge decanters. Then, the clarified wastewater is fed to the oxidation tank, where organic matter and remaining nutrients are depleted. The harvested microalgae biomass can be processed, following the biorefinery concept (see 1.2.1) and residuals of this treatment can be digested with the excess sludge.

This configuration has several advantages:

- gas exchange between mixed liquor and microalgae solution. Dissolved oxygen produced by microalgae metabolism can diffuse into the mixed liquor, decreasing the activated sludge oxygen demand. At the same time, the CO_2 produced by aerobic bacteria can enter the microalgae solution, where it is exploited for microalgal biomass production. The tubular arrangement of the photobioreactor increase the gases

exchange thanks to its high exchange surface, respect to a unique floating “mattress” photobioreactor.

- land requirement. Since the photobioreactor is placed over a conventional oxidation tank, no further land is required.
- Unique flue gas supply system: both CO_2 and oxygen supply is achieved by only one system; the mixture air/CO_2, in fact, is furnished by means of a series of perforated plates at the bottom of the oxidation tank.

Of course, several aspects must be carefully analyzed and further researched and developments are necessary to understand if this type of system is feasible in reality:

- membrane strength. The photobioreactors must be proved to resists to the inner pressure; a breaking of the membrane will result in the overall process failure.
- inner biomass concentration. Since the residence time is controlled by the oxidation tank extension, the obtainable inner biomass concentration must be checked for each case. Too low biomass concentrations will result in insufficient nutrients depletion and, therefore, in an outlet concentration over the law limits.
- systems compatibility. The oxidation tank requires a series of facilities, which have to be adapted for the new configuration.

Concerning the polyethylene membrane, a prototype is currently under developing at the NASA’s Ames Research Center (California), where it is exploited for microalgae offshore cultivation in batch photobioreactors made with this material (www.nasa.gov/omega/).

4.3.2 FLOATING MATTRESS PHOTOBIOREACTOR

A process scheme similar to that analyzed in paragraph 4.3 consists of a floating photobioreactor (“floating mattress”), arranged on the oxidation basin of a conventional treatment plant. This particular photobioreactor should be made with a selective permeable membrane, permeable to gases, such as CO_2 and O_2, and to nutrients, but impermeable to biomass (both bacteria and microalgae). As it can be seen from figure 4.8, the systems floats over the oxidation basin.

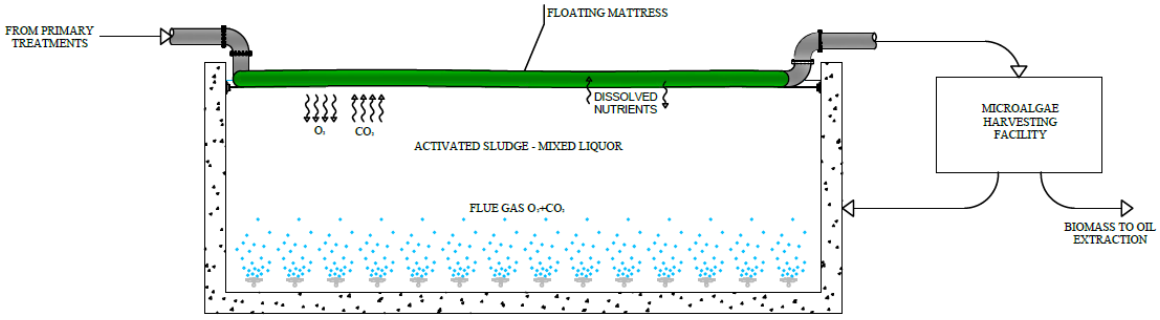

Figure 4.8 Concept representation of a floating mattress photobioreactor.

The wastewater enters the photobioreactor, where microalgae biomass can grow depleting a part of the nutrients content. The height of the mattress should not exceed a value of 0.2÷0.5 meter, thus to avoid self-shading effects (Enzo 2011). The mattress could also contain a series of septa, in order to give a path to the wastewater and avoid the formation of death zones.

After the photobioreactor, microalgae are harvested by means of a gravity clarifier (with or without chemicals adding) or by means of centrifuge decanters.

The harvested microalgae biomass can be processed, following the biorefinery concept (see 1.2.1) and residuals of this treatment can be digested with the excess sludge.

Concerning the photobioreactor material, a suitable one was not already found, but we are confident that it will soon be feasible, since the semi-permeable membrane technologies are subjected to rapid developments.

This configuration has several advantages similar to those showed in paragraph 4.3.1.

The residence time inside the floating mattress is governed by the residence time of the activated sludge basin. Assuming that wastewater flowrate and surface area are the same for the two reactors, the relationship between the residence times of activated sludge and floating mattress is straightforward,

$$\frac{A * H_{AS}}{\tau_{AS}} = \frac{A * H_{FM}}{\tau_{FM}} \qquad \text{(Eq. 4.37)}$$

where:

- H_{AS} is the oxidation basin height [m]
- H_{FM} is the floating mattress height [m]
- τ_{AS} is the oxidation basin residence time [d]
- τ_{FM} is the floating mattress residence time [d]
- A is the reactors surface [m^2]

Considering an average height of the oxidation basin of 6 m, which is a common value for typical wastewater treatment plants (Metcalf & Eddy 2004) and a mattress height of 0,5 m:

$$H_{AS} = 12 * H_{FM} \quad \text{(Eq. 4.38)}$$

Substituting into equation and assuming a residence time of 0.33 d (8 h) for the oxidation basin (Metcalf & Eddy 2004):

$$\tau_{FM} = \frac{\tau_{AS}}{12} = 0.028\ d \quad \text{(Eq. 4.39)}$$

In table 4.6, inlet and outlet nitrogen concentration are reported. Inlet concentrations refer to table 4.1. Concerning outlet nitrogen concentration, its value is calculated with equation 4.4 (which takes into account that a certain amount of nitrogen is consumed by the activated sludge process) and increased of 12 g/m^3 to avoid an excessive loading, however remaining below the law limits (15 g/m^3).

Table 4.10 Nutrient concentration before and after the activated sludge treatment step.

PARAMETER	VALUE	UNIT
C_{Ni}	37.99	gN/m^3
C_{Pi}	4.14	gP/m^3
C_{No}	18.8	gN/m^3

Substituting results of Eq. 4.39 and nitrogen values reported in table 4.10 into equation 4.10, the requested biomass concentration is obtained.

$$C_x = 2.2\ \frac{g}{l} \quad \text{(Eq. 4.40)}$$

a value too high, so that a recirculation of the harvested biomass is therefore necessary. The corresponding productivity is 80 g/(l*d).

The outlet phosphorous concentration is obtained through Eq. 4.18.

$$C_{Po} = 1.48\ \frac{g}{l} \quad \text{(Eq. 4.41)}$$

4.4 DESIGN MODEL VERIFICATION

In order to verify the Monod-based model, experimental data collected through continuous flow experiments running at constant illumination will be compared with calculated results obtained

with the same starting conditions (Inlet nitrogen and phosphorous) and running parameters (Residence time and measured biomass concentration).

4.4.1 VERIFICATION BASED ON BIOMASS YIELDS

In this paragraph, experimental data will be verified through biomass yields ($Y_{x/_N}$ *and* $Y_{x/_P}$), with equation 4.16 and 4.23.

$$C_x = (C_{Ni} - C_{No}) * Y_{x/_N}$$
$$C_x = (C_{Pi} - C_{Po}) * Y_{x/_P} \quad \text{(Eq. 4.42)}$$

Substituting experimental measures of inlet nutrients (C_{Ni} , C_{Pi}) and biomass inner concentration (C_x), and solving with respect to C_{No} and C_{Po}, outlet nutrients concentration can be estimated. Results of these calculations will be compared with measured nutrients concentration in each experiment, as shown in table 4.11.

Table 4.11 Comparison between measured and calculated parameters based on biomass yields.

				Residence time [d]				
	Parameter	*Symbol*	*Unit*	*0.64*	*0.79*	*1.01*	*1.26*	*1.97*
Measured parameters	Biomass conc.	C_x	mg/l	307.00	468.00	540.00	640.00	800.00
	Inlet N	C_{Ni}	mgN/l	41.01	41.01	54.81	54.81	54.81
	Inlet P	C_{Pi}	mgP/l	5.32	5.32	3.08	3.08	3.08
	Outlet N	C_{No}	mgN/l	11.50	0.94	8.44	10.78	11.03
	Outlet P	C_{Po}	mgP/l	0.76	0.91	0.68	0.26	0.26
	N consumption	ΔN_m	mgN/l	29.51	40.07	46.37	44.03	43.78
	P consumption	ΔP_m	mgN/l	4.56	4.41	2.40	2.82	2.82
	N over P consumption ratio	$\Delta N_m / \Delta P_m$	mgN/mgP	6.47	9.09	19.32	15.61	15.52
Calculated parameters	Outlet N	$C_{No,c}$	mgN/l	10.92	-4.85	1.89	-7.91	-23.59
	Outlet P	$C_{Po,c}$	mgP/l	3.78	2.97	0.36	-0.14	-0.94
	N consumption	ΔN_c	mgN/l	30.09	45.86	52.92	62.72	78.40
	P consumption	ΔP_c	mgP/l	1.54	2.35	2.72	3.22	4.02
	N over P consumption ratio	$\Delta N_c / \Delta P_c$	mgN/mgP			19.48		

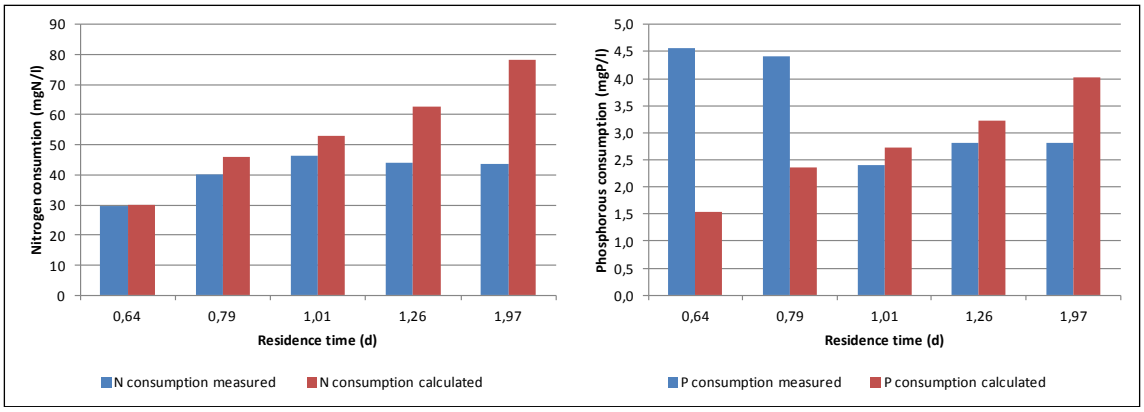

Figure 4.9 Comparison between calculated and measured nutrients consumption based on biomass yields.

Concerning nitrogen removal, looking at figure 4.9 it's clear that this model can be applied only for low residence times. In fact, after 1 day of residence time, the difference between calculated and measured values increases quite linearly. This can be due to changes in microalgae metabolism which lead to different cells composition.

Concerning phosphorous, this model foresee with a good approximation only results for high residence time (> 1 d). At low residence time the expected phosphorous removal is less than half the effective removal measured in continuous flow experiments. This can be due to a phosphorous accumulation on microalgae cells: Richmond (2004) observed that microalgae can store and/or adsorb excess phosphorous during the exponential growth, and then use it when the external supply becomes limited. Therefore, at short residence time, a higher amount of phosphorous than expected is depleted from the culture solution, since microalgae exit the reactor before using it.

4.4.2 VERIFICATION BASED ON NUTRIENTS BALANCE

Nitrogen and phosphorous balances expressed by equations 4.9 and 4.18 will be used to compare experimental and simulated results, substituting the inlet nutrient concentrations ($C_{N,i}$ and $C_{P,i}$), residence time (τ) and biomass concentration (C_x) measured in each experiment, and solving them respect to $C_{N,o}$ and $C_{P,o}$. Results of these calculations are reported in table 4.12. and figure 4.10.

$$C_{Ni} - C_{No} - \frac{\mu_{N,max} * C_{No}}{k_N + C_{No}} * C_x * \tau = 0 \qquad \text{(Eq. 4.10)}$$

$$C_{Pi} - C_{Po} - \frac{\mu_{P,max} * C_{Po}}{k_P + C_{Po}} * C_x * \tau = 0 \qquad \text{(Eq. 4.18)}$$

Table 4.12 Comparison between measured and calculated parameters based on nutrient balances.

				Residence time [d]				
	Parameter	*Symbol*	*Unit*	*0.64*	*0.79*	*1.01*	*1.26*	*1.97*
Calculated parameters	Outlet N	$C_{No,c}$	mgN/l	7.66	3.99	3.69	2.44	1.22
	Outlet P	$C_{Po,c}$	mgP/l	0.79	0.44	0.18	0.12	0.06
	N consumption	ΔN_c	mgN/l	33.35	37.02	51.12	52.37	53.59
	P consumption	ΔP_c	mgP/l	4.53	4.88	2.90	2.96	3.02
	N over P consumption ratio	$\Delta N_c/\Delta P_c$	mgN/mgP	7.36	7.59	17.61	17.71	17.77

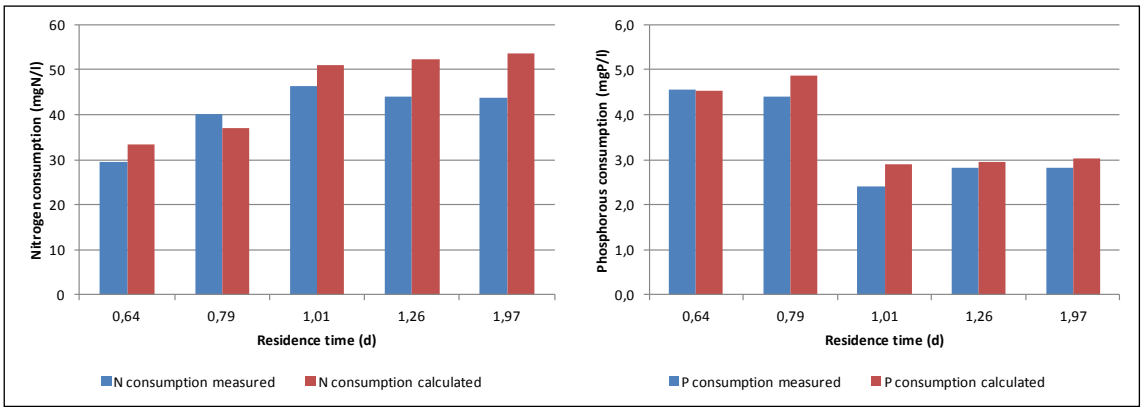

Figure 4.10 Comparison between calculated and measured nutrients consumption based on nutrient balances.

Concerning nitrogen removal, the adopted model seems to simulate the real conditions with low error under 1 day of residence time. For higher values, nitrogen consumption increase slightly instead of decreasing as experimental results pointed out, but this error seems to be quite low. For phosphorous removal, the model simulates real conditions with small errors at each residence time tested, confirming its forecasting validity at all.

4.5 EXISTING PLANTS ANALYSIS

Nowadays no commercial wastewater plants integrated with microalgae are running all over the world, but a series of pilot plants are being studied and operated; since the most of these projects are financed by private companies and/or are protected by patents, it is currently difficult to find reliable information of process parameters and on real performances. Despite of these difficulties, in the following paragraph, an analysis of a pilot plant in the U.S.A will be carried out, exploiting data found on the internet. This analysis will be useful to scale up our photobioreactor systems in future research activities.

4.5.1 PROCESS WITH BIOFUEL PRODUCTION EMPHASIS

The process flow diagram in figure 4.11 represents an integrated process of wastewater treatment and microalgae production (with an emphasis in biofuel production) by Tryg Lundquis and his algal research group at the California Polytechnic State University (Lundquist et al. 2012).

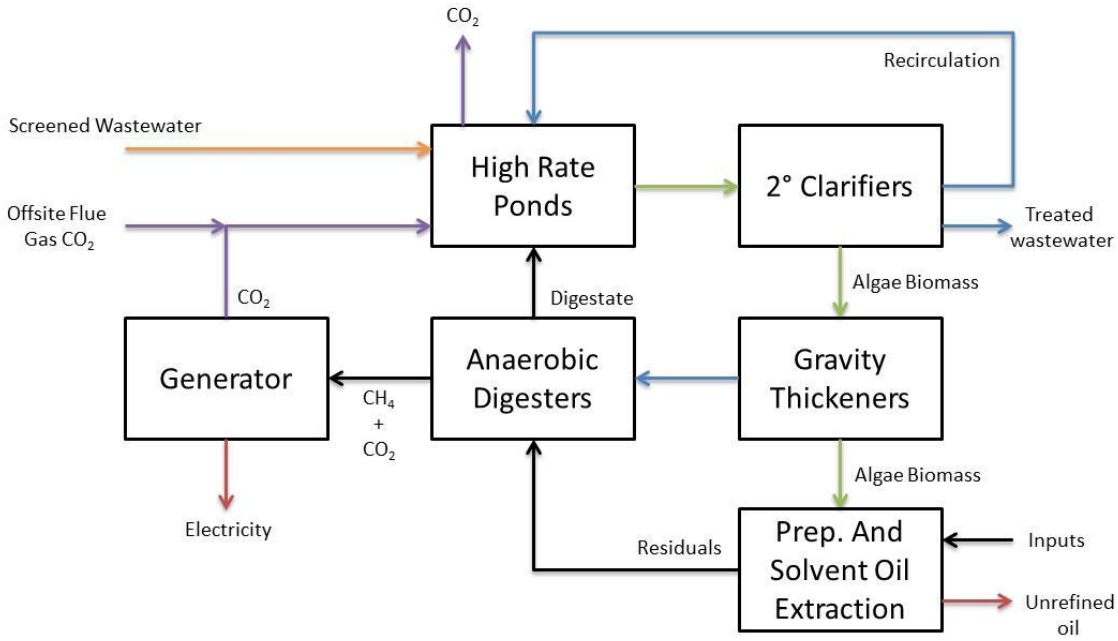

Figure 4.11 Flowsheet of an integrated wastewater treatment with emphasis on biofuel production. Derived from (Lundquist et al. 2012).

Screened wastewater enter the high rate ponds (HRP), where flue gas enriched in CO_2 is supplied in order to enhance microalgal growth. HRP are paddlewheel mixed, with a residence time of about 3-5 days; nine HPR of 40 m^2 and nine of 4 m^2 are used for this pilot plant. A nitrogen abatement of 99% is achieved thanks to nutrients recirculation from the secondary clarifiers, while if recirculation is not provided, the nitrogen abatement range from 84% to 94%. NO_x content is negligible. The pH in the pond, reaches values of 9.5-10 during day, leading to a consistent killing of *E. coli* and pathogenic bacteria. Concerning phosphorous, the dissolved fraction is depleted up to 0.1 mg/l, while the particulate fraction is not depleted at all and needs to be removed by settling and filtration. The algal biomass is recovered by means of a secondary clarifier, where only the bioflocculating capacity of microalgae are exploited, without adding chemicals, resulting in lower overall costs. However, the bioflocculation is not homogeneous and depends on CO_2 addition, nutrients loading, recirculation and other factors. A further biomass concentration is done by means gravity thickeners, thus to achieve a final concentration suitable for the processes downstream.

The concentrated algal biomass is processed for oil extraction, and the residues from this treatment step are used for feeding an anaerobic digester, producing methane and, therefore, electricity. The flue gas produced with biogas burning is supplied to the HRPs.

A carbon print analysis of the overall process shows a consistent GHG saving, compared to typical wastewater treatment methods, as shown in figure 4.12.

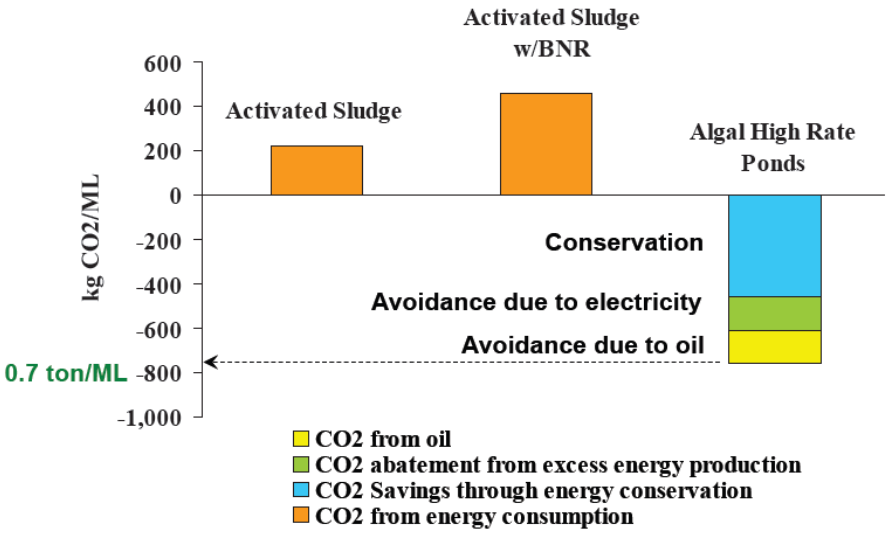

Figure 4.12 GHG savings at Cal. Poly Algae Field Station (Lundquist, 2012).

A cost-benefits analysis shows a 50% saving of the total process cost, with respect to a typical activated sludge process, and a 67% saving of electricity, without considering the biogas exploitation. Besides, there is a net power production, considering biogas use, unlike the conventional treatment plants, where the biogas exploitation is almost never sufficient to match the plant electricity operating demand.

Despite of all these advantages, biofuel production from microalgae is still not convenient, since it is not competitive in price with the standard oil, and more researches and developments are needed.

Besides, it is not clear if BOD depletion is obtained in the HRPs system, as there are no data concerning this aspect. However, in previous works (F.B. Green, L. S. Bernstone 1996) Advanced Facultative Ponds (AFP) were installed before HPRs in order to achieve BOD depletion. In these AFPs the organic matter is consumed through anaerobic methane fermentation, which occur in deep pits designed to avoid the intrusion of dissolved oxygen. The wastewater is introduced at the bottom of these pits, and overflow velocities are designed to allow the settlement of solids. The sludge is consumed day by day: in almost 30 years of operation no sludge removal was necessary. BOD depletion achieved with well-designed AFPs ranges between 60% to 80%.

However, this system seems extremely interesting and promising, and it deserve to be deeper analyzed. A careful analysis should be done in order to understand if it can be applied to Italian urban wastewaters, as wastewater quality can consistently vary between different countries. Besides, environmental conditions, such as temperature and solar irradiation, can greatly influence the algal growth (see 3.3), and must be taken into account. Another challenge in implementing this system in our country could be the land availability; Italy has a higher population density, and finding a suitably extended location is harder than in the U.S.A. Finally, our environmental legislation is much more restrictive, and further treatments could be necessary to achieve the law limits, above all in sensitive areas, such as the Venice Lagoon.

Concerning BOD removal through AFPs, a depletion capacity of 80% will not lead to discharge concentration under the Italian law limit, which are more severe respect to the U.S.A.. Therefore it is probable that HPRs will have to be coupled with conventional activated sludge processes.

5 CONCLUSIONS

In this thesis work, the possibility of coupling wastewater treatment and microalgae biomass production was investigated experimentally.

Initially, batch experiments with *C. prototothecoides* were performed to address the possibility of treating source-separated urine: despite of preliminary results, experiments carried out at 1/10 and 1/100 dilutions did not show a growth at all. Literature analysis suggests that the failure of these experiments could be due to a wrong synthetic human urine composition; further investigation is needed to find a composition able to simulate the real one, without complicating it too much.

Then, a batch experiments with urban wastewater from Camposampiero (PD) was carried out without inoculating microalgae. After a lag period of about 1 week, a microalgae consortium developed inside the medium, showing a high growth rate constant. The strain composition of this consortium is currently under research at the Biology Department of Padua University.

The behavior of *C. prototothecoides* at different temperatures was investigated with batch experiments: results show that at temperatures from 10°C to 30°C, the growth rate constant increase linearly from a minimum of 1.16 d^{-1} to a maximum of 1.9 d^{-1}. Concerning nitrogen removal, a consistent depletion was observed at all the temperatures tested, except for 10°C, where the final nitrogen concentration was more than 5 ppm. Orthophosphate analysis showed a peculiar behavior: their concentration decreased dramatically in 1 day in all the experiments, thus suggesting that *C. prototothecoides* can adsorb/accumulate orthophosphates and use them when the external concentration is too low. This result should be confirmed with further investigations, in order to assess if the fast depletion observed was due to precipitation processes or to algal adsorption/accumulation. Besides, a decreasing in cell densities was registered at increasing temperatures: literature analysis suggested that it can be due to a different cell composition. This aspect is quite important, since a change in lipid or protein contents can influence the overall process yield.

Finally, *C. prototothecoides* was cultured in a continuous flow flat-panel photobioreactor run at steady state. Results of experiments at constant illumination, integrated with data from a previous thesis (Morandini 2012), showed a peak in biomass productivity at 0.79 d of residence time. Besides, the inner biomass concentration showed an exponential behavior: increasing the residence time, the biomass concentration tended to a maximum value; this trend can be due to a limiting conditions, such as the light irradiation which is attenuated by self-shading effects at high biomass content.

Concerning continuous experiments under day/night cycles condition, consistent nutrients depletion were observed, resulting in outlet concentrations below the law limits. The biomass

productivity was observed to vary between dark and light period, showing a higher value (+ 35%) at the end of the latter. Besides, CO_2 influence in bacteria concentration was testes, showing that it cannot be considered an inhibiting factor for bacteria growth at the environmental conditions tested.

Finally, the experimental data obtained were exploited to design two possible wastewater treatment processes integrated with microalgal biomass production. In a first configuration, the microalgal reactor is placed before a conventional activated sludge treatment, while in second one, the order of the two treatments is inverted, thus allowing a better control on the final pollutants concentration. However, this proposal led to an almost halved microalgae biomass production. An alternative configuration with a floating “mattress” photobioreactor was analyzed, showing advantages and possible challenges of such a system. Further research and developments are necessary to address its feasibility.

A comparison between experimental results and model calculations was performed for process design purposes: the kinetic model showed to represent satisfactorily real data, confirming its validity at each residence time tested. The biomass model led to higher errors, which can be probably due to difference in microalgal composition at different residence times.

BIBLIOGRAPHY

Abdel-Raouf, N., Al-Homaidan, a. a. & Ibraheem, I.B.M., 2012. Microalgae and wastewater treatment. *Saudi Journal of Biological Sciences*, 19(3), pp.257–275. Available at: http://linkinghub.elsevier.com/retrieve/pii/S1319562X12000332 [Accessed May 27, 2013].

Anna L Stephenson, John S Dennis, Christopher J Howe, S.A.S.& A.G.S., 2010. Influence of nitrogen-limitation regime on the production by Chlorella vulgaris of lipids for biodiesel feedstocks. *Biofuels*, 1(1), pp.47–58.

APHA-AWWA-WEF., 1992. Standard methods for the examination of water and wastewater. , 18.

Burton, F.L., 1996. Water and wastewater industries: characteristics and energy management opportunities.

De Castro Araújo, S. & Garcia, V.M.T., 2005. Growth and biochemical composition of the diatom Chaetoceros cf. wighamii brightwell under different temperature, salinity and carbon dioxide levels. I. Protein, carbohydrates and lipids. *Aquaculture*, 246(1-4), pp.405–412. Available at: http://linkinghub.elsevier.com/retrieve/pii/S0044848605001365 [Accessed June 3, 2013].

Chang, Y. et al., 2013. Cultivation of Spirulina platensis for biomass production and nutrient removal from synthetic human urine. *Applied Energy*, 102, pp.427–431. Available at: http://linkinghub.elsevier.com/retrieve/pii/S0306261912005363 [Accessed June 18, 2013].

Cheng, K., Ren, M. & Ogden, K.L., 2012. Statistical optimization of culture media for growth and lipid production of Chlorella protothecoides UTEX 250. *Bioresource Technology*, 128(2013), pp.44–48. Available at: http://dx.doi.org/10.1016/j.biortech.2012.09.085.

Chisti, Y., 2007. Biodiesel from microalgae. *Biotechnology Advances*, 25(3), pp.294–306. Available at: http://dx.doi.org/10.1016/j.biotechadv.2007.02.001.

Enzo, M., 2011. *Development of a pilot plant for microalgae production: laboratory measurements and plant design*. Università degli Studi di Padova.

F.B. Green, L. S. Bernstone, T.J.L. and W.J.O., 1996. Advanced integrated wastewater pond systems for nitrogen removal. *Wat. Sci. Tech*, 33(7), pp.207–217.

Facca, M., 2013. *Coltivazione e caratterizzazione di una microalga per la produzione di biomassa su scala industriale*. Università degli Studi di Padova.

Gupta, D. & Singh, S., 2012. Greenhouse Gas Emissions from Wastewater Treatment Plants: A Case Study of Noida. *Journal of Water Sustainability*, (June 2012). Available at: http://www.jwsponline.com/uploadpic/Magazine/pp 131-139 JWS-A-12-008.pdf [Accessed June 20, 2013].

Hernandez-Sancho, F., Molinos-Senante, M. & Sala-Garrido, R., 2011. No Titleenergy efficiency in Spanish wastewater treatment plants: A non-radial DEA approach. *Science of The Total Environment*, 409(14), pp.2693–2699.

Jorquera, O. et al., 2010. Comparative energy life-cycle analyses of microalgal biomass production in open ponds and photobioreactors. *Bioresource technology*, 101(4), pp.1406–13. Available at: http://www.ncbi.nlm.nih.gov/pubmed/19800784 [Accessed May 21, 2013].

Lam, M.K. & Lee, K.T., 2012. Microalgae biofuels: A critical review of issues, problems and the way forward. *Biotechnology advances*, 30(3), pp.673–90. Available at: http://www.ncbi.nlm.nih.gov/pubmed/22166620 [Accessed May 23, 2013].

Lardon, L., Hélias, A. & Sialve, B., 2009. Life-cycle assessment of biodiesel production from microalgae. *… science & technology*, pp.3–9. Available at: http://pubs.acs.org/doi/abs/10.1021/es900705j [Accessed June 19, 2013].

Larkum, A.W.D. et al., 2012. Selection, breeding and engineering of microalgae for bioenergy and biofuel production. *Trends in biotechnology*, 30(4), pp.198–205. Available at: http://www.ncbi.nlm.nih.gov/pubmed/22178650 [Accessed June 13, 2013].

Larsen, T.A. et al., 2009. Source Separation: Will We See a Wastewater Paradigm Shift in Handling? *Environmental Science & Technology*, 43(16), pp.6126–6130. Available at: http://pubs.acs.org/doi/abs/10.1021/es9010515 [Accessed May 30, 2013].

Lundquist, T., Osundeko, O. & Kunz, S., Algae Wastewater Treatment Webinar.

Mata, T.M., Martins, A. a. & Caetano, N.S., 2010. Microalgae for biodiesel production and other applications: A review. *Renewable and Sustainable Energy Reviews*, 14(1), pp.217–232. Available at: http://linkinghub.elsevier.com/retrieve/pii/S1364032109001646 [Accessed May 21, 2013].

Maurer, M, Pronk, W. & Larsen, T. a, 2006. Treatment processes for source-separated urine. *Water research*, 40(17), pp.3151–66. Available at: http://www.ncbi.nlm.nih.gov/pubmed/16949123 [Accessed May 30, 2013].

Mayrovitz, H.N. & Sims, N., 2001. Biophysical effects of water and synthetic urine on skin. *Advances in Skin & Wound Care*, 14(6), p.302.

Mbaya, A. et al., THE IMPACT OF SOURCE SEPARATION OF URINE ON BIOLOGICAL NUTRIENT REMOVAL ACTIVATED SLUDGE. Available at: http://www.ewisa.co.za/literature/files/263_213 Mbaya.pdf.

Metcalf & Eddy, 2004. *Wastewater Engineering: Treatment and Reuse* Fourth Edi. M. Hill, ed.,

Milani, A., 2013. *Microalghe per la depurazione di reflui urbani: cinetiche di crescita e di abbattimento degli inquinanti*. Università degli Studi di Padova.

Morandini, M., 2012. *Investigation on wastewater treatment with microalgae: a way to improve existing processes*. Università degli Studi di Padova.

PVGIS© European Communities, 2007. Solar Irradiation Data. Available at: http://re.jrc.ec.europa.eu/pvgis/apps/radmonthphp?lang=en&map=europe/.

Raehtz, K.D., 2009. Challenges and Advantages in Making Microalgae Biomass a Cost Efficient Source of Biodiesel. *Basic Biotechnology eJournal*, 5(1), pp.37–43.

Rawat, I. et al., 2013. Biodiesel from microalgae: A critical evaluation from laboratory to large scale production. *Applied Energy*, 103, pp.444–467. Available at: http://linkinghub.elsevier.com/retrieve/pii/S0306261912007088 [Accessed May 22, 2013].

Rawat, I. et al., 2011. Duel role of microalgae: Phycoremediation of domestic wastewater and biomass production for sustainable biofuels production. *Applied Energy*, 88(10), pp.3411–3424.

Rojas, J. & Zhelev, T., 2012. Energy efficiency optimisation of wastewater treatment: Study of ATAD. *Computers & Chemical Engineering*, 38, pp.52–63. Available at: http://linkinghub.elsevier.com/retrieve/pii/S0098135411003371 [Accessed June 20, 2013].

Sander, K. & Murthy, G.S., 2010. Life cycle analysis of algae biodiesel. *The International Journal of Life Cycle Assessment*, 15(7), pp.704–714. Available at: http://link.springer.com/10.1007/s11367-010-0194-1 [Accessed May 21, 2013].

Sharma, K.K., Schuhmann, H. & Schenk, P.M., 2012. High Lipid Induction in Microalgae for Biodiesel Production. *Energies*, 5(12), pp.1532–1553. Available at: http://www.mdpi.com/1996-1073/5/5/1532/ [Accessed May 23, 2013].

Shelef, G., Moraine, R. & Sandback, E., 1977. *Combined algae production wastewater treatment and reclamation systems*, West Germany: Pergamon Press.

Singh, J. & Gu, S., 2010. Commercialization potential of microalgae for biofuels production. *Renewable and Sustainable Energy Reviews*, 14(9), pp.2596–2610. Available at: http://linkinghub.elsevier.com/retrieve/pii/S1364032110001619 [Accessed May 21, 2013].

Su, Y., Mennerich, A. & Urban, B., 2012. Synergistic cooperation between wastewater-born algae and activated sludge for wastewater treatment: influence of algae and sludge inoculation ratios. *Bioresource technology*, 105, pp.67–73. Available at: http://www.ncbi.nlm.nih.gov/pubmed/22189078 [Accessed June 10, 2013].

Woertz, I., Fulton, L. & Lundquist, T., 2009. Nutrient Removal & Greenhouse Gas Abatement with CO₂ Supplemented Algal High Rate Ponds. *Proceedings of the Water Environment Federation*, 2009(7), pp.7924–7936. Available at: http://openurl.ingenta.com/content/xref?genre=article&issn=1938-6478&volume=2009&issue=7&spage=7924.

Yen, H. et al., 2011. Biore source Tec hnology Microalgae-based biorefinery – From biofuels to natural products. *Bioresource Technology*, 135(2013), pp.166–174. Available at: http://dx.doi.org/10.1016/j.biortech.2012.10.099.

Zhang, L., Thomas, H. & Anastasios, M., 2002. Biochemical and morphological characterization of sulfur-deprived and H2-producing Chlamydomonas reinhardtii (green alga). *Planta*, 214(4), pp.552–561.

RINGRAZIAMENTI

Desidero innanzitutto ringraziare il prof. Bertucco, per avermi dato l'opportunità di approfondire questo campo di ricerca e avermi guidato durante l'intero svolgimento della tesi.
Un ringraziamento particolare a Barbara ed Elia per avermi pazientemente assistito negli esperimenti di laboratorio e nella stesura dell'elaborato.
Ringrazio Marco, senza di lui non avrei nemmeno iniziato questa tesi, e Andrea, che mi ha trasmesso le sue conoscenze e la sua esperienza in laboratorio;
Un saluto a tutti i colleghi di laboratorio: Matteo, Stefania, Renata, Sonia, Carlos, Carlotta e Myriam.

Vorrei ringraziare poi, tutto lo staff del Centro di Biotrattamento di Camposampiero, in particolar modo Annamaria, per la gentilezza e la disponibilità che hanno sempre dimostrato;

Grazie ai miei genitori, che mi hanno supportato (e sopportato) in tutti questi anni, il vostro appoggio e la vostra comprensione sono stati fondamentali, senza di voi noi avrei mai raggiunto questo traguardo. E come non ringraziare mio fratello, Samuele: nonostante i nostri innumerevoli contrasti, sarai sempre un punto di riferimento per me. Flò, silenziosa compagna, grazie per avermi tenuto compagnia nelle infinite sessioni di studio alla scrivania.
I nonni: Arrigo, per tutti i pranzi e le cene scroccate e le verdure del tuo fantastico orto, e Giannina, la pazienza e comprensione dimostrati, permettendomi di occupare la tua Mansarda fino a notte fonda, e per molte notti, sono ormai leggenda.

Un pensiero speciale va a Tommaso e Filippo, compagni di studio e "avventure" (e chiamiamole pure così) in questi ultimi anni di università.

And last but not least, ringrazio i miei amici Ale, Andrea, Niccolò e Mattia, per la vostra compagnia, le pokerate nebbiose, e i passaggi in macchina che non mi avete mai negato. E anche Alberto, Elena , Gianluca, Mattia B., Marco, Massimo, Valentina e Valentino, grazie a tutti!